CLONAL ANALYSIS OF HUMAN MAMMARY CELL TRANSFORMATION AND X-RAY SENSITIVITY

by

Sneha Balani

B.Sc. (Hons.), University of Delhi, 2009

M.Sc., University of Delhi, 2011

A THESIS SUBMITTED IN PARTIAL FULFILLMENT OF

THE REQUIREMENTS FOR THE DEGREE OF

DOCTOR OF PHILOSOPHY

in

THE FACULTY OF GRADUATE AND POSTDOCTORAL STUDIES

(Interdisciplinary Oncology)

THE UNIVERSITY OF BRITISH COLUMBIA

(Vancouver)

April 2018

Abstract

Intra-tumoural biological, transcriptional and genomic heterogeneity are hallmarks of human breast cancers. However, tumour propagating activity appears confined to subsets of cells within each tumour. This finding is thought to indicate a persistence of mechanisms that maintain a hierarchical growth and differentiation structure in the normal mammary gland. Because little is known about the responses of either primary normal or malignant human mammary cells to existing therapies, this thesis sought to examine the intrinsic sensitivity of different purified human mammary colony-forming cell (CFC) types and tumours derived from them to ionizing radiation.

Luminal progenitor (LP) CFCs were found to be ~1.5-fold more radioresistant than basal cell (BC) CFCs and LPs also showed evidence of checkpoint adaptation, slower repair activity and greater predisposition of γH2AX foci accumulation. Two human breast cancer cell lines (MDA-MB231 and SUM149) and a non-tumorigenic human mammary cell line (MCF-10A) were all found to be more radioresistant than the normal LP-CFCs. CFCs isolated from 8-week tumours generated in mice transplanted with normal human BCs or LPs transduced with $KRAS^{G12D}$ showed even greater radioresistance and this was further increased in serially passaged derivative lines with more aggressive growth properties.

To examine the responsiveness of malignant cells with tumor-initiating cell (TIC) activity *in vivo*, a dose-response analysis was first undertaken of their frequencies in the MDA-MB231 and SUM149 cells. Limiting dilution analysis (LDA) and single-cell transplants showed the frequency of TICs in both to be very high (<10%), but with

increasingly marked inhibition of their detection in tumours initiated from innocula containing $2x10^4$ cells or more. Analogous LDA measurements of the TICs in *KRAS*^{G12D}-transduced BCs and LPs, yielded frequencies of ~0.2% and ~0.07%, respectively, in contrast to the frequencies of 0.02-0.5% for BCs and 0.01-0.6% for LPs for tumours initiated from $3x10^4$-10^6 cells.

These results demonstrate the heterogeneity of treatment responses in normal human mammary cells with innate proliferative ability that can be heightened by transformation. They also reveal the complex clonal dynamics operative in the growth of TICs *in vivo* that may confound interpretation of treatment effects assessed only by measuring immediate changes in tumor size.

Lay Summary

Radiotherapy is widely used to treat breast cancer patients, yet little is known about how it affects the normal breast cells or cancers that arise from them. Since the breast contains different types of cells, the mechanisms that control their different behaviours may also affect how different breast cancers respond to radiation. To test this idea, the sensitivity of two different types of normal breast cells and tumours derived experimentally from each to ionizing radiation was examined. The results revealed differences between the two normal breast cell types that became increasingly resistant in their increasingly aggressive malignant progeny. Additional studies revealed complex interactions in the detection of their tumour-initiating activity *in vivo*. This finding indicates the importance of measuring the effect of treatments on this *in vivo* tumour-initiating activity separate from immediate changes in tumour size.

Preface

Under the supervision and conceptual guidance of my supervisor Dr. Connie Eaves, I performed all of the experiments included in this thesis, as well as the analysis and interpretation of the data obtained. Dr. Nagarajan Kannan, Dr. Maisam Makarem, Dr. Long Nguyen and Dr. Sylvain Lefort helped with designing experiments and interpreting data in Chapters 2 and 3. Dr. Sylvain Lefort and Dr. Davide Pellacani provided technical assistance with the experiments involving transplants into mice that contributed to the results in Chapter 3. Zhencheng He (Maxwell Lab, BC Children's Hospital Research Institute) helped with the γH2AX assay. Glenn Edin helped in the acquisition of luciferase data. Darcy Wilkinson consented, collected and prepared cryopreserved samples of dissociated cells from patient reduction mammoplasty samples, and performed the immunohistochemical staining.

Sections of Chapter 1 (Section 1.9, Figure 1.6, Figure 1.7, and Table 1.1) and Chapter 4 (Section 4.2) have been published as a review in Nature Communications: Balani S., Nguyen, L.V., Eaves, C.J. (2017) Modeling the process of human tumorigenesis. Nature Communications 8, Article number: 15422.

Chapter 2 is being prepared for submission as a manuscript entitled "Analysis of the intrinsic sensitivity of normal and transformed human mammary clonogenic cells to ionizing radiation" for publication in a peer-reviewed journal.

Chapter 3 is being prepared for submission as a manuscript entitled "Development of a method to quantify the *in vivo* treatment response of transformed cells with clonogenic activity" for publication in a peer-reviewed journal.

All human cells were obtained with consent and used according to University of British Columbia Research Ethics Board protocols under certificate number H06-00210 and H11-02531. Animal experiments were carried out in accordance with the policies and guidelines presented by the University of British Columbia Animal Care Committee. Canadian Council on Animal Care Approval was granted under the certificate number: #A15-0024.

Table of Contents

List of Tables

List of Figures

List of Abbreviations

2D	2-dimensional
3D	3-dimensional
ALL	acute lymphoid leukemia
AML	acute myeloid leukemia
APC	allophycocyanin
BC	basal cell
BSA	bovine serum albumin
CD	cluster of differentiation
CDK	cyclin dependant kinase
CFC	colony-forming cell
CIC	clone-initiating cell
CK	cytokeratin
CML	chronic myeloid leukemia
CNV	copy number variation
DAPI	4’,6-diamidino-2-phenylindole
DMEM	Dulbecco’s minimal essential media
DMSO	dimethylsulfoxide
DNA	deoxyribonucleic acid
DSB	double stranded break
EDTA	ethylene diamine tetraacetic acid
EGF	epidermal growth factor
EGFR	epidermal growth factor receptor
EGTA	ethylene glycol-bis(β-aminoethyl ether)-N,N,N',N'-tetraacetic acid
EpCAM	epithelial cell adhesion molecule
ER	estrogen receptor
FACS	fluorescence activated cell sorting
FBS	fetal bovine serum
FITC	fluoroscein isothiocyanate

GFP	green fluorescent protein
HER2	human epidermal growth factor receptor-2
H&E	hematoxylin and eosin
HF	hank's balanced salt solution with 2% FBS
iPSCs	induced pluripotent stem cells
LC	luminal cell
LDA	limiting dilution analysis
LP	luminal progenitor
MDS	myelodysplastic syndromes
MLL	mixed lineage leukemia
MRU	mammary repopulating unit
MUC1	mucin-1
NaCl	sodium chloride
NOD-SCID	non-obese diabetic-*Scid*
NP40	nonidet P40
NRG	non-obese diabetic-Rag1-null, IL2Rgamma chain-null
PBS	phosphate buffered saline
PCR	polymerase chain reaction
PD-1	programmed death-1
PD-L1	programmed death ligand-1
PDX	patient-derived xenograft
PE	phycoerythrin
PI	propidium iodide
PLK1	polo-like kinase 1
PMSF	phenylmethylsulfonyl fluoride
PR	progesterone receptor
PRb	retinoblastoma protein
PVDF	polyvinylidene fluoride
RIPA	radioimmunoprecipitation assay
RNA	ribonucleic acid
ROS	reactive oxygen species

rpm	revolutions per minute
SDS	sodium dodecyl sulfate
SEM	standard error of the mean
SMA	smooth muscle actin
SNV	single nucleotide variant
TF	transcription factor
TIC	tumour-initiating cell
TBST	tris-buffered saline with polysorbate 20
YFP	yellow fluorescent protein

Acknowledgements

I would like to acknowledge my exceptional supervisor and mentor Dr. Connie Eaves for her commitment, dedication and support in guiding my doctoral degree. I thank her for giving me the opportunity of training with the best and for providing the perfect environment to discuss and engage in scientific concepts and ideas; for teaching me how to ask important biological questions and how to critique my own and others' work. I thank her for her guidance, attention to detail and for her full support of my various extracurricular involvements as well as future career goals.

I would like to acknowledge my supervisory committee members Dr. Kelly McNagny, Dr. Sharon Gorski and Dr. Victor Ling for their advice, criticism, scientific expertise, and help in guiding my thesis project.

I want to thank my colleagues, past and present; particularly, Dr. Maisam Makarem, Dr. Raj Kannan, Dr. Long Nguyen, Dr. Claire Cox, Dr. Sylvain Lefort, Dr. Davide Pellacani and Susanna Tan for insightful discussions and support in turbulent times. I further thank Maisam, Long and Sylvain for being excellent mentors and friends. I acknowledge Darcy Wilkinson, Glenn Edin and Margaret Hale for technical assistance and Dr. Chris Maxwell and Dr. Peter Stirling for their scientific input.

I thank other members of the Eaves' Lab for their contribution and feedback through the years; especially, Dr. Paul Miller, Dr. David Knapp, Dr. Naoto Nakamichi, Lisa Bulaeva, Colin Hammond, Margie MacAldaz and Fangwu Wang. I would like to acknowledge current and past members of the Terry Fox Laboratory for being my friends and family and the staff; particularly, Dr. Amanda Kotzer, Alice Chau, Vincent Chui, Shera Paterson and Cynthia Wong for their help in navigating administrative hurdles.

I want to thank my program, Interdisciplinary Oncology, Dr. Angie Brooks-Wilson and Sharon Ruschkowski for support in completing this degree, as well as acknowledge Dr. Sanjay Katiyar and Dr. Poonam Sharma at University of Delhi for helping me gain my first firm footing into the world of research.

I was fortunate to be involved extensively at the University of British Columbia. I would like to acknowledge the role of GrasPods and UBC Graduate Student Society for launching me as a student leader and that of StemCellTalks Vancouver, Let's Talk Science and Stem Cell Network for helping me fulfill my passion for public outreach. I would also like to thank Amy Stewart and staff, colleagues and friends at UBC Residence Life for shaping me into a well-rounded individual, and Jacqui Brinkman, Graduate Pathways to Success and Faculty of Graduate and Postdoctoral Studies for their professional guidance and generous support.

I thank my friends, including but not limited to Jacqueline, Shannon, Marta, Vincent, Jason, Catherine, Rachel, Kat, Gaby, Kajal and Robert for providing me an unparalleled support system. I thank Monika Kodnani for being my family in the city and my extended family all over the world for being a supportive part of this process.

And lastly, I want to thank my parents, Shweta and Dinesh Balani and my brother Vishesh, for their unconditional love, undying belief and continuous support in every aspect of my life.

Dedicated to my Mom and Dad

Chapter 1: Introduction

1.1 Normal human mammary gland: structure and cell types

The adult human mammary gland is a bilayered network of cells that form a structure of interconnecting ducts all joining together at the nipple. The entire mammary gland is surrounded by a basement membrane consisting primarily of laminin and collagen IV, embedded in a collagen-rich stroma containing fibroblasts, adipocytes, blood and lymphatic vessels and hematopoietic cells [1]. Histologically, the two cell layers are morphologically quite distinct. The outer basal layer that lines the inner surface of the basement membrane consists of cells with myoepithelial features. The inner layer of cells line the continuous lumen that extends throughout all of the ducts and alveolae where they can be stimulated to produce milk (Figure 1.1a).

Histological markers characteristic of the cells of the outer basal layer (referred to as basal cells, or BCs) are smooth muscle actin (SMA), cytokertins (CKs) 5 and 14, CD10, Thy-1 (CD90) and apha-6 integrin (CD49f). Distinguishing features of cells of the luminal layer are high expression of EpCAM, CK8/18, CK19, and MUC1. However, these EpCAM+ cells can be further subdivided into multiple cell types. Those that co-express CD49f and KIT include cells that can proliferate in response to epidermal growth factor (EGF) in 2D cultures and make colonies of progeny with luminal features (see below). Accordingly, they are referred to as luminal progenitors (LPs). The remainder that are $CD49f^-$ KIT^- do not proliferate under these conditions and are referred to as

luminal cells (LCs) [2, 3] (Figure 1.1b). The LP fraction can be further subfractionated according to the expression of ALDH1 activity into relatively more ($EpCAM^+CD49f^+ALDH^-$) or less differentiated ($EpCAM^+CD49f^+ALDH^+$) LPs. The ALDH+ LPs in humans are analogous to the ER- LPs in mouse [4]. These subsets constitute all of the epithelial cells in the mammary gland and are phenotypically distinct from the other cells present in the breast, including various blood- and lymph-borne $CD45^+$ leukocytes, $CD31^+$ endothelial cells, and stromal cells (SCs) (that are $CD49f^-$ and $EpCAM^-$).

1.2 Molecular characterization of human mammary cells

The molecular regulators that specify the unique features of each of the normal human mammary subsets have only recently been investigated in depth with many genes now implicated as exerting important effects on the growth and functional behaviour of different cell types within the mammary gland. Transcriptome profiling and functional studies have identified several key transcriptional factors (TFs) in the subpopulations of normal human and analogous mouse mammary cell types. Thus implicated in BCs are *SLUG, TP63, TP53, SOX9, STAT3, MYC* and *TAZ* [5-9]. In cells with luminal features, *CEBPB* and *NOTCH3* [10], together with *GATA3* and *ELF5* [11], and *FOXA1*, which regulates ER activity [12], have been identified as important. Epigenomic profiles have provided global annotation of active enhancer regions [13] as well as more comprehensive analysis of human mammary subsets [14]. For example, the latter revealed that the LP and LC epigenomes differ greatly, with LPs sitting intermediate

between BCs and LCs. This study also confirmed the presence of previously described TFs and identified a number of their binding sites that are unique to the different cell types. These included *EGR1*, *EGR2*,*TP53* and members of the *TEAD EBF* and *TCF* families for BCs, AP-1 TF complex, *ESR1* and *FOXP1* for LCs and *GRHL2*, *ELF1* and *ETS1* for LPs [14]. Furthermore, the use of mass cytometry has recently generated profiles of signaling activities associated with external cues for all 3 major human mammary subsets [15]. This study also identified a subset of phenotypically defined LPs that display an elevated content of active caspase-3 that, nevertheless, remain viable.

1.3 Clonal growth-based assays of proliferative potential

Clonal growth-based assay systems are critical for analyzing the cell output potential of individual cells within heterogeneous populations. *In vitro* and *in vivo* assay conditions have been developed that allow a hierarchy of cells with different proliferative and differentiation potentialities to be identified and quantified. These include an *in vivo* assay for cells with the regenerative properties of a stem cell (referred to operationally as a mammary-repopulating unit or MRU) and *in vitro* 2D and 3D colony-forming cell (CFC) assays detecting both bipotent and lineage-restricted progenitors (Figure. 1.2 & 1.3) [2, 10, 16]. Briefly, the method for detecting human mammary CFCs in 2D cultures involves the seeding of cells on collagen-coated wells along with irradiated fibroblasts in SF-7 media for 8-10 days at 37ºC. The method for detecting *human* MRUs involves generating a single-cell suspension and embedding the cells together with irradiated supportive fibroblasts in a collagen gel that is then transplanted under the kidney capsule

of highly immunodeficient adult female mice with slow-release pellets of estrogen and progesterone to mimic pregnancy and enhance cell production from the transplanted cells [17]. MRUs can be similarly detected by implanting the gels subcutaneously in Matrigel (D Pellacani, personal communication). The gels are then retrieved 4-6 weeks later, dissociated into single cells and assayed for CFCs. The human mammary CFCs obtained from the gels include the same spectrum of CFCs found in the normal human breast. Incorporation of irradiated fibroblasts into the initially transplanted gels, allows the recovered CFC numbers to be linearly related to the number of cells transplanted over a wide range down to limiting numbers of input cells. This, in turn, enables their presence to be used to infer that at least one MRU was in the cells transplanted in limiting dilution transplant experiments and hence the calculation of human MRU frequencies in the original test cell suspensions using Poisson statistics. The frequency of MRUs in bulk dissociated reduction mammoplasty samples has been shown to be ~1/1,000 to 1/10,000 cells and the average number of CFCs obtained per MRU to be 4.1 ± 0.6 CFCs [17]. Cell purification experiments have further shown that MRU activity is exclusively detected in the BC subset with minimal to no MRU detected in the LC and LP subsets [2, 17].

A second *in vivo* detection system allows for orthotopic growth of human mammary epithelial cells in the mouse mammary fat pad that has been previously injected with human mammary fibroblasts [18]. However, a limiting dilution analysis (LDA) of the frequency of MRUs in the injected cells using a histological endpoint was lower than that reported for the kidney capsule MRU assay, although the BC-restricted phenotype of the cells thus identified was the same [3].

If subsets are sufficiently enriched in their content of transplantable cells with regenerative activity, single-cell assays can be performed. To date, this has been possible with mouse mammary BCs [19] but not human mammary cells. Moreover, both of these approaches lack the feasibility and precision required for addressing larger scale questions. An alternative is to detect the progeny of individual starting cells based on their engineered acquisition of a unique but biologically neutral genetic feature. This latter approach has the great advantage of enabling many (100's – 1,000's) of clones to be tracked simultaneously in a single transplant. However, this approach also necessarily introduces the possibility of clonal competition, incomplete activation of the test cells and consequent effects on the resultant clonal dynamics obtained that may or may not reflect a more homeostatic condition.

Because lentiviral transduction involves a semi-random insertion of the viral genome into each transduced host cell, the clonal progeny can then be uniquely identified by restriction fragment size analysis on a Southern blot [20] or by a PCR-based method to detect the unique sequences flanking the insertion site [21]. In the latter case where a single insertion site per cell can be assumed using transduction protocols that achieve suboptimal gene transfer efficiencies, this method can also be used to infer clone sizes [22-24]. Nevertheless, ~50% of insertion sites are still elusive to detection using the latest versions of this methodology [21].

A derivative of this approach with more comprehensive coverage makes use of a large library of vectors each of which contains a different short DNA "barcode" in its genome so that each transduced cell will contain a different single barcode when transduced at appropriately low efficiencies [25, 26]. Clone numbers and sizes of their

expanded progeny are then inferred from the relative representation of different barcodes in sequenced DNA extracts of the harvested tissue (Figure 1.5). The use of this methodology to analyze the clonal composition of regenerating normal human mammary cell populations has revealed a greater diversity of differentiation in primary transplants of purified normal human BCs than noted in BC-derived colonies *in vitro* and delayed growth of the BCs that regenerate mammary tissue in secondary hosts [27]. Notably, for both vector strategies, phenotypic purification of the cells to be analyzed prior to extracting the DNA for insert site or barcode analysis allows the phenotypic composition of each clone to also be characterized [28-35].

1.4 Inferred hierarchical organization of mammary cell subsets

Organization of the mammary gland has historically been conceptualized as a hierarchy in which self renewing MRUs with a basal phenotype produce bipotent as well as myoepithelial and luminal-restricted progenitors that, in turn, give rise to mature terminally differentiated cells within their respective lineages (Figure 1.4). Although *in situ* lineage tracing studies are not feasible in humans, one study showed that purified human mammary LCs can produce multilayered acinar structures *in vivo* that contain cells of both the luminal and myoepithelial lineages, suggesting some LCs retain bipotent differentiation abilities [4]. Thus, the control of differentiation within the normal human mammary gland may not be as rigidly coordinated as implied by conventional lineage maps.

Lineage tracing which involves the genetically engineered expression of a detectable marker/reporter in a cell- or tissue-specific manner, has implied that unipotent rather than bipotent mammary cells play a major role in separately maintaining the two major lineages of the gland in adult mice. In a first study, the use of inducible Cre reporter strains to track the fate of mammary progenitor cells during embryogenesis, adulthood and pregnancy showed that embryonic K14+ progenitors gave rise to all lineages in the adult gland, but maintained separate luminal (K8+/K18+) and basal (K5+/K14+) lineages in the adult [36]. This study thus introduced the concept that unipotent luminal and basal cells, rather than bipotent mammary stem cells, maintain the epithelial lineages throughout adulthood in mice. In humans, it has long been known that the adult human mammary gland is of polyclonal origin. Studies that have mapped the patterns of X-chromosome inactivation, a process occurring early in prenatal development, revealed that the gland contains contiguous patches of tissue of different clonal origin [37]. This would also be consistent with a model in which single bipotent cell types sustain both lineages in discrete local regions of the gland. However, these findings do not exclude the alternative possibility that these are merely associations by chance.

1.5 Human breast cancer

Breast cancer develops over time and may go through an *in situ* phase. The most common physical sign is a painless breast lump. Swollen and enlarged lymph nodes may be present within the axillary region during the early stages of metastasis. Evidence of a

bloody nipple discharge, heaviness, redness, swelling, deformity, or retractions of the breast are less common but substantial indicators of breast malignancy, usually when the disease is at an advanced stage [38].

Worldwide about 1.7 million cases of breast cancer are diagnosed every year, translating to approximately one new case every 18 seconds [39]. Interestingly, a higher incidence is documented in higher income regions (92 per 100,000 in North America compared to 27 per 100,000 in Middle Africa and Eastern Asia) [40-42]. In Canada, breast cancer continues to be the most common diagnosis of cancer in women (25%) and is the second leading cause of cancer deaths in women after lung cancer. In men, breast cancers make up 0.2 percent of all cancer cases [43]. The probability a Canadian woman will die from breast cancer during her lifetime is 1 in 30 [43]. Risk factors for breast cancer include increasing age, race, early menarche, late menopause, fibrous breast tissue, reproductive patterns (including greater number of children, first childbirth at a younger age and longer duration of breast feeding), hormone use (combined estrogen and progestin therapy increases the risk of developing breast cancer), high alcohol use, tobacco use, diet (fruit and vegetable consumption has been shown to be inversely related to breast cancer risk), and lack of physical activity [44]. Mutations in the *BRCA1* and *BRCA2* genes are significantly associated with the development of breast and ovarian cancer by the age of 70 [45].

Early detection and screening is an important strategy to improve outcomes. In Canada, the Canadian Task Force on Preventive Health Care recommends screening every 2-3 years for women aged 50-74 years with special considerations for certain ethnic groups that may have a higher or lower risk of breast cancer, hence requiring more

or less frequent screens [46]. Survival depends on stage of diagnosis and disease characteristics, but overall survival in Canada is 87% at 5 years for women and 79% for men. Women who are diagnosed between the ages of 40 and 69 have the highest 5-year survival rates (89-90%) and lowest rates are among older women 80-99 (78%) [43].

1.5.1 Classical Definitions and Evolving Classification

Breast cancers comprise a heterogeneous group of complex diseases characterized by intra- as well as inter-tumoral differences in their biological, transcriptional and genomic features. Clinically, breast cancers are categorized at diagnosis according to their size, invasive status, morphology, and certain molecular characteristics ascertained by immunohistochemistry (i.e., as ER-positive or negative, HER2-positive or negative, luminal or basal features, and proliferative activity) [47].

Transcriptome analysis initially suggested six different subtypes: Luminal A, Luminal B, Luminal C, ERBB2+ (HER2+), normal-like and basal-like [48, 49]. These were later reduced to four subtypes by combining Luminal B with Luminal C and the exclusion of normal-like as a subtype because of the lack of clarity as to whether they represented a distinct group of breast tumours with shared prognostic implications [50]. Another subtype of breast cancers referred to as claudin-low was then later introduced based on additional studies of human and mouse tumours [51] and breast cancer cell lines [52].

Luminal A breast cancers are characterized predominantly by expression of *ESR1*, as well as other genes such as *BCL2* [53]. Luminal B breast cancers are characterized by

increased expression of proliferation genes such as *MKI67* and *PCNA* [54]. HER2+ breast cancers have high expression of HER2 and GRB7, whereas basal-like breast cancers have high expression of basal-associated KRT5 and a high prevalence of the *TP53* mutation [48]. Claudin-like subtype are clinically ER-PR-HER2- and have frequently metastasized already at diagnosis, just like triple negative breast cancers [50].

Detection of these intrinsic subtypes has been shown to be obtained using just 50 genes (PAM50 test) [55] and is now being investigated in clinical trials for its predictive value in assessing clinical outcomes [56]. Other prognostic tests developed for assessing the likelihood of relapse based on gene expression have also been devised [57-60]. Furthermore, integrative clustering analysis of nearly 2,000 breast tumours, has identified 10 subgroups termed IntCluster 1 to 10. These have different gene expression profiles, CNVs and distinct clinical outcomes [61, 62]. More recent genomic analyses suggest that the IntClusters can be further subdivided into subgroups with different prognoses based on their DNA content, CNVs and specific mutations [63].

1.5.2 Heterogeneity in Human Breast Cancer

Advances in DNA sequencing technology allow genomic profiles of breast tumours to be analyzed [64]. SNVs, as well as indels, are detected at various frequencies, and used to infer clonal genotypes based on algorithms used to model clonal and sub-clonal mutation clusters. It has been possible to infer early driver mutations from analyses of such models [64-66]. An example of this is the high prevalence of *TP53* mutation in triple negative and basal-like breast cancers consistent with a driver function. However, this may not be

true for other tumours where mutations in *TP53* are present in low-abundance, and hence may not be a founding mutation in these cases. Such observations support a model of branched clonal evolution where subclones acquire different mutations [67]. Advances in sequencing have also enabled researchers to estimate levels of intra-tumoural heterogeneity using mutant-allele fractions. For example, associations between *PIK3CA* mutations and reduced survival are identified in subgroups of ER-positive cancer. High levels of intra-tumoural heterogeneity are generally associated with highly aggressive tumours and poorer outcomes [68]. However, definitive evidence of different clonal genotypes within tumours requires the application of single-cell sequencing methods or the sequencing of clonally derived tumour populations [69].

The study of the process of clonal diversification can involve either a forward or retrospective approach to identify changes in clonal populations over time. One approach is to study metastasis and compare the genomic clonal diversity in the metastases versus the primary tumour. These types of studies have been performed in human breast [64, 65], kidney [70], lung [71] and pancreatic cancers [72]. A second approach is to transplant a patient's primary tumour into immunodeficient mice and then examine the clonal evolution of the xenograft over serial passages [73-76]. However, this latter approach has two caveats. First, only a part of the patient's tumour is transplanted thus introducing a selection of the clones that can be assessed. Second, clonal selection may occur within the subset of clones that engraft and their subsequent growth may also be differentially affected by the mouse microenvironment. The advantage of generating such xenografts, however, is their potential use to study the effects of targeted or

chemotherapy treatments in order to determine the effects of such treatments on tumour-propagation [77, 78].

Recent advances in the use of DNA barcoding to track the clonal evolution of serially transplanted tumours have enabled the study of clonal dynamics in breast cell lines [28]. These studies showed that the spectrum of clones detected in serial passages of the same starting populations fluctuated. More recently, clonal tracking of xenografted primary glioblastoma showed that slow-cycling stem-like cells give rise to more rapidly cycling progenitor population with extensive self-maintenance capacity [79]. The aforementioned caveat of clonal selection has also been partly solved by the use of single cell transplants of patient xenografts [69] and single nucleus genome sequencing [80] in some studies of breast cancer. As such studies are further developed, they may have important implications for improving the diagnosis and treatment of breast cancer.

1.6 Treatment of Breast Cancer

Current therapies for breast cancer patients include surgery and ionizing radiation for localized disease plus chemotherapy and molecularly targeted therapies for metastatic disease. Surgery and radiation, although generally effective for early stage breast cancers, are also disfiguring, moderately traumatic, and not optimized. Primary neoadjuvant chemotherapy is usually given for locally advanced but operable breast cancer to reduce tumour size and facilitate breast conservation. Doxorubicin, which stops the growth of cancer cells by blocking topoisomerise 2, was the first chemotherapeutic drug to be introduced into clinical trials in 1967 and became the most effective agent against breast

cancer by the early 1970s [81, 82]. Anthracycline-based combinations with cyclophosphamide have since been the standard of care in both metastatic and adjuvant setting [83]. The introduction of taxanes: paclitaxel and docetaxel, which disrupt microtubule function thereby inhibiting cell division, represented a major milestone in the systemic therapy of breast cancer, showing activity similar to and sometimes exceeding that of the anthracyclines [84]. This was followed by the development of other cytotoxic agents that stop cell cycle progression such as vinorelbine [85] and other vinca alkaloids, gemcitabine [86], capecitabine [87], ixabepilone [88], and eribulin [89]. These agents are used for the management of metastatic breast cancers.

The planning of adjuvant postsurgical therapy is dictated by the pathology report, in which tumour biology is classified by histological grade, and ER, PR, and HER2 status. Since 80% of all breast cancers are ER+, tamoxifen, a selective ER modulator, remains the standard of care for premenopausal women [90] and aromatase inhibitors are generally used for postmenopausal women [91]. About 15% of breast cancers have amplification of the *HER2* gene, which carries a worse prognosis [92], but can often be effectively treated with the monoclonal anti-HER2 antibody called trastuzumab [93]. For *HER2*-amplified breast cancers, trastuzumab added to taxane therapy has improved overall survival in patients who have not received adjuvant trastuzumab [94]. Alternatively, lapatinib, a small kinase inhibitor of HER2 has also been used in combination with capecitabine [95]. Other monoclonal antibodies include Pertuzumab, which is given with trastuzumab and chemotherapy, either before surgery to treat early-stage or advanced disease and ado-trastuzumab emtansine, also known as TDM-1, which

is attached to a chemotherapy drug and used to treat advanced breast cancer in women who have already been treated with trastuzumab and chemotherapy [96].

However, in most patients with advanced local or metastatic disease, resistance to therapy is inevitable. In ER+ tumours, a combination of everolimus, an inhibitor of mammalian target of rapamycin (mTOR) with the aromatase inhibitor exemestane is currently being tested [97]. Palbociclib, ribociclib and abemaciclib are approved for post-menopausal women with advanced ER/PR+ HER2- breast cancer. These agents block cyclin-dependant kinases (CDKs) 4 and 6, and hence have been anticipated to stop breast cancer cells from dividing [98]. Bone metastases are found in 60-80% of patients with advanced disease [99] and brain metastases are common in patients with HER2+ disease, because trastuzumab cannot cross the blood-brain barrier [100]. Denosumab is used for bone metastasis that prevents the activation of osteoclast-mediated bone destruction [101], while whole brain radiotherapy is the standard treatment for multiple brain metastases and surgical debulking for solitary metastases [102].

Treatments currently in the pipeline include PI3K inhibitors such as the pan-PI3K inhibitor Buparlisib and the PI3Kα-selective inhibitor alpelisib [103] and immune checkpoint inhibitors that target the programmed death-1 (PD-1) receptor. PD-1 inhibitors (e.g., nivolumab and pembrolizumab) are currently being tested in phase II and III trials of metastatic TNBC, respectively [104]. Additional agents in different stages of clinical development include atezolizumab, avelumab and durvalumab that target programmed death ligand-1 (PD-L1), a T-cell inhibitory molecule [105].

1.6.1 Inadequacy of current treatment strategies

Surgery and radiation, although generally disfiguring and modestly traumatic, are reasonably effective for managing early stage breast cancers. However, this means that for many other patients, including most female carriers of mutations in *BRCA1*, *BRCA2* or *TP53* who develop breast cancer, curative treatments are not available. Historically, the introduction of new therapies has relied on clinical trials that are either initiated in patients with end-stage disease, or are focused on targeting abnormalities evident in dominant clones. It is therefore not surprising that resistance remains an important clinical challenge. Some patients do not respond to the targeted therapies they are given from the start, which is referred to as *de novo* resistance. In other patients, most of the malignant cells present may be killed in the short term, but then later (even after many years) relapses occur that are commonly refractory to the same treatments. This is often called "acquired" resistance, although it is most likely that unresponsive cells were already present as rare variants before the treatment was first applied. In addition, the effect of currently used treatments may be diminished or even prevented by the status of the tissue microenvironment of the malignant cells during the treatment.

1.7 Modulators of radiation response in human breast cells

Ionizing radiation produces both single and double-stranded DNA breaks that can cause chromosomal aberrations and genetic mutations, which may be lethal to the cell in which they occur usually when the cells attempt to divide. This may be due to direct action,

where the atoms of the target cell are ionized or excited. Alternately, it may be due to indirect action, where radiation may interact with other atoms or molecules in the cell, mostly water to produce free radicals that cause damage to nearby DNA. About two-thirds of the biological damage caused by X-rays are due to indirect action and can thus be modified by chemical protectors or sensitizers. In addition, ionizing radiation can activate an immediate apoptotic response in some cells [106].

Historically, radiation effects on human breast cancer cells have been studied in cell lines. A study that defined cancer-initiating cells as CD44+/CD24- used the breast cancer cell lines MCF-7 and MDA-MB231 and propagated them both as monolayer cultures and mammospheres. They showed that the cells in the primary mammospheres were more resistant than those in the monolayer to a single dose of radiation. Fractionated doses of radiation increased the activation of Notch-1 and the percentage of the cancer-initiating cells [107]. Another study showed that breast cancer cells with the tumorigenic CD44+/CD24- phenotype contained lower reactive oxygen species (ROS) levels than the other cell types [108].

The presence or absence of molecular oxygen has historically been found to dramatically influence the biological effects of X-rays. A highly efficient ROS scavenging system or generally low levels of ROS in cancer stem cells may contribute to their high resistance to ionizing radiation [108-110]. Some of the candidates that have been suggested to be responsible for resistance of cancer stem cells to radiation are Wnt and beta-catenin signaling [111]. Wnt and beta-catenin signaling has been linked to chromosomal instability through regulation of the mitotic spindle [112]. Additional candidates are Notch-1, the expression of which increased the radiation response of cells

in mammospheres [107]; *PTEN*, the loss of which altered *CHK1* localization and, led to genomic instability [113] and conferred radioresistance to glioblastoma cell lines [114]; *EGFR* that was shown to mediate radioresistance in glioma models [115, 116]; and *HIF-1*α which sensitized tumour cells to radiation through induction of ATP metabolism, proliferation and p53 activation [117].

There is, however, little information about how primary mammary cells respond to ionizing radiation. A previous study from our group compared the effect of increasing X-ray doses on the clonogenic activity of primary human mammary epithelial cells and observed that one fraction was more radioresistant compared to the other. This fraction also expressed higher levels of peroxidases that are capable of combating ROS [118].

1.8 Cell of origin and tumour-initiating cell concepts relevant to human breast cancer

A popular theory is that the different molecularly defined subgroups of breast cancer reflect their origin from corresponding cell types in the normal mammary gland [119]. However, this concept differs from the prevailing view of the multi-step origin of many acute myeloid leukemias (AMLs) and the observation that most breast cancers share a multiplicity of mutations that would likely be accrued very slowly over time in self-sustaining cell types in addition to those mutations indicative of subclonal diversification. Prevailing evidence suggests that the first driver mutations of future AML clones arise in hematopoietic stem cells where they then accrue additional mutations that ultimately establish a fully malignant, self-perpetuating leukemic stem cell state in clonal

derivatives. Thus, the AML clone may appear to be comprised of cells at later stages of differentiation; however, these cells are not self-perpetuating and rely on rarer subsets for the continued production of leukemic progeny (Figure 1.6). Some types of human breast cancer now appear to more closely resemble this AML-like model. However, confusion stems from the observation that while breast tumours that arise from human *BRCA1* mutant carriers have a distinctive basal-like morphology and gene expression profile, it has been suggested that these actually derive from an expanded population of LPs [120]. Similarly, deletion of *Brca1* in mouse luminal cells has been found to result in tumours with a basal-like phenotype [121]. Recent evidence also suggests that some breast cancer cells have unstable phenotypes [5, 122]. Thus, the phenotypes of breast cancer cells do not *a priori* offer reliable indicators neither of their growth properties, nor of the likely effectiveness of a proposed treatment beyond the detection of ER, PR or HER2. It has also been reported that in human breast cancers, as in normal human mammary tissue, only rare cells of a defined phenotype perpetuate the growth of the tumour in xenograft experiments [123]. However, this remains controversial as it has also been found that such cells may display phenotypic instability [124]. Interestingly, the genetic heterogeneity evident within tumours demonstrates that this must arise within cells that have clonogenic activity that may then be variably displayed in xenografted mice [28, 69]. Primary tumorigenic cells cannot currently be quantified *in vitro,* but *in vivo* this activity can be inferred from their contributions to tumour formation in highly immunodeficient xenotransplanted mice, hence the term “tumour-initiating cells” (TICs). It has been suggested that these TICs would display similar properties in xenograft assays as they would within the patients from which they were obtained, hence explaining the

current interest in the use of this methodology to investigate treatment sensitivities of patients' cells [125]. Nevertheless, whether such assays detect all cells important to be eliminated to achieve complete remission is not yet clear and remains a caveat of this approach.

1. 9 *De novo* models of human tumorigenesis

Experimental models of *de novo* tumorigenesis starting from cells isolated directly from normal human tissues are attractive because they circumvent the caveats inherent in extrapolating from immortalized cell line data, necessarily incomplete retrospective studies, or species differences (Figure 1.7). However, the frequency of success has thus far been very limited, perhaps due to a historic lag in the development of appropriate methods to isolate the relevant target cells in viable form, and/or to transduce them at an adequate efficiency with the appropriate combination of genetic alterations. Indeed, where these issues have been carefully addressed, some models have been generated (Table 1). For example, normal human basal prostate cells transduced with a combination of vectors encoding cDNAs for *AKT*, *ERG*, and the androgen receptor have been found to produce tumours when transplanted in immunodeficient mice [126]. In contrast, in the same study, transplants of co-isolated luminal prostate cells transduced with the same vectors did not yield tumours. This result is interesting because the gene expression profile of prostate cancers appears closer to that of the luminal cells of the normal prostate. One explanation is that prostate cancers in which these genes are characteristically altered actually originate in basal cells that then generate progeny with

luminal features [126]. Alternatively, it may be argued that a malignant phenotype can originate *in vivo* directly in luminal cells but the conditions used to date simply fail to support this process experimentally.

De novo models of tumorigenesis starting from primary human cells have also now been reported for colon and mammary cells. For example, a recent study demonstrated the formation of tumours in immunodeficient mice transplanted with organoids expanded *in vitro* from colon cells genetically edited by CRISPR/Cas9 to generate suppressive mutations in *APC*, *SMAD4* and *TP53* and activating mutations in *KRAS* and *PIK3CA* [127]. *De novo* genesis of human breast tumours has also now been achieved in immunodeficient mice transplanted with primary isolates of normal cells transduced with *p53(R175H)*, *CCND1*, *PIK3CA*, and *KRAS(G12V)* [128], *SV40* plus *KRAS(G12V)*[129], and more recently with just *KRAS(G12D)* alone [130]. However, in contrast to the results described for the prostate model, immunohistological analyses of these human breast tumours have indicated the presence of a mixture of phenotypes, possibly related to the polyclonal composition of the tumours generated [130]. The robustness of these models and speed of the tumorigenesis observed in at least some cases should make them useful for future elucidation of the minimal cellular and extrinsic factors required for their generation.

Examples of *de novo* leukemogenesis using primitive ($CD34^+$) subsets of hematopoietic cells isolated from human cord blood are also accruing. In this case, examples of genes whose vector-mediated forced overexpression in normal cells have produced overt leukemic populations in immunodeficient mice include cDNAs for *MLL-AF9* [35, 131], *MLL-AF4* [132], *MN1* plus *NUP98HOXD13* [133], *BCR-ABL* plus a

dominant-negative form of *IKAROS [134]*, and *MYC* plus *BCL* [135]. The Mixed Lineage Leukemia (*MLL*) gene is rearranged and fuses with multiple partner genes in both spontaneously arising human AML and acute lymphoid leukemia (ALL), but the *MLL-AF9* fusion oncogene is associated almost exclusively with AML in humans [131]. Interestingly, overexpression of *MLL-AF9* in normal human cord blood cells produced ALL in transplanted Non-obese diabetic-*Scid* (NOD-SCID) hosts, but AML in the same mice engineered to express three human growth factors. This result illustrates the ability of external factors to dictate the phenotype of the malignant cells produced and further underscores the fallacy in assuming that the predominant cell type necessarily reflects the cell of origin or the specific oncogene driving the tumorigenic state. The *MN1-NUP98HOXD13* model also serves to illustrate the difference between effects obtained in analogous mouse and human target cells. In mouse cells, *MN1* alone was sufficient to induce a myeloid leukemia, whereas in human cord blood cells, it induced only a transient myeloproliferation. Only when an activated *HOX* gene (i.e., *NUP98HOXD13*), was also introduced was a serially transplantable AML obtained in the human cells.

These studies demonstrate some of the unique aspects of tumorigenesis in primary human cells that are not well predicted by mouse models. They also provide examples of experimentally generated *de novo* human tumours whose characteristics are heavily influenced by factors beyond the cell of origin, or the genetic alterations used.

1.10 Characterizing the functional diversity of subclones within human tumours

Most studies attempting to analyze the sub-clonal diversity of malignant human populations that arise in patients have relied on retrospective inferences derived from genomic or phenotypic characterization of primary samples and/or changes incurred in serial transplants of these cells in immunodeficient mice [69, 136-140]. However, these approaches generally do not allow the frequency of clonogenic cells to be quantified, or their genomic or phenotypic properties to be defined. These are important parameters because the genomic instability of many established neoplastic human populations can produce genetic alterations that are irrelevant to the continued growth of the tumour. Examples of such mutations have been well documented in genetic analyses of the leukemic cells from patients with chronic phase chronic myeloid leukemia (CML) [141].

LDA and vector-based tracking of clonogenic cells offer powerful approaches to quantify malignant cells with proliferative potential *in vivo*. The LDA approach has been extensively applied to a number of primary human tumour types that can engraft immunodeficient mice. These include malignant populations that arise in the human brain [142, 143], colon [144, 145], prostate [146], breast [123], ovary [147], skin [148, 149] and the hematopoietic system [150-154]. Coupling these approaches to prospectively isolated phenotypes of cells within the transplanted populations has been the basis of identifying the subset(s) of cells actually possessing the tumorigenic activity detected in the recipients. However, in order to exploit this approach to characterize the clonal growth properties of *single* tumorigenic cells, the transplants must be initiated with cell numbers that produce tumours at a frequency of less than one in three mice. The large

numbers of mice required to obtain clonal data can thus rapidly become prohibitively expensive, if not impractical, particularly when clonal outputs may vary quantitatively as well as phenotypically and dynamically within and between different primary tumours being assessed. The use of vector insert analysis to identify clones based on their semi-random integration sites [21] circumvents many of the limitations of LDA approaches and an even more powerful approach is afforded by the use of DNA-barcoded lentiviral vector libraries [155].

1.11 Thesis objectives

Breast cancer treatment failures are thought to be due to the inability to eradicate all tumour cells. However, very little is known about the sensitivity of either normal or primary malignant human mammary cells to current therapies, including radiation which is the most commonly used modality for local control. In the emerging era of "personalized medicine", a possible solution would be to develop a large-scale system for quantifying the response of individual human mammary tumour cells with the capacity to proliferate to candidate treatments. Given the extensive use of radiation in breast cancer therapy and the surprising lack of information about normal or malignant human mammary cell sensitivity to ionizing radiation, I chose this modality to serve as the primary test treatment to investigate.

Since tumours typically retain many features of their tissue of origin, I first sought to determine the baseline sensitivities of clonogenic cells from both normal human LP and BC fractions and potential mechanisms that might explain any sensitivity-related

properties thus revealed. These results were then used as a baseline to compare with the radiation sensitivities of various sources of malignant clonogenic human mammary cells (both cell lines and primary cells) and determine if and how those derived from LPs and BCs might differ from the normal cells from which they were derived. For this, I took advantage of a novel *de novo* model of breast tumorigenesis that offers the unique opportunity to study the acquisition of changes in treatment response in different types of normal human mammary cells before, during and after transformation with a single, defined oncogenic perturbation (forced expression of $KRAS^{G12D}$, [130]). The results of these experiments are presented in Chapter 2.

I was then interested to determine how the above findings might predict the responses of TICs defined by an *in vivo* assay. However, this necessitated a first analysis of how to quantitate these in a meaningful manner. At the time, other members of our lab had just discovered from DNA barcoding analyses of serially propagated tumours produced in xenografted immunodeficient mice that the number of clones produced was *inversely* related to the number of cells transplanted for widely used sizes of input innocula [28]. Therefore, before using a TIC assay to examine radiation responses of TICs, I first undertook experiments to establish a quantitative *in vivo* assay for cells with this property of inverse relationship. Chapter 3 reports the design and results of those experiments.

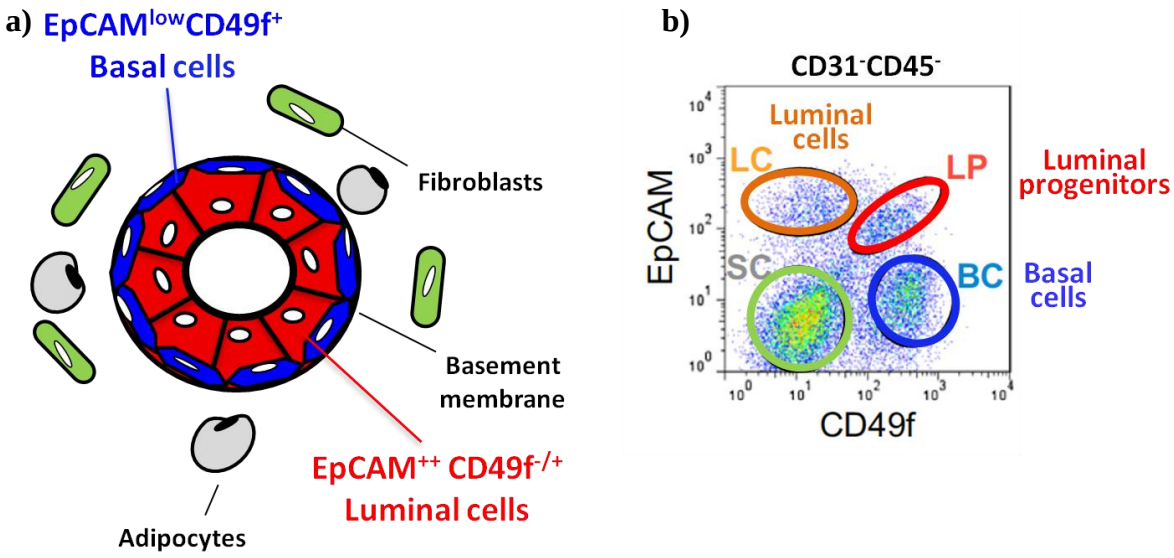

Figure 1.1: Cellular make-up of the normal adult human female breast.

a) Schematic of the bilayered structure of the adult human mammary gland showing the cells of the outer basal layer in blue and the inner luminal layer in red. b) Representative FACS plot showing the different populations of cells within the mammary gland based on their surface expression of CD49f and EpCAM. Basal cells (BCs) express EpCAM^{lo}CD49f^{+}, while the luminal fraction can be further subdivided into those with clonogenic activity (LPs) expressing EpCAM^{+}CD49f^{lo} and a more mature compartment of cells (LCs) expressing EpCAM^{+}CD49f^{-}. Stromal cells (SCs) are EpCAM^{-}CD49f^{-}.

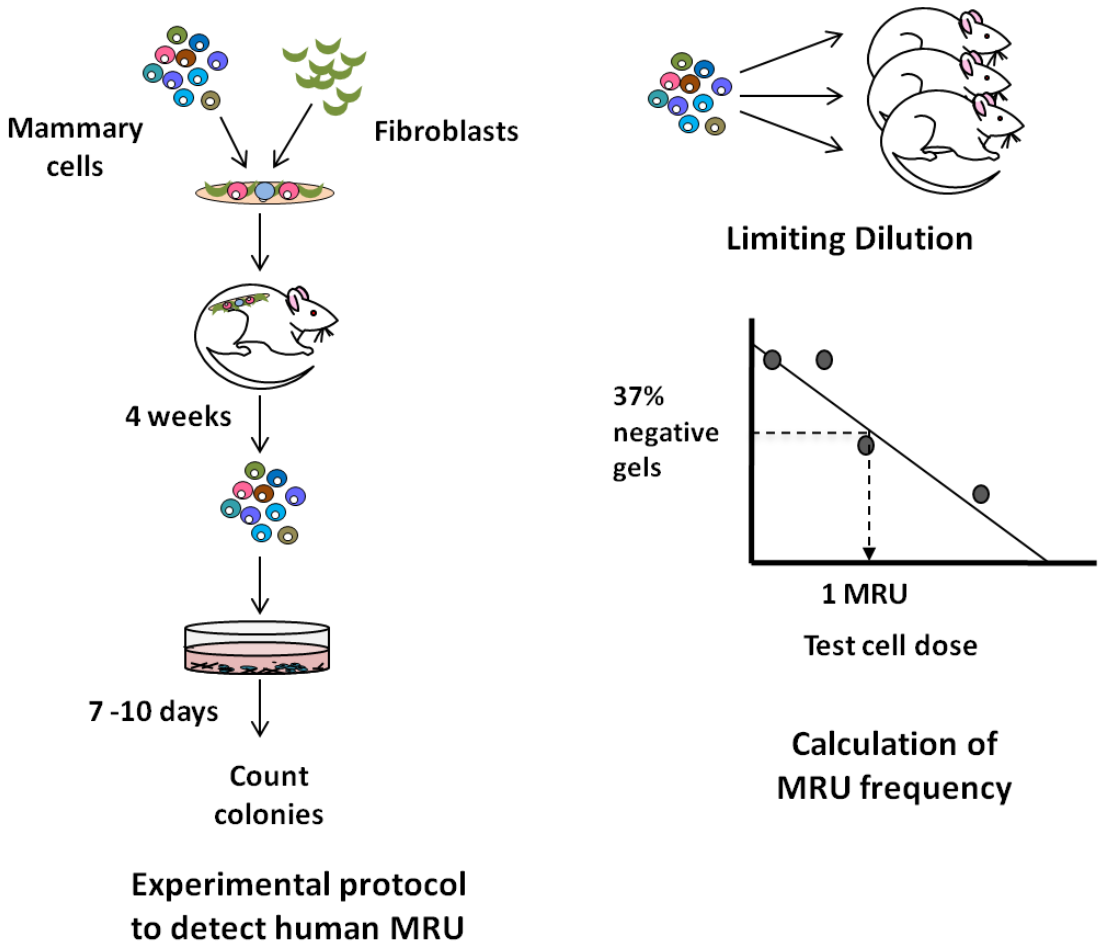

Figure 1.2: LDA to quantify Mammary Repopulating Units (MRUs).

Shown is a depiction of the human MRU assay. Human mammary epithelial cells in suspension are embedded in a solid collagen gel along with irradiated C3H-10T1/2 mouse embryonic fibroblasts and then then transplanted under the renal capsule of immunodeficient mice. After 4 weeks the gels are retrieved, digested with collagenase, the cells dissociated into a single cell suspension, and plated into a 2D tissue culture plate to measure the CFC content. The number of regenerated CFCs was shown to be a linear function of the number of input cells, and can thus be used to calculate the input MRU frequency [2, 17].

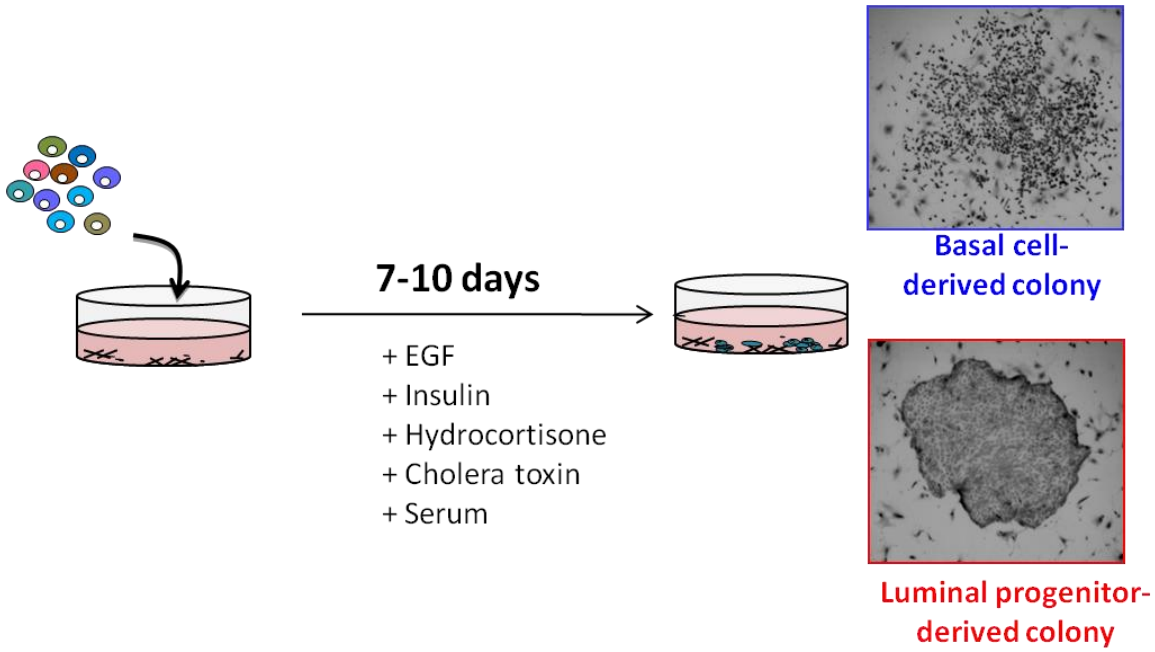

Figure 1.3: *In vitro* 2D CFC assay for mammary cells with proliferative ability. Cells are dissociated into single-cell suspension and plated at a sufficiently low density for individual colonies to be scored as non-overlapping entities in tissue culture plates preloaded with irradiated mouse NIH-3T3 fibroblasts. Purified mammary cells are cultured in medium supplemented with EGF, insulin, hydrocortisone, cholera toxin and 5% fetal bovine serum (FBS) for 7 to 10 days at 37ºC. At the end of the assay, the plates are fixed, stained with Giemsa and colonies are then scored using an inverted microscope. Images on the right show typical colonies derived from BCs and LPs.

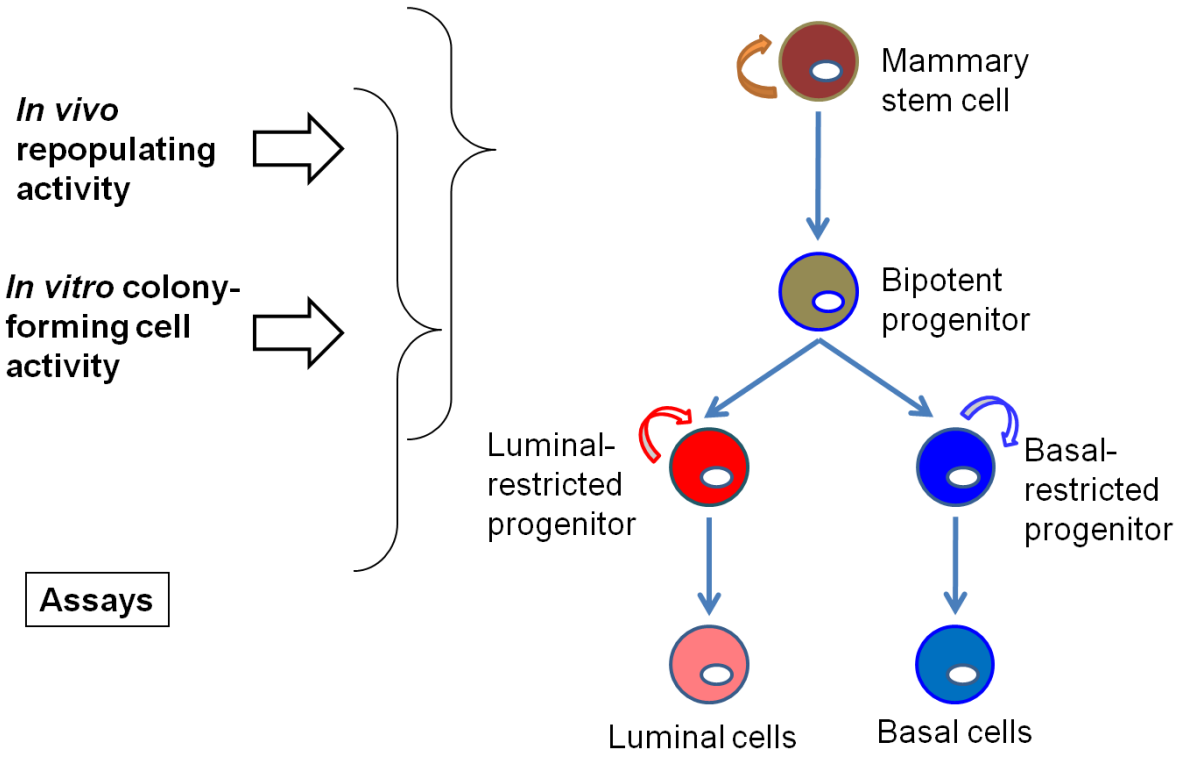

Figure 1.4: Mammary epithelial cell differentiation hierarchy.

Shown above is a simplified model of the mammary epithelial cell differentiation hierarchy in humans. However, accruing evidence suggests that this hierarchy may not be rigidly adhered to and cells may show variable levels of uncoordinated changes. Lineage unrestricted as well as lineage-restricted cells can be studied by their potential to make colonies in *in vitro* assays. Mammary stem cells defined by an ability to regenerate complete gland structures containing CFCs *in vivo*, hence the term "mammary repopulating unit" or MRU to identify the cells thus detected.

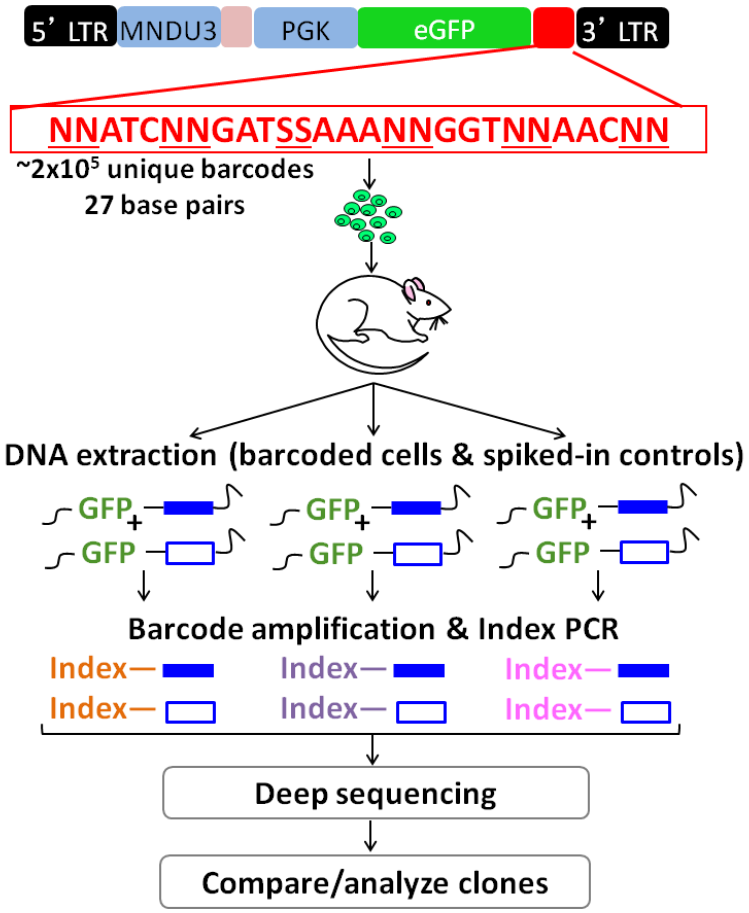

Figure 1.5: Schematic representation of the use of DNA barcoding in clonal tracking experiments.

Cells are transduced at a limiting infection frequency with a library of lentiviral vectors each of which contain a unique DNA barcode and expresses GFP. The cells are then transplanted into immunodeficient mice for a required period of time (4-8 weeks), after which the progeny are harvested and DNA extracted. This is followed by barcode amplification by Index PCR and deep sequencing to generate data for the number, size and composition of each clone, depending on the markers used for their isolation. Spiked-in controls consisting of known numbers of cells are used as an internal calibration for normalization and clone size calculations. This method allows for the detection of barcoded clones with high sensitivity, specificity and reproducibility.

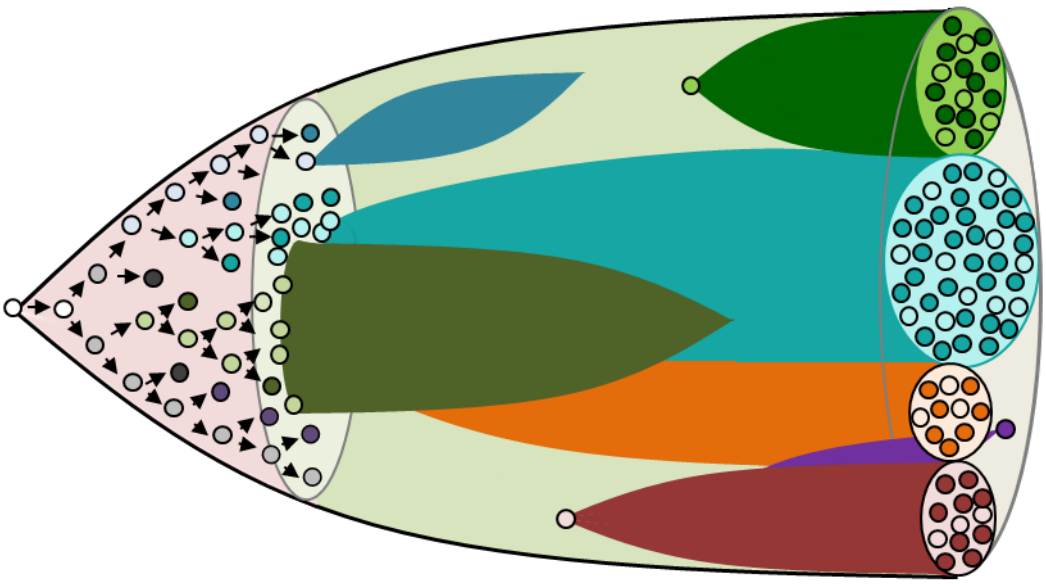

Figure 1.6: Schematic depiction of subclonal evolution and diversification of cell types in developing malignant populations.

In this diagram, subclones identified by accumulating genetic changes are shown by different colours. Cells within each clone that have proliferative potential are shown as pale cells in contrast to some of their progeny that can no longer divide and are shown as dark cells. This illustrates the diversification of biological properties that occurs both within and between subclones, with some clones being transient, whereas others are persistent but variably expanding.

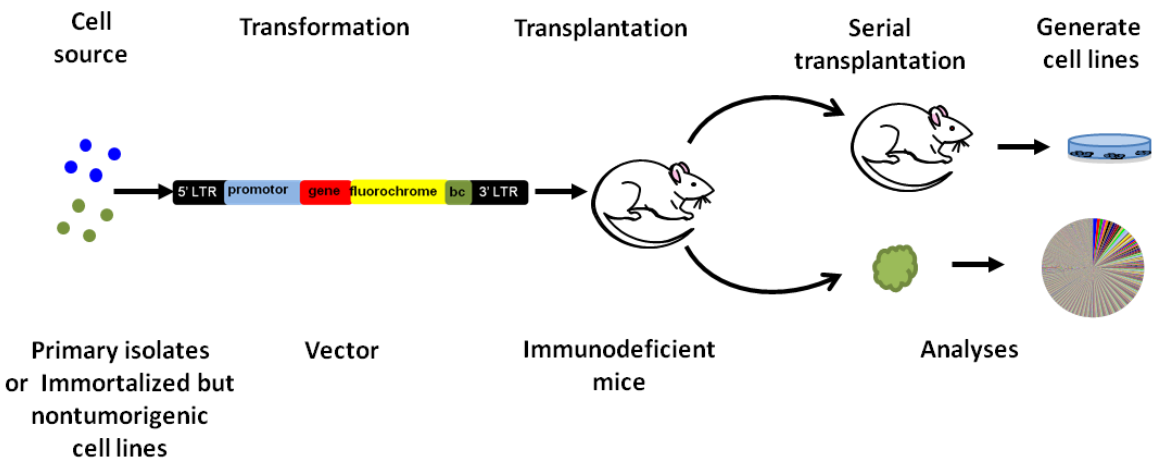

Figure 1.7: *De novo* generation of tumours from genetically manipulated "normal" human mammary cells.

Most examples of successful transformation of primary sources of normal human cells (or non-tumorigenic human cell lines) have used retro- or lentiviruses encoding one or more oncogenes and a fluorochrome (e.g., GFP) to enable transduced cells to be later isolated and characterized. The transduced cells are then transplanted into a receptive site in immunodeficient mice. When a tumour forms, the cells can then be removed for morphological, immunohistochemical, flow cytometric and/or various molecular and clonal analyses. When this method is efficient, polyclonal tumours may be generated (as illustrated by the pie chart). Retrieved viable cells can also be further transplanted in secondary hosts or used to generate cell lines.

Table 1.1: Examples of *de novo* tumour models from primary sources of human cells

Human Tissue	Gene	Finding	Ref
Prostate	*AKT, ERG, AR*	Tumour formation in basal cells but not in luminal cells.	[126]
Colon	*APC, SMAD4, TP53, KRAS, PIK3CA*	Organoids engineered to express all five mutations grew independently of niche factors *in vitro*, and could be transplanted to form tumours in mice.	[127]
Mammary	*SV40 large-T hTERT HRAS(V12)*	Transformed cells showed presence of c-myc and made tumours efficiently with the addition of Matrigel or fibroblasts demonstrating an influence of stromal cells on tumorigenecity.	[156]
	ERα, BMI1, MYC, TERT	Transformed cells expanded *in vitro* in an estrogen-dependent manner and transplantation generated ERα-positive tumours that metastasize to multiple organs.	[157]
	p53(R175H), CCND1, PIK3CA, & *KRAS(G12V)*	Cells with mutant BRCA1 form tumours and showed increased basal differentiation compared to cells from non-carrier tissues. EpCAM+CD10- luminal cells from both BRCA1+/+ and BRCA1mut/+ tissues were enriched for tumour- forming ability.	[128]
	SV40 & *KRAS(G12V)*	Transformation of EpCAM+ cells yielded common forms of breast cancer, including ER+ and ER- tumours with luminal and basal-like characteristics, respectively. Transformation of CD10+ (basal) cells yielded rare metaplastic tumours similar to the claudin-low subtype.	[129]
	KRAS(G12D)	Both basal and luminal cells generated polyclonal serial transplantable tumours containing mixed phenotypes and clones with variable growth dynamics revealed in serial transplants.	[130]
Blood	*MLL-AF9*	Some leukemia stem cells were multi-potent and could be lineage directed by altering either the growth factors or the recipient strain of mouse, highlighting the importance of the microenvironment. Others were strictly lineage committed, demonstrating the heterogeneity of the stem cell compartment in the MLL diseases produced.	[35, 131]
	MLL-AF4	Generation of a model of t(4;11) pro-B ALL that fully recapitulated the immunophenotypic and molecular features of the disease that appears in patients.	[132]
	MN1 and *NUP98HOXD 13*	Co-transduction of an activated HOX gene (NUP98HOXD13) with MN1 induced a serially transplantable AML.	[133]
	BCR-ABL1 & dnIKAROS (IK6)	An aggressive AML with disseminated myeloid sarcomas developed within 4 weeks following transplantation of cord blood cells transduced with both genes.	[134]
	MYC & *BCL*2	A model of lymphoma that recapitulated the histopathological and clinical aspects of steroid-, chemotherapy- and rituximab-resistant human “double-hit” MYC-BCL2 lymphoma.	[135]
	DEK-NUP214	A human cell AML with phenotypic characteristics of a t(6;9) disease and CD45+CD13+CD34+CD38+ immunophenotype.	[158]
	ZMYM2-FGFR1	Development of myeloproliferative disease that progressed to AML. Mice showed hepatospenomegaly, hypercellular bone marrow and a CD45+CD34+CD13+ immunophenotype.	[159]

Chapter 2: Analysis of the intrinsic sensitivity of normal and transformed human mammary clonogenic cells to ionizing radiation

2.1. Introduction

Normal human LPs and BCs have many different phenotypic, metabolic, as well as growth properties. Human LPs display more limited proliferative activity and generate only luminal progeny, whereas BCs include cells that can display full gland regenerative activity *in vivo* and bilineage differentiation activity *in vitro*. Interestingly, invasive tumours are generated rapidly and efficiently in immunodeficient mice transplanted with either LPs or BCs transduced with a $KRAS^{G12D}$–encoding lentiviral vector [130]. Since the properties of the clonogenic cells in breast cancers may be influenced in part by the cell type from which they have arisen, as well as the mutations they acquire, it may be important to understand the mechanisms that control normal mammary cells to treatments relevant to breast cancer as well as those caused by specific mutations. Thus the ability to control the "cell-of-origin" of tumours by creating tumours *de novo* starting from a defined population of cells using a single defined oncogene, offers an attractive model to interrogate this idea.

Radiotherapy is used as adjuvant therapy alongside surgery for breast cancers that are thought to be localized to the breast and in advanced cases to treat brain metastasis in breast cancer patients. Interestingly, while we may now have well developed methods to isolate, assay and manipulate different subsets of normal human mammary cells, not

much is known about their responses to ionizing radiation. In many cells, treatments like ionizing radiation that damage DNA, activate cell cycle checkpoints to delay cell cycle progression and allow repair of the damage. Other mechanisms lead to cell death, such as apoptosis and necrosis, or pro-survival, such as autophagy while additionally inducing cell cycle arrest or senescence. When repair of the DNA lesions is complete, the signal(s) caused by the recognition of DNA damage are no longer produced, and cell cycle progression is resumed. Another process whereby re-entry into the cell cycle can occur in the presence of *unrepaired* damage (called checkpoint adaptation) has been studied in *Saccharomyces cerevisiae* and *Xenopus*. This process was originally defined in *S. cerevisiae* as the ability to divide in the presence of irreparable DNA breaks [160-162]. When exposed to an extra chromosome lacking telomeres, or an irreparable endonucleolytic DNA double-strand break, *S. cerevisiae* cells first entered a G_2M arrest. However, this G_2M arrest was not maintained and cells eventually resumed progression through the cell cycle [160, 161]. A similar process was described in *Xenopus* eggs where treatment with aphidicolin, a replication inhibitor, caused an initial checkpoint arrest in S phase, but later the eggs were able to enter mitosis despite the presence of incompletely replicated DNA [162].

Many checkpoint responses are conserved from yeast to mammals, and in 2006 it was confirmed that checkpoint adaptation also occurs in human cells exposed to ionizing radiation [163]. This study showed that upon exposure to ionizing radiation, human U2OS osteosarcoma cells undergo an extended G_2 arrest and adaptation to the G_2 checkpoint required Plk1 kinase [163]. Evidence of checkpoint adaptation has also been suggested to occur in lymphocytic leukemia [164], colon carcinoma [165], hepatocellular

carcinoma [166], normal human fibroblast [164] and colorectal adenocarcinoma cell lines [165]. However, evidence of checkpoint adaptation in primary human mammary cells has not been previously reported.

To investigate innate properties of BCs and LPs that may contribute to differential radiation sensitivities of their CFCs, experiments were designed to examine a model (Figure 2.1) in which radiosensitivities can be predicted by γH2AX foci formation, the early apoptotic response, the ability to repair sublethal damage, and the expression of repair proteins and other elements that affect radiosensitivity. The results show some coherence with this model but also some examples that do not fit, as discussed below.

2.2 Materials and Methods

2.2.1 Generation of viable single cell suspensions from human breast tissue samples

Discard tissue from reduction mammoplasty surgeries was obtained with informed consent, and used according to protocols approved by the University of British Columbia Research Ethics Board. The tissue was minced with scalpels and dissociated overnight for ~18 hours at 37ºC in Dulbecco's Minimal Essential Media (DMEM)/Ham's F12 media (1:1, STEMCELL Technologies) supplemented with 2% bovine serum albumin (BSA, Gibco), 300 U/ml collagenase (Sigma) and 100 U/ml hyaluronidase (Sigma). "A" pellets, rich in mammary epithelial organoids were obtained by an initial centrifugation at 80 g for 4 minutes. "A" pellets were cryopreserved at -180ºC in fetal bovine serum (FBS, STEMCELL Technologies) containing 6% dimethylsulfoxide (DMSO). Prior to use, vials of cryopreserved "A" pellets were thawed and rinsed with Hank's Balanced Salt Solution

supplemented with 2% FBS (referred to as HF). The cells were then enzymatically dissociated in 2.5 mg/ml trypsin with 1 mM EDTA (STEMCELL Technologies) and 5 mg/ml dispase (STEMCELL Technologies) with 100 µg/ml DNase I (Sigma), with washing of the cells in HF between each step. The resulting cell suspension was passed through a 40 µm mesh to obtain a single-cell suspension.

2.2.2 Flow cytometry to separate cell subsets

Mammary cells were depleted of hematopoietic and endothelial cells using antibodies to CD45 (Pacific Blue, Clone HI30, BioLegend) and CD31 (Pacific Blue, Clone WM59, BioLegend), respectively. Cells were also exposed to 4', 6-diamidino-2-phenylindole (DAPI) to eliminate dead (DAPI+) cells. Anti-EpCAM phycoerythrin (PE) (Clone 9C4, BioLegend) and anti-CD49f allophycocyanin (APC) (R&D Systems) were used to isolate the BC and LP fractions free of mature luminal cells and stromal cells. BCs were isolated according to their $EpCAM^{low/-}CD49f^{+}$ phenotype and LPs were isolated according to their $EpCAM^{high}CD49f^{+}$ phenotype. FACS was performed using a FACSAria III or Fusion cell sorter (BD Biosciences).

2.2.3 Irradiation of cells for viability assays

Cells were irradiated in suspension in HF at a concentration of 10^6 cells/ml at room temperature in a total volume of ~100 µl using an X-ray irradiator, X-RAD 320 from Precision X-ray. Doses used ranged from 1 Gy to 8 Gy with programs set at 300kV (volts) and 10mA (amp).

2.2.4 2D *in vitro* CFC assay

Mammary cells and irradiated NIH-3T3 fibroblasts were co-cultured for 7-10 days in SF-7 media supplemented with 5% FBS. SF-7 medium consists of 1:1 DMEM/F12 (STEMCELL Technologies) supplemented with 0.5 µg/ml hydrocortisone (Sigma), 1 µg/ml insulin (Sigma), 10 ng/ml EGF (Sigma), and 10 ng/ml cholera toxin (Sigma) as previously described [2].

2.2.5 H2AX assay

Cells were seeded on collagen-coated 8-well chamber slides and the next day, irradiated with 1 Gy X-rays. After varying times, the wells were washed with phosphate buffered saline (PBS), and a solution of 2% paraformaldehyde and 0.2% Triton X-100 in PBS was added for 20 minutes. After 3 washes with PBS, 0.5% Nonidet P40 (NP40, Merck) was added for another 20 minutes at room temperature, followed by 3 more washes with PBS. A blocking solution of 2% BSA and 1% rabbit serum (Sigma) was then added for 1 hour, and then replaced with an anti-phospho-histone H2A.X (Ser139) antibody (clone JBW301, Merck Millipore) and the slides were subsequently incubated in the dark, overnight at 4ºC, on a rocker. The next day, the antibody was removed and cells were washed with a solution of 0.5% BSA and 0.175% Tween 20 in PBS for 5 minutes, repeatedly 3 times. The cells were finally washed with DAPI (1:50) for 1 minute followed by washes with PBS and fixed in Vectashield (Vector Laboratories Inc.), covered with a cover slip that was then sealed with clear nail polish.

2.2.6 Apoptosis assay

Cells were analyzed after being stained with Annexin V-fluorescein isothiocyanate (FITC) (Cat: 640906, BioLegend) and 1 mg/ml Propidium Iodide (PI, Sigma) to distinguish different stages of apoptosis and death according to their positivity for Annexin V only, both Annexin V and PI or PI only.

2.2.7 Cell cycle analysis

Cells were washed with cold PBS and fixed by vortexing in ice-cold 70% ethanol. After another hour on ice, fixed cells were left overnight at -20ºC. The next day, cells were centrifuged at 1,500 revolutions per minute (rpm) for 10 minutes at 4ºC and the supernatant gently aspirated. Cells were then re-suspended in a solution of 1 mg/ml PI and 10 mg/ml DNase-free RNase in PBS and incubated at 37ºC for 30 minutes prior to FACS analysis.

2.2.8 Western blot analysis

Radioimmunoprecipitation (RIPA) buffer was prepared using the following recipe: 10 mM Tris-Cl (pH 8.0, Sigma), 1 mM Ethylenediaminetetraacetic acid (EDTA, Life Technologies), 0.5 mM ethylene glycol-bis(β-aminoethyl ether)-N,N,N',N'-tetraacetic acid (EGTA, Sigma), 1% Triton X-100 (Sigma), 0.1% sodium deoxycholate (Sigma) , 0.1% sodium dodecyl sulfate (SDS, Life Technologies), 140 mM Sodium Chloride (NaCl, Sigma) and 1 mM Phenylmethylsulfonyl fluoride (PMSF, Sigma). Frozen samples were resuspended in RIPA buffer supplemented with 1 µl PIC, 1 µl of 1M sodium fluoride and 1 µl of 1M sodium orthovanadate, incubated on ice and centrifuged at

10,000 rpm for 10 minutes. In a 96-well plate, samples were mixed with Bradford solution (BioRad) and incubated at room temperature for 5 minutes. Samples were next mixed with loading dye (Invitrogen), vortexed and boiled at 95ºC for 5 minutes. Samples were loaded with DNA ladder (Thermo Fisher Scientific) and run at 200 V for 40 minutes. A polyvinylidene fluoride (PVDF) membrane was activated by washing in methanol, double distilled water and stored in transfer solution containing methanol, double distilled water and transfer buffer. Gel and membrane were sandwiched, topped with transfer buffer and run at 30 V for 3 hours. Ponceau S staining was used to visualize proteins. The membrane was blocked in 5% BSA for 30 minutes and incubated with primary anti-phospho-PLK1 (Thr210) antibody (Cell Signaling, 5472, generously provided by Dr. Helen Chen, Maxwell lab, BC Children's Hospital Research Institute) overnight at 4°C. The membrane was then washed with tris-buffered saline with polysorbate 20 (TBST) and incubated with a secondary antibody (mouse anti-rabbit, IgG-horseradish peroxidase, Santa Cruz Biotechnology) for 1 hour. Following further washing with TBST, the membrane was visualized using a ChemiDoc Gel Imaging system (Bio-rad). Data was quantified using ImageJ.

2.2.9 Cell lines

MDA-MB231 and MCF-10A cells were obtained from ATCC (#HTB 26 and #CRL-10317) and maintained as cultures of adherent cells in DMEM/F12 + 10% FBS for MDA-MB231 and DMEM/F12 + 5% horse serum (STEMCELL Technologies), 20 µg/ml EGF, 5 µg/ml hydrocortisone, 100 ng/ml cholera toxin, 1 mg/ml insulin (all from Sigma) and 1 mg/ml penicillin-streptomycin (Life Technologies) for MCF-10A. SUM149 was

obtained from Sandra Dunn's lab at BC Children's Hospital and maintained as cultures of adherent cells in DMEM/F12 + 5% FBS (STEMCELL Technologies) supplemented with 5 µg/ml insulin, and 1 µg/ml hydrocortisone (both from Sigma).

2.2.10 Lentiviral vectors

Two lentiviruses were used: a MNDU3-PGK-mCherry-KRAS^{G12D} vector, which is a variation of the MNDU3-PGK-GFP construct containing a KRAS cDNA altered by site-directed mutagenesis to obtain the G12D mutant as previously described [130] and a MNDU3-PGK-YFP-CBR-Luc virus encoding YFP in place of GFP and a Click Beetle Red Luciferase cDNA.

2.2.11 Transduction protocol

Cells were incubated in suspension at a concentration of $<10^6$ cells in 100 µl of SF-7 media supplemented with 5% FBS and $\sim10^6$ infectious units of virus and incubated at 37ºC for 4 hours to achieve ~50-70% transduction efficiency, and then washed twice with HF prior to being used for any subsequent experimental procedure.

2.2.12 Mice

Highly immunodeficient adult virgin female NRG (NOD/*Rag1*$^{-/-}$*IL2rγc*$^{-/-}$) mice, 8-12 weeks old, were used for all experiments according to procedures that had been approved by the Animal Care Committee of the University of British Columbia.

2.2.13 Transplantation of human cells into mice

Cells were transplanted subcutaneously on the back of highly immunocompromised NRG mice, together with 50 µl of Matrigel (Corning/BD Biosciences).

2.2.14 Generation of *de novo* tumours and isolation of cells from *de novo* tumours

Freshly isolated BCs and LPs were transduced simultaneously with one or more lentiviral vectors and injected into NRG female mice. Eight weeks later, mice were euthanized and tumours harvested, minced with scalpels, dissociated in DMEM/F12 supplemented with 5% FBS, 300 U/ml collagenase (Sigma) and 100 U/ml hyaluronidase (Sigma) and 1% penicillin-streptomycin and incubated at 37ºC for 1-2 hours with intermittent vortexing every 20 minutes. After washing with HF, tumour tissue was further enzymatically dissociated using trypsin and dispase and then stained with anti-human CD298 APC (Clone LNH-94, BioLegend) and anti- human EpCAM PE-Cy7 (Clone 9C4, BioLegend) and DAPI. Human cells with phenotype $CD298^{+}EpCAM^{+}$ were isolated by FACS using a FACSAria III or Fusion cell sorter (BD Biosciences).

Secondary and quaternary cell lines derived from primary *de novo* tumours initiated from BCs were kindly provided by Dr. Sylvain Lefort in the Eaves' lab and cultured in SF-7.

2.2.15 Statistics

All reported p-values were calculated using the parametric unpaired Student's t-test. Values shown on plots with a log scale on the Y-axis are geometric means ± standard

error of the mean (SEM), and those shown on plots with a linear scale on the Y-axis are arithmetic means ± SEM.

2.3 Results

2.3.1 Normal human clonogenic LPs are more resistant to X-rays than matched isolates of clonogenic BCs

To examine the X-radiosensitivity of the two types of CFCs identified in freshly isolated normal human mammary tissue, FACS-purified BCs and LPs were irradiated with different doses and their CFC activity immediately determined. The results showed that LP CFCs are ~1.5-fold more resistant to X-irradiation than BC CFCs ($p=0.0005$ and 0.0003 at 3Gy and 4Gy, respectively, Figure 2.2). This is in accordance with previous data in our lab obtained from studies of similarly irradiated un-separated normal human mammary cells CFC activity scored on the basis of the phenotype of the colonies generated [118].

2.3.2 LPs show more damage after radiation as seen by the presence of γH2AX foci

To assess the damage caused, induced foci of H2AX phosphorylation were measured as an indicator of DNA double strand breaks in FACS purified BCs and LPs from 15 minutes up to 24 hours after being X-irradiated at 1 Gy. Control cells were sham irradiated and fixed after 60 minutes. Both irradiated BCs and LPs showed an increase in γH2AX foci compared to their control counterparts that was most pronounced at the

earliest time point examined (15 minutes) and then declined slowly over the ensuing hour ($p=<0.0001$ for all time points for BCs, except at 24 hours when $p=0.034$, and $p=<0.0001$ for all time points for LPs). However, the number of foci was significantly higher in the LPs at 15 minutes post radiation compared to BCs ($p=0.0004$, Figure 2.3).

2.3.3 X-irradiation initially produces more early apoptotic LPs than BCs but a lower proportion of late apoptotic cells

To obtain baseline values, freshly isolated BCs and LPs were cultured for 2 days in SF-7 medium and then sorted for Annexin-V-negative cells. The cells were then harvested 1, 24 or 48 hours later, fixed and analyzed by FACS as described (Figure 2.4). LPs showed a higher proportion of overall apoptotic cells although the total number of dying cells as defined by the fraction of input cells that were $Annexin^{+}PI^{+}$ was higher in the BC fraction (Figure 2.5). However, when early and late apoptotic fractions were analyzed separately, the LPs had the highest yield of $Annexin^{+}PI^{-}$ (pre-apoptotic) cells and BCs contained more $Annexin^{-}PI^{+}$ (late apoptotic) cells. In cells examined in parallel after being exposed to 4 Gy X-rays, these ratios were similar but the representation (and yield) of cells in the apoptotic compartment increased for both BCs and LPs.

2.3.4 LPs show a greater number of irradiated cells arrested in G_2 compared to BCs

To determine whether LPs and BCs might differ in the ability of X-irradiation to arrest their progression through the cell cycle, freshly isolated cells were first cultured for 2

days to stimulate their proliferation, then irradiated at 4 Gy and then fixed and stained with PI 1, 24 or 48 hours later. Control cells were sham irradiated and fixed similarly at all 3 time points. FACS analysis of their DNA content showed both subsets were not fully cycling until 36 hours after first being placed *in vitro* (24 hours after being sham irradiated). In parallel, an increased accumulation of the irradiated LPs in G_2 was observed (p=0.0247) that had resolved by 48 hours. In contrast, there was no evidence of a corresponding G_2 arrest by the irradiated BCs. Interestingly the proportion of cell in S phase was also greatly reduced, suggesting a G_1-S arrest (p=0.0212, Figure 2.6 and 2.7).

2.3.5 PLK1 in LPs suggests they possess a mechanism of checkpoint adaptation

To test the hypothesis that LPs arresting in G_2 after irradiation may progress through the cell cycle by showing checkpoint adaptation, the presence of PLK1 was assessed in both BCs and LPs. On performing western blot analysis on 2 BCs and 4 LPs (2 matched) samples, a significant amount of activated phospho-PLK1 was detected in LPs (p=0.0464) and not in BCs. PLK1 levels were also significantly increased in LPs after irradiation (p=0.0021) (Figure 2.8).

2.3.6 Fractionation experiments suggest the presence of a stronger repair mechanism in BCs compared to LPs

To determine how cells may be able to repair sub-lethal damage caused by X-irradiation and if this may be different between BCs and LPs, cells were assessed in a fractionation

experiment. Briefly, freshly isolated cells were cultured for 2 days to allow for the selection of a more robust population of cells. Post the 2-day culture, cells were seeded in a 2D CFC assay. The plates were then X-irradiated at an initial dose of 2 Gy. These plates were X-irradiated at another 2 Gy after 1, 2, 4 and 6 hours. Controls were sham irradiated and a control plate was irradiated at 4 Gy. The plates were fixed and counted 8-10 days later. On assessing the surviving CFC population, it was seen that BC show better CFC survival compared to LPs at all time points (p=0.0004, 0.0007, 0.0037 and 0.0099 at 1, 2, 4 and 6 hours respectively, Figure 2.9).

2.3.7 Use of published RNA-Seq data to explain checkpoint adaptation in LPs and more efficient repair mechanism in BCs

To look for potential associated mRNA evidence to support the different radiation sensitivities of normal LPs and BCs, published data from donor-matched populations [130] was examined for the presence of transcripts of *PLK1* and genes involved in DNA damage and mitotic re-entry (Figure 2.10).

The activation of the G_2M checkpoint involves the activation of *CHK1/2* by *ATM/ATR*-mediated phosphorylation. The activated *CHK1/2* phosphorylates *CDC25*, causing *CDC25* inhibition by the cytoplasmic sequestration of *CDC25*. Consequently, *CDK1* remains inactive by sustained inhibitory phosphorylation by *Wee1*, resulting in the rapid inhibition of entry into mitosis [167-169]. No significant differences were seen between the 2 cell populations in the levels of *PLK1*, *CHK1*, *CHK2*, *CDC25C* and *CDK1*.

However, *ATM*, *ATR* and *WEE1* were found to be upregulated in LPs compared to BCs (p=0.0205, 0.0016 and 0.0085 respectively, Figure 2.11).

Another layer of control for the G_2M checkpoint is provided by the p53 pathway [170]. *P53* is capable of upregulating cell cycle proteins such as p21 (CDKN1A) which play essential roles in DNA damage response by participating in cell cycle progression, apoptosis and transcription [171]. The main role of p21 in the G_1 checkpoint lies in its ability to inhibit the activity of *CDK2* required for the G_1S phase transition, thereby contributing to G_1-phase arrest [172]. Consequently, the Retinoblastoma protein (pRb) remains hypo-phosphorylated thereby sequestering the transcription factor E2F, whose activity is required for S-phase entry [173]. Increased cytoplasmic p21 is also known to facilitate repair. RNA-seq data shows upregulation of p21 in addition to that of levels of CDK2 and CDK4, in BCs compared to LPs (p=0.0009, 0.0178 and 0.0325, respectively, Figure 2.11).

2.3.8 Culture-adapted tumorigenic human mammary epithelial cell lines are more radioresistant than normal BCs and LPs

Having established the baseline radiosensitivity in normal cells, the next step was to explore the response of malignant cells to radiation. In a first test of the radiosensitivity of clonogenic cells, the response to radiation on one non-tumorigenic but immortalized human mammary epithelial cell line (MCF-10A) and two tumorigenic cell lines (MDA-MB231 and SUM149) was tested. Cells in suspension *in vitro* were exposed to different doses of X-radiation and then plated in 2D CFC assays to determine effects on their *in*

vitro clonogenic activity. The proportion of surviving CFCs from all three lines were observed to be very similar to one another and more resistant to radiation when compared to normal primary LP and BC CFCs (p=0.0117 for LP vs. SUM149, p=0.0028 for LP vs. MCF-10A, p=0.0223 for BC vs. SUM149, p=0.0026 for BC vs. MCF-10A and p=0.018 for BC vs. MDA-MB231at 4 Gy, Figure 2.12).

2.3.9 MCF-10A cells transduced with oncogenic *KRAS*^{G12D} show no change in radiosensitivity

MCF-10A cells were transduced with the lentiviral *KRAS*^{G12D} vector and the resulting cells were assayed in a 2D CFC assay after being exposed to increasing doses of X-rays as for previous cell types. The resultant effects on on the clonogenic activity were similar between both transduced and untransduced MCF-10A cells (p>0.05, Figure 2.13).

2.3.10 *KRAS*^{G12D}-transduced human mammary cells show increased radioresistance

Having established how cell lines may not be the right model for studying the effects of radiation, primary cells transduced with lentiviral *KRAS*^{G12D}-encoding vector were next used to determine how quickly a change in radiosensitivity might be seen in a BC or LP population. Cells were analyzed in 2D CFC assays 72 hours after transduction to allow expression of the *KRAS*^{G12D} transgene. Although these transduced cells showed a slight increase in resistance to radiation as compared to freshly isolated cells, a similar effect

was also seen with cells transduced with a control mCherry lentiviral vector (p=0.0172 for LP vs. LP+KRAS^{G12D}, p=0.0270 for LP vs. LP+mCh at 4Gy, Figure 2.14).

2.3.11 Cell cycle analysis of transduced cells show similar trends

Cell cycle analysis of *in vitro* transduced cells showed that *KRAS*^{G12D} or the control mCherry vector showed similar response of X-irradiation on their cell cycle progression (Figure 2.15). Irradiated BCs transduced with *KRAS*^{G12D} were arrested in G_2 (p=0.0497), and both *KRAS*^{G12D} and control mCherry vector transduced LPs were arrested in G_1S as well as in G_2 (p=0.0003 for LP+KRAS^{G12D} in S phase, p=0.0029 for LP+KRAS^{G12D} in G_2 and p=0.004 for LP+mCh in S phase, p=0.003 for LP+mCh in G_2). While the idea for trying the oncogenic transformation *in vitro* was to study early transformation events and possible effects that could have an effect on radiation response, these observations suggest that just a brief period in culture is sufficient to change the radiation sensitivity of human mammary cells.

2.3.12 *In vivo* generated clonogenic cells from *KRAS*^{G12D}-transformed normal human LPs and BCs display increased X-ray resistance

To test the radiosensitivity of cells from tumours generated from *KRAS*^{G12D}-transformed BCs or LPs, 8-week tumours were dissociated and human cells isolated by FACS prior to being irradiated *in vitro* and then assayed in 2D CFC assays as in previous experiments. CFCs from both BC- and LP-derived *de novo* tumours appeared to be more radioresistant

than CFCs from the normal cells from which they were derived (p=0.0035 for BC-derived and p=0.0041 for LP-derived tumours at 4 Gy, Figure 2.16).

2.3.13 CFCs from serially passaged *de novo* *KRAS*^{G12D}-transformed human mammary cells show extreme radio-resistance

Cells from serially passaged derivative lines obtained from two different primary *de novo* tumours (kindly provided by S Lefort), were irradiated *in vitro* and then assessed also in 2D CFC assays. The results show these cells had acquired an even greater radioresistance (p=0.0018 and 0.0011) than normal BCs at 4 Gy (Figure 2.17).

2.3.14 Analysis of RNA-seq data for BCs and LPs obtained pre- and post *KRAS*^{G12D}-induced transformation

Comparison of RNA-seq data for normal BCs and LPs and the cells generated in primary tumours obtained from them after their transduction with *KRAS*^{G12D} showed upregulated *PLK1* expression in BC-derived *de novo* tumours compared to normal BCs (p=<0.0001) and upregulated *WEE1* in *de novo* tumours derived from both BCs and LPs compared to their corresponding normal counterparts (p=0.0029 for BCs and p=0.0027 for LPs). Conversely, *CDK4* was significantly downregulated in BC-derived *de novo* tumours compared to normal BCs (p=0.0051, Figure 2.18). No statistically significant differences were seen in the relative expression of *CHK1, CHK2, CDC25C, CDK1, ATM, ATR, CDKN1A* and *CDK 2* between *de novo* derived tumours and their corresponding starting cell populations.

2.4 Discussion

There are four major findings emanating from these studies. First, we have established an intrinsically determined reduced radiosensitivity of human LP-CFCs compared to BC-CFCs. Second, we have obtained evidence that this difference may reflect a superior checkpoint adaptation ability of LPs. Third, even though the BC-CFCs seem to be more radiosensitive compared to LP-CFCs, they may have a more robust repair mechanism as also suggested by the results of their superior survival after exposure to a split-dose treatment. Fourth, the cell of origin may play a role in how their malignant derivatives respond to radiation.

The biological consequences of irradiation leading to cell death are highly influenced by the activation of the DNA damage response mechanisms. It is established that the creation of a DNA double-strand break (DSB) represents the principal lesion that, if not adequately repaired, can lead to cell death via the generation of lethal chromosomal aberrations or the direct induction of apoptosis. Apoptosis, or programmed cell death is highly regulated and essential for various biological events such as morphogenesis. However, it is also important for the elimination of potentially harmful cells. If a cell becomes damaged beyond repair, the cell may undergo apoptosis [174]. The terminal apoptotic pathway of mammalian cells depends on the activation of caspases, which is a family of proteases, and their modification of protein substrates within the nucleus and cytoplasm [175]. From the experiments described in this chapter, it was observed that there were more early apoptotic cells in the LP subset, in accordance to a recent study

which showed that LPs exhibiting the Cas3 phenotype still had proliferative ability in 2D assays *in vitro* [15].

After irradiation, cells are also known to phosphorylate H2AX, as shown by γH2AX foci and stop their progression through the cell cycle. Some cells are known to escape this arrest, engage in the phenomenon of checkpoint adaptation and continue to cycle with genomic alterations still present. Others may want to repair their DNA before progressing through the cycle. It was observed that both BCs and LPs were able to show the presence of γH2AX foci within 15 minutes of being irradiated. Importantly, the number of foci observed in LPs was higher than that in BCs. Additionally, LPs were found to be arrested in G_2 phase 24 hours after radiation while BCs did not show a G_2 arrest. To test for the presence of checkpoint adaptation, the levels of phospho-PLK1 in both the fractions with and without radiation were assessed. Western blotting showed a strong presence of activated phospho-PLK1 in LPs in irradiated as well as untreated cells. RNA-seq data showed the upregulation in LPs of *WEE1* previously found to regulate G_2 arrest. Conversely, fractionated radiation experiments suggest the possibility of the presence of a repair mechanism in BCs not seen in LPs.

DNA damage induces checkpoint kinase signaling pathways such as ATM-CHK2 and ATR-CHK1, which delay cell cycle progression in order to allow DNA repair. The efficacy of the DNA repair machinery activated by the DNA damage signaling network is critical and determines cell death or repair. While ATM, ATR are observed to be expressed at higher levels in LPs, BCs express higher levels of p21 and CDKs 2 and 4 in addition to showing a better CFC survival in the split X-ray dose-response experiment.

All of the above observations, including the increased γH2AX foci, the cell cycle arrest in G_2 phase, evidence of checkpoint adaptation and a lower repair activity in the LP subpopulation, point to a greater predisposition to genomic instability in the LPs. Previous studies have shown telomere shortening in LPs [8] and a mechanism to combat ROS accumulation [118]. These observations together with those discussed in this chapter are consistent with the possibility of LPs being a cancer-prone population.

We next examined the radiation response of the non-malignant human MCF-10A cell line, obtained from cells from a patient with benign fibrocystic disease [176], with the expectation that these cells might prove an ideal tool to study molecular mechanisms imposed by induced transformation. However, we found that the non-tumorigenic MCF-10A cells are more radioresistant than primary human mammary CFCs and further transformation of the MCF-10A (with $KRAS^{G12D}$) did not alter their X-ray sensitivity. However, in retrospect, this finding may not be surprising since we subsequently learned that the MCF-10A cells harbor a spontaneously acquired deletion in the p16/ARF gene [176], and *P16* has recently been shown to influence the radiosensitivity of head and neck squamous cell carcinoma cells [177].

Another interesting observation was that although transduced cells could be cultured, they might not respond similarly to cells harvested directly from a tumour *in vivo*. Indeed, even the culture period required for transduction may be sufficient to elicit a decreased radiosensitivity, as suggested by the altered responses of cells exposed to a control vector. Notably, higher levels of PLK1 and *WEE1* were observed in the same type of *de novo* induced tumours compared to the normal subsets of mammary cells from which they were generated. .In addition, cells from serially passaged *de novo* human

mammary tumours also derived by *KRAS*^{G12D} transduction, showed a progressive increase in radioresistance.

Taken together, these results support the hypothesis that ionizing radiation may cause LPs to arrest in the cell cycle and then activate an ability to undergo checkpoint adaptation and thus promote their continued proliferation. In contrast, BCs may lack such a mechanism and thus end up with a greater death response. Although further experiments would be required to address these possibilities more definitively, it may be important to consider mechanisms regulating checkpoint adaptation as playing a role in how breast cancer cells respond differentially to DNA-damaging treatments.

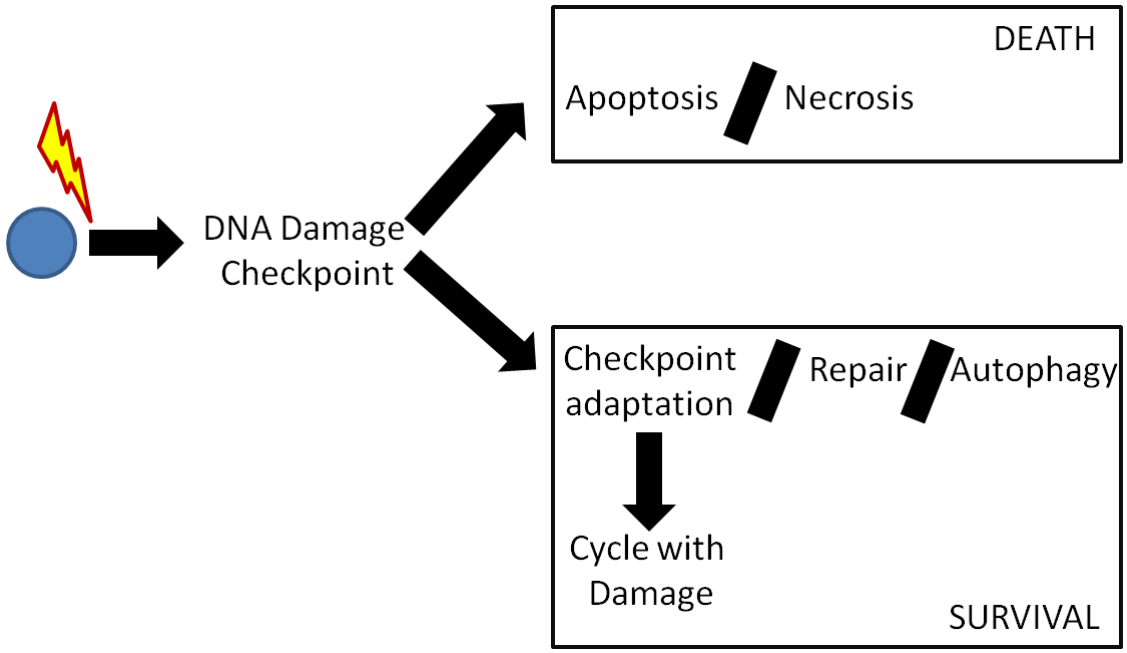

Figure 2.1: Proposed model of mechanisms activated by ionizing radiation that affect survival responses of clonogenic mammary cells.

Irradiated cells activate a checkpoint at which time they either die through apoptosis or necrosis or survive by one of three mechanisms. They may stay blocked from further progression through the cell cycle and repair DNA damage, or they may show "checkpoint adaptation" and accumulate damage, or activate autophagy as a pro-survival mechanism.

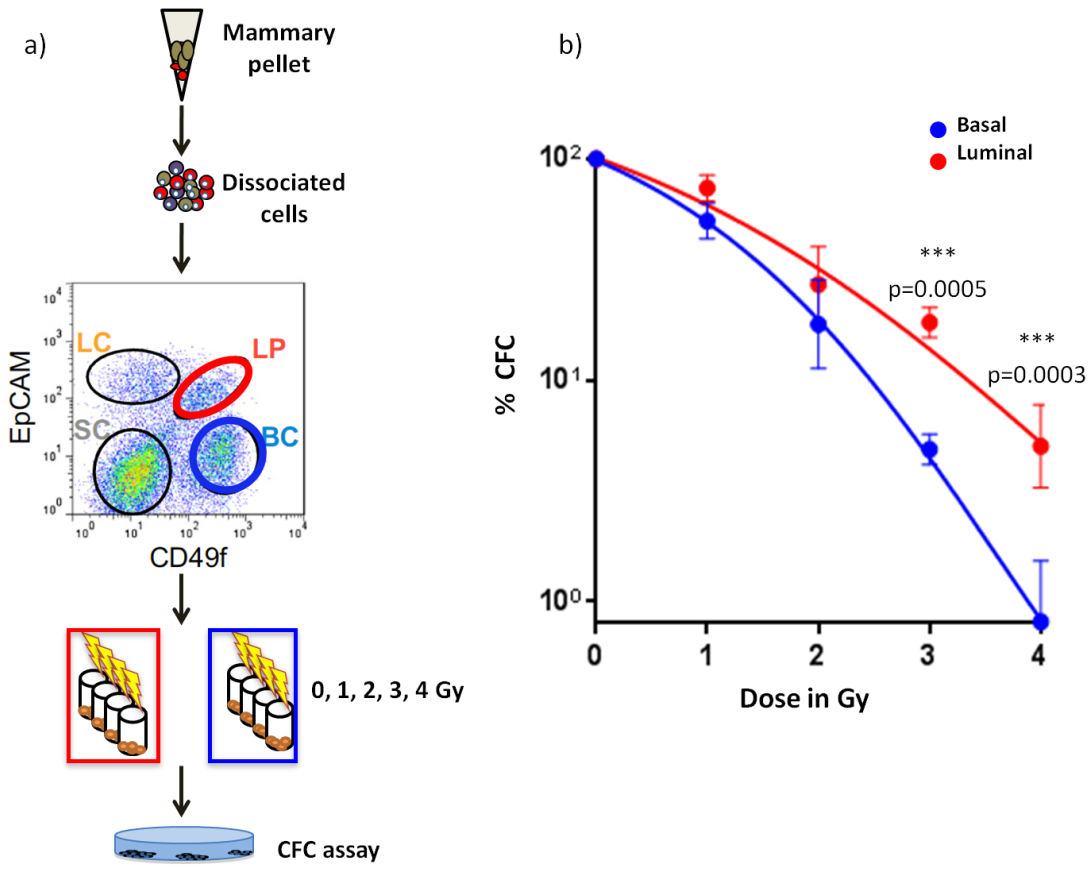

Figure 2.2: Assessment of the radiosensitivity of normal human mammary CFCs.

a) Experimental design. Primary isolates of normal human mammary cells were dissociated into single-cell suspensions and purified BCs and LPs isolated by FACS. These cells were then exposed to different doses of X-rays and assayed in a 2D CFC assay. After 7-10 days, colony numbers were counted to enable CFC survival values to be calculated. b) Results showing the % surviving CFCs with increasing doses of radiation. LP-CFCs (red) are found to be 1.5x more resistant than BC-CFCs (blue). Results are pooled from 7 experiments with cells from different donors.

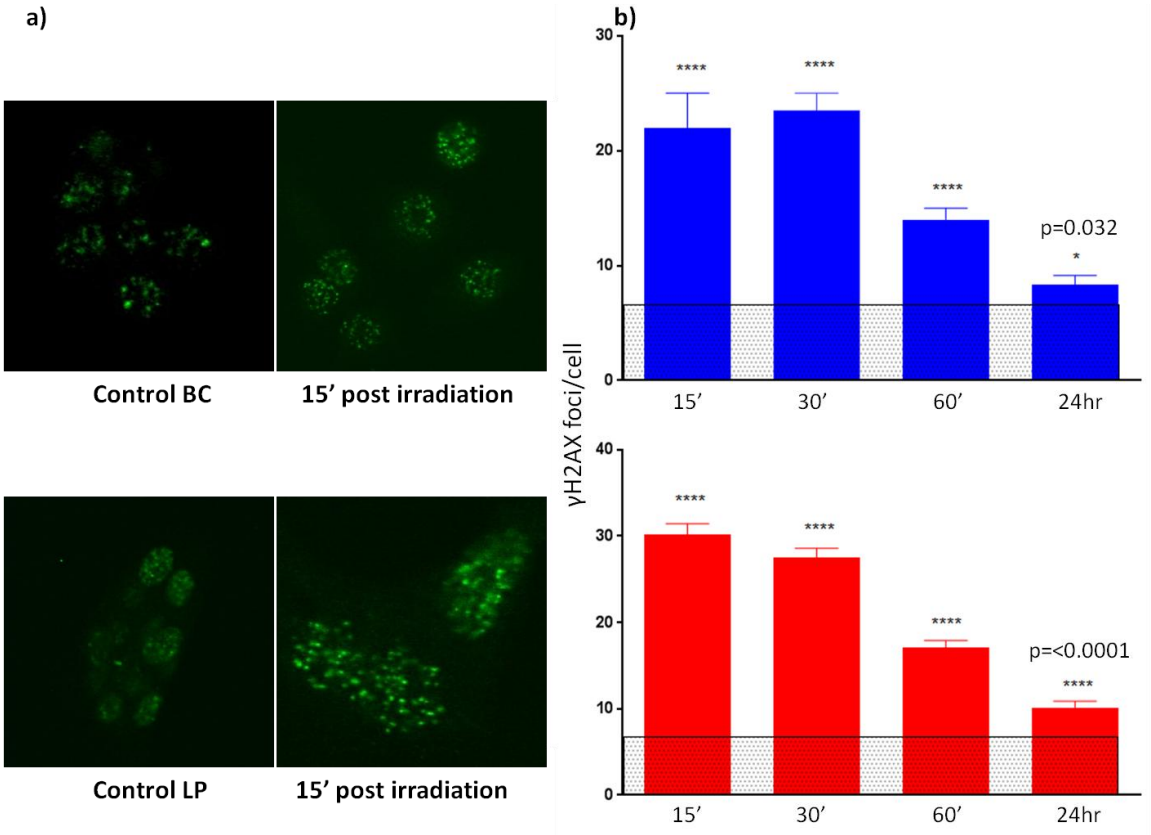

Figure 2.3: Assessment of γH2AX foci in BCs and LPs as a function of time after exposure to 1 Gy.

a) Representative images of control and test cells analyzed for γH2AX foci 15 minutes post irradiation at 1Gy. b) Quantification of the number of foci. Both cell fractions showed an increased number of γH2AX foci after being irradiated. Shaded area shows number of γH2AX foci present in control, non-irradiated cells. This effect was most pronounced after 15 minutes. At this time the number of foci per LP (red) was significantly higher (p=0.0004) than per BC (blue). Results are pooled from 4 experiments with matched LP and BC isolates from different donors (2500 cells/time tested/experiment). Asterisks show significance relative to control un-irradiated cells, where **** indicates p =<0.0001.

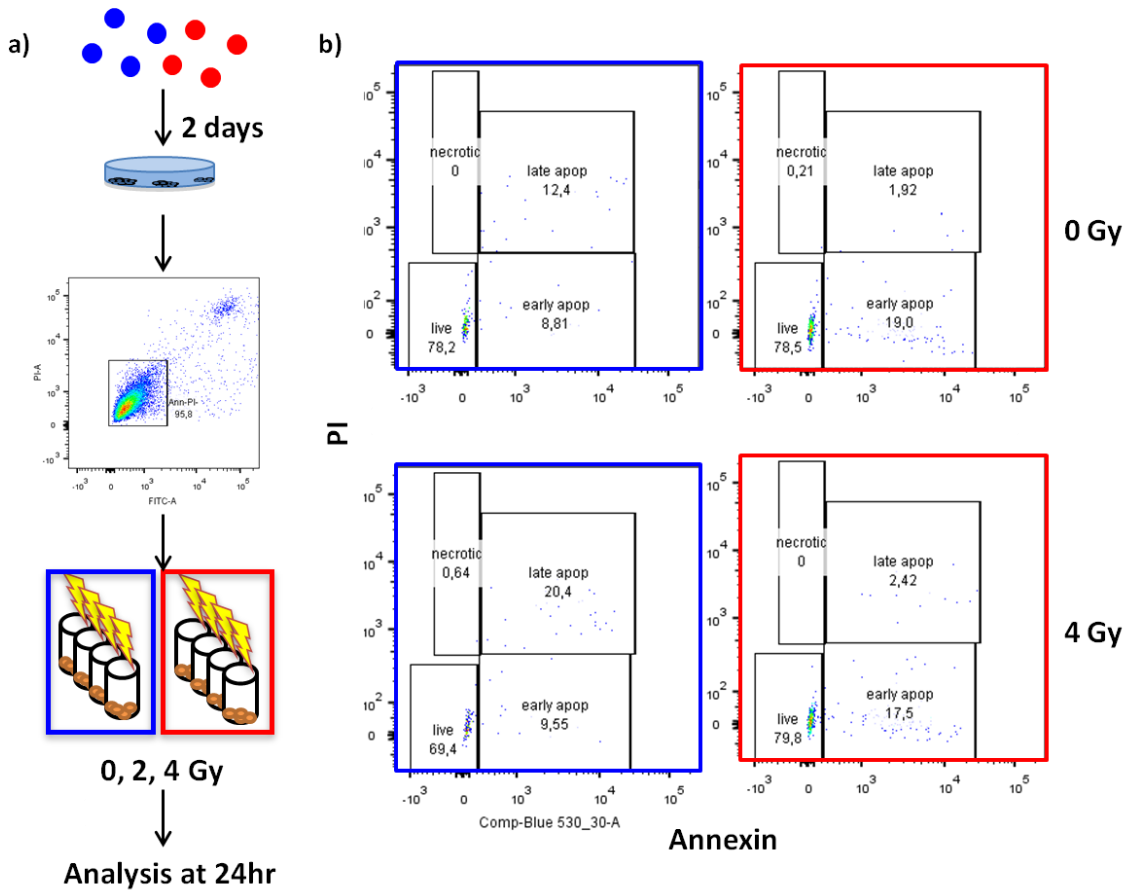

Figure 2.4: Assessment of the production of apoptotic response of LPs and BCs to irradiation.

a) Experimental design. BCs (blue) and LPs (red) were stained with Annexin-V and PI and analyzed by FACS 24 hours after being irradiated. b) Representative FACS plots for 1 sample in each case showing the relative distribution of cells in different apoptotic fractions in cultures of LPs and BCs assessed 24 hours after exposure to 0 or 4 Gy. (as a % of total cells in that sample). Different fractions are marked as live: PI-Annexin-, early apoptotic: PI-Annexin+, late apoptotic: PI+Annexin+, and necrotic: PI+Annexin-.

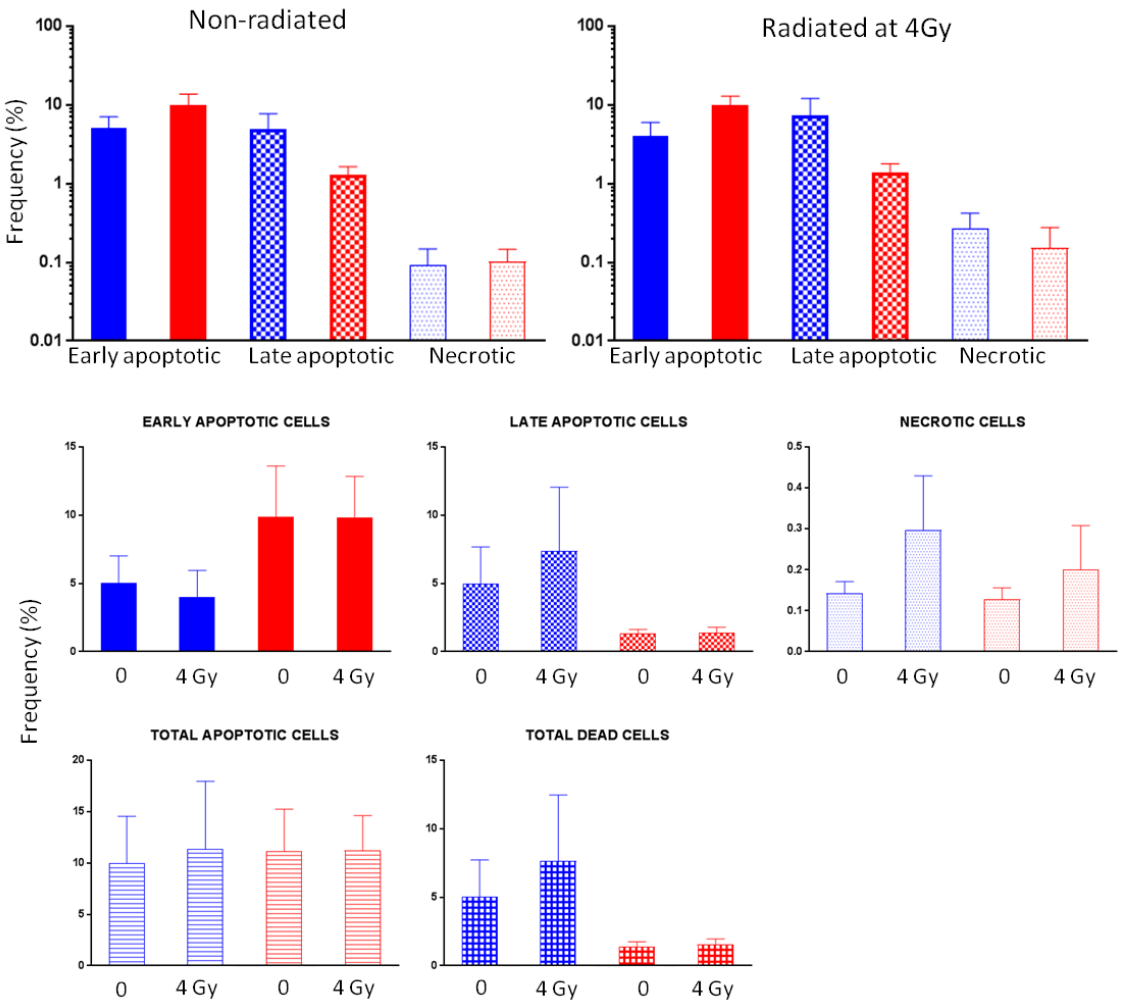

Figure 2.5: Quantification of apoptotic cells in cultures of BCs and LPs for 24 hours after exposure to 0 or 4 Gy.

The top two panels show LPs (red) contain a higher frequency of early apoptotic cells (solid bars) but fewer late apoptotic cells (intermediate bars) irrespective of irradiation, as compared to BCs (blue). Results are pooled from 4 experiments with matched LP and BC isolates from different donors (2,500 cells analyzed/condition/experiment). No significant differences ($p>0.05$) are observed as computed by student's t-test between BCs and LPs in the various apoptotic stages irrespective of irradiation.

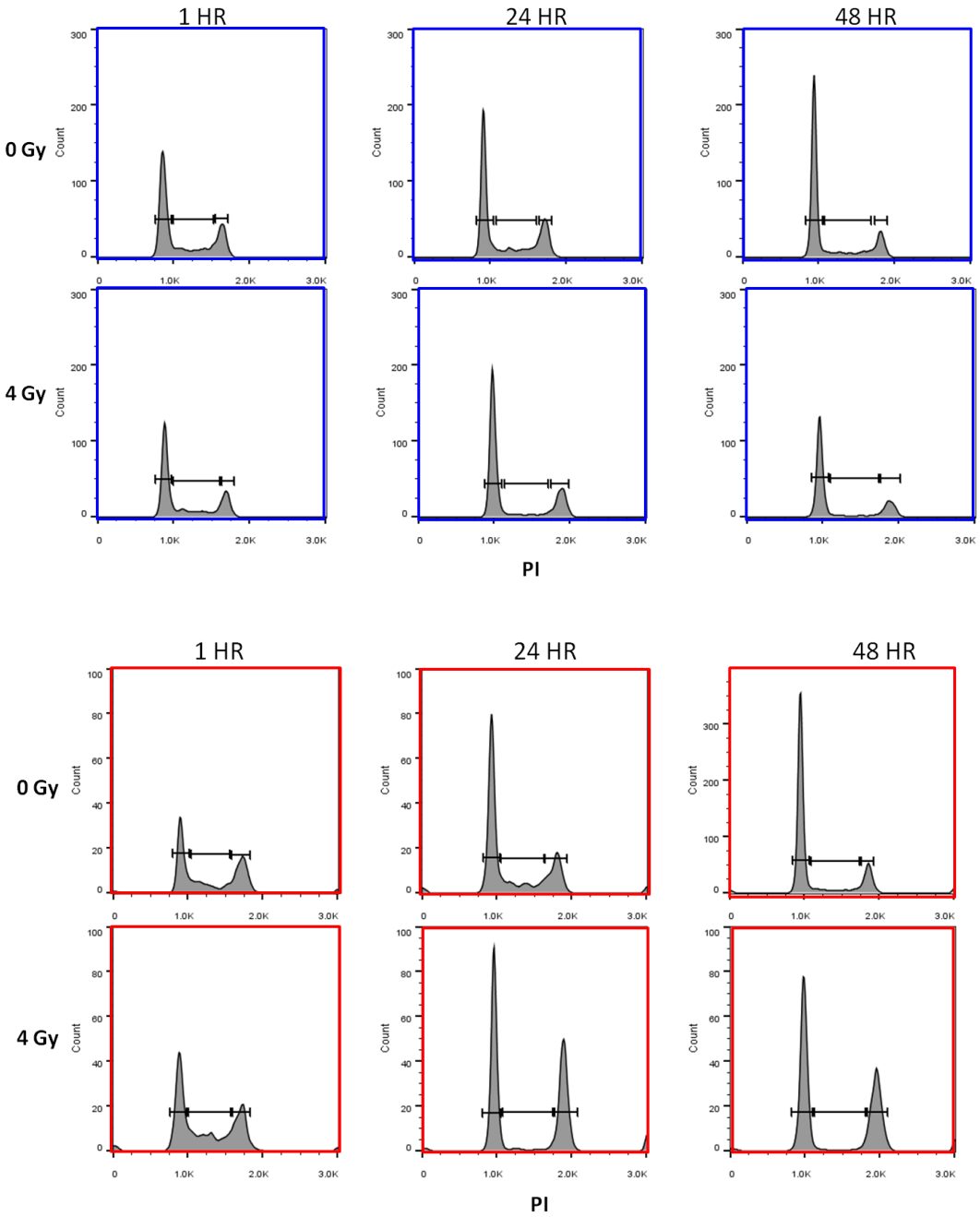

Figure 2.6: Representative FACS profiles of cell cycle distributions of BCs (blue) and LPs (red) cultured for the times shown after exposure to 0 or 4 Gy.

LPs show a G_2 arrest 24 hours after being irradiated with 4 Gy.

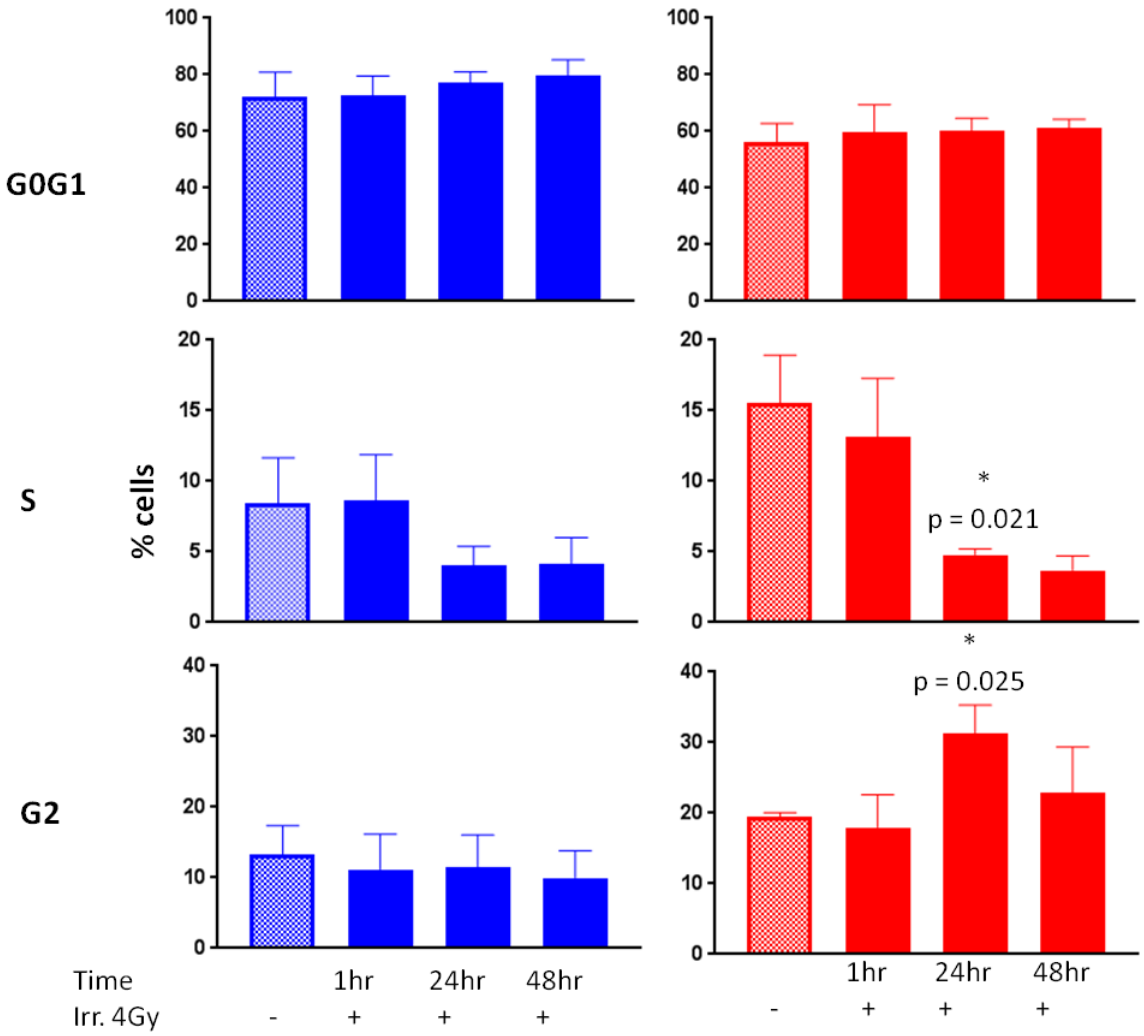

Figure 2.7: Quantification of cell cycle distribution of cultures of BCs (blue) and LPs (red) assessed at different times after exposure to 0 or 4 Gy.

LPs show a significant decrease in the proportion of cells in S-phase (p=0.021) and increase of cells in G_2-phase (p=0.025), 24 hours after being irradiated with 4 Gy compared to non-irradiated cells, as computed by student's t-test. Although not statistically significant, BCs show a slight decrease in the proportion of cells in S-phase (p=0.250). Results are pooled from 4 experiments with matched LP and BC isolates from 4 different donors.

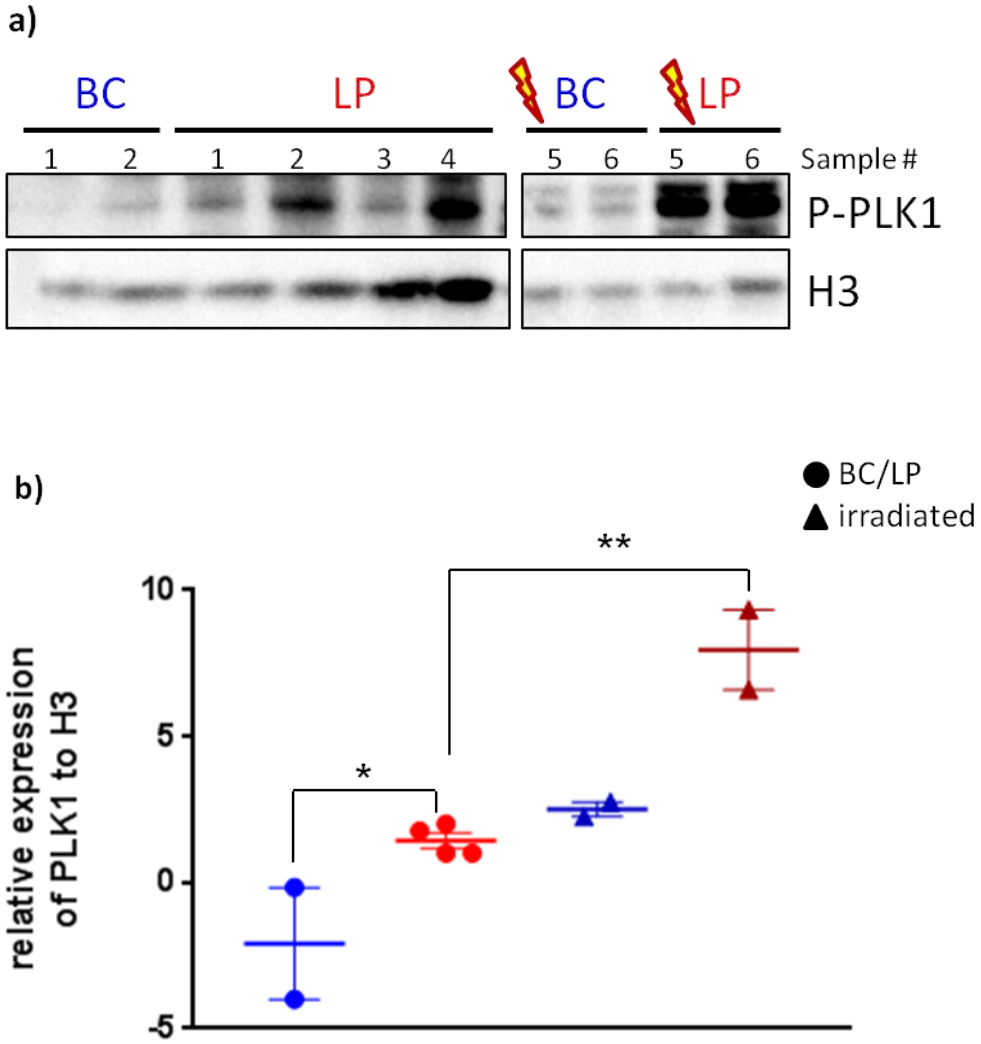

Figure 2.8: Presence of P-PLK1 shown by Western blotting.

Matched BCs and LPs were immunoblotted with anti-phospho-PLK1 and a control anti-histone H3 antibody. Phospho-PLK1 is seen at higher levels in LPs compared to BCs (p=0.0464) without radiation. Phospho-PLK1 expression after irradiation shows further increase in LPs (p=0.0021). Significance computed by student's t-test.

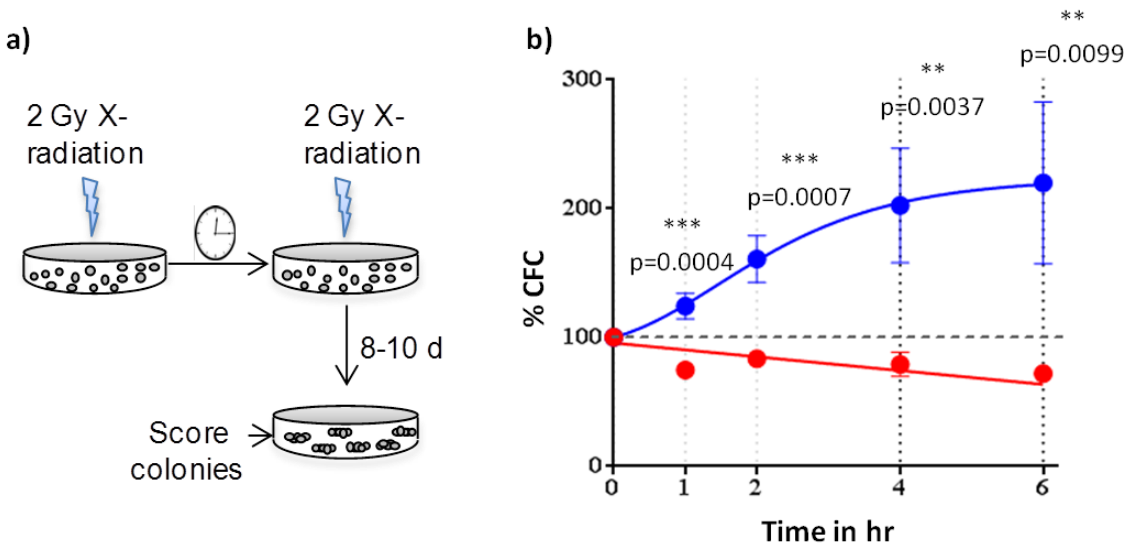

Figure 2.9: Assessment of LP- and BC-CFC capacity to repair sublethal damage caused by radiation.

a) Experimental design. The same numbers of cells were initially X-irradiated with 2Gy, and again with another 2 Gy either immediately or 1, 2, 4 or 6 hours later. Colonies were counted 8-10 days later. b) Results show a significant increase at all time points in surviving BC-CFCs (blue) indicative of their ability to repair sublethal damage; not displayed by LPs (red) (p=0.0004 at 1hr, p=0.0007 at 2hrs, p=0.0037 at 4hrs and p=0.0099 at 6 hrs computed by student's t-test). Results are pooled from 4 separate experiments with matched LP and BC isolates from different donors in each experiment.

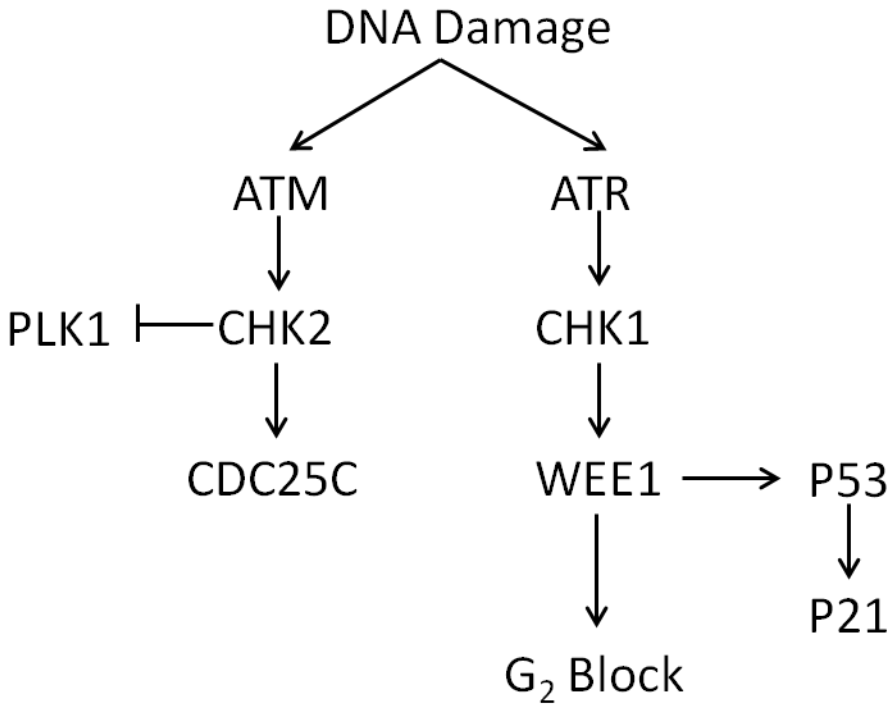

Figure 2.10: Model showing key players in DNA damage responses involving PLK1 and WEE1.

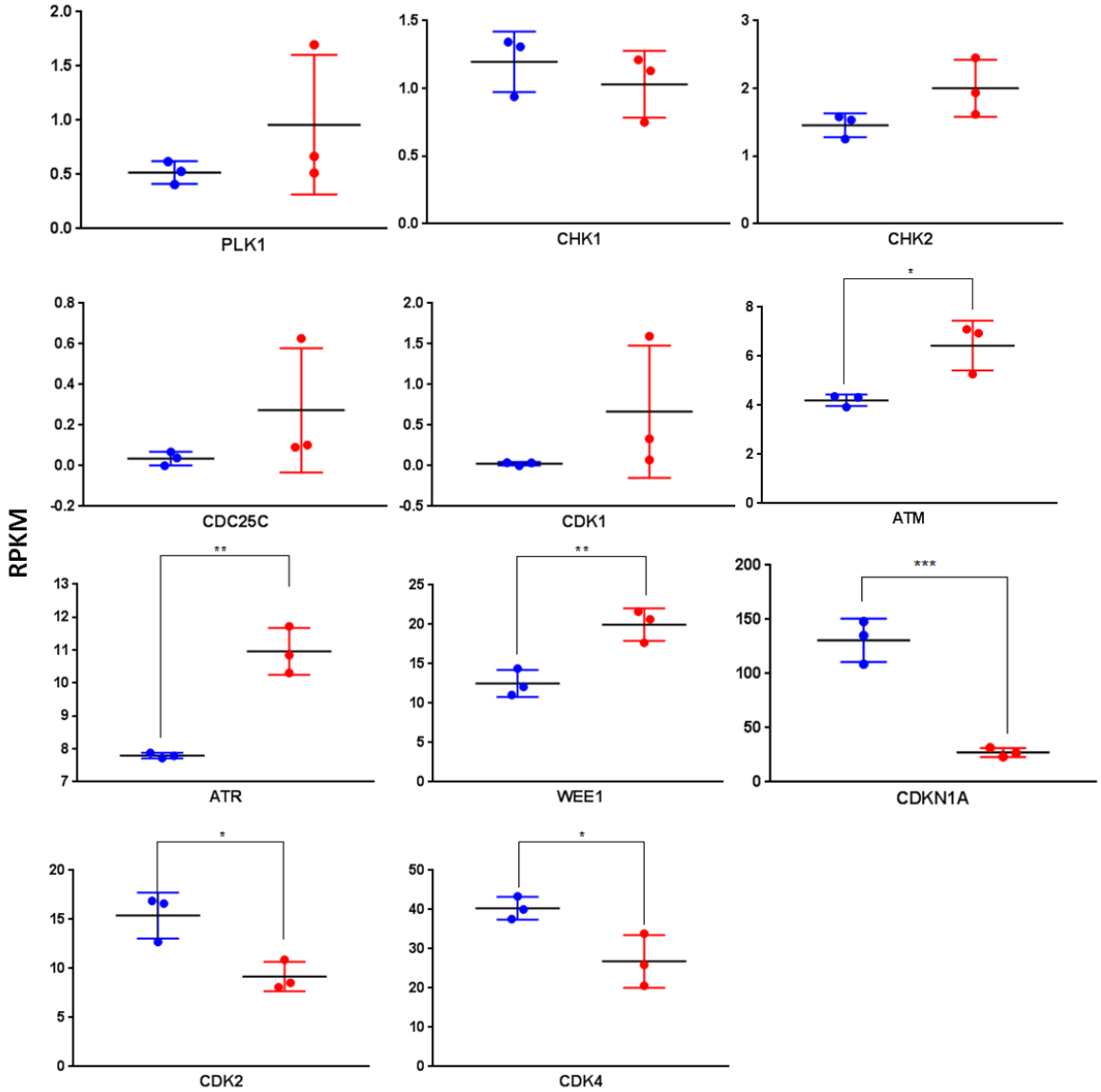

Figure 2.11: Comparison of the relative levels of *PLK1*, *CHK1*, *CHK2*, *CDC25C*, *CDK1*, *ATM*, *ATR*, *WEE1*, *CDKN1A*, *CDK2* and *CDK4* in BCs (blue) and LPs (red) derived from published RNA-seq data [130].

LPs show significantly higher expression of *ATM*, *ATR* and *WEE1* and lower expression of *CDKN1A*, *CDK2* and *CDK4* compared to BCs. Significance shown by asterisks, where * indicates p=<0.05, ** is p=<0.01 and *** is p=<0.001, computed by student's t-test.

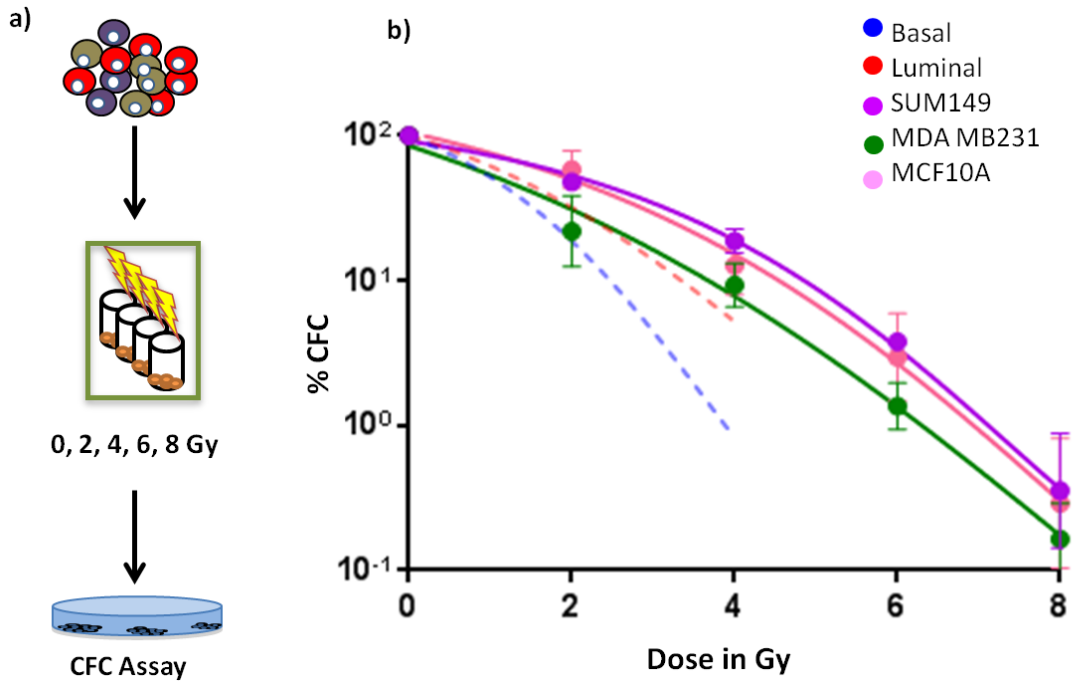

Figure 2.12: Comparison of the radiosensitivity of non-tumorigenic (MCF-10A) & tumorigenic (SUM149 & MDA-MB231) human breast cell line CFCs to normal LP-CFCs and BC-CFCs.

a) Experimental design. Cells from different sources were irradiated in suspension and assayed in a 2D CFC assay. After 7-10 days, colony numbers were counted and the percentages of CFC survival were calculated. b) Results showing the % CFCs surviving increasing doses of radiation. Cell line CFCs (solid lines) are found to be more radioresistant (p=0.0117 for LP vs. SUM149, p=0.0028 for LP vs. MCF-10A, p=0.0223 for BC vs. SUM149, p=0.0026 for BC vs. MCF-10A and p=0.018 for BC vs. MDA-MB231 at 4 Gy, computed by student's t-test) than primary normal BC- and LP-CFCs (dotted lines –redrawn from Fig. 2.2). Cell line results are pooled from 4 experiments.

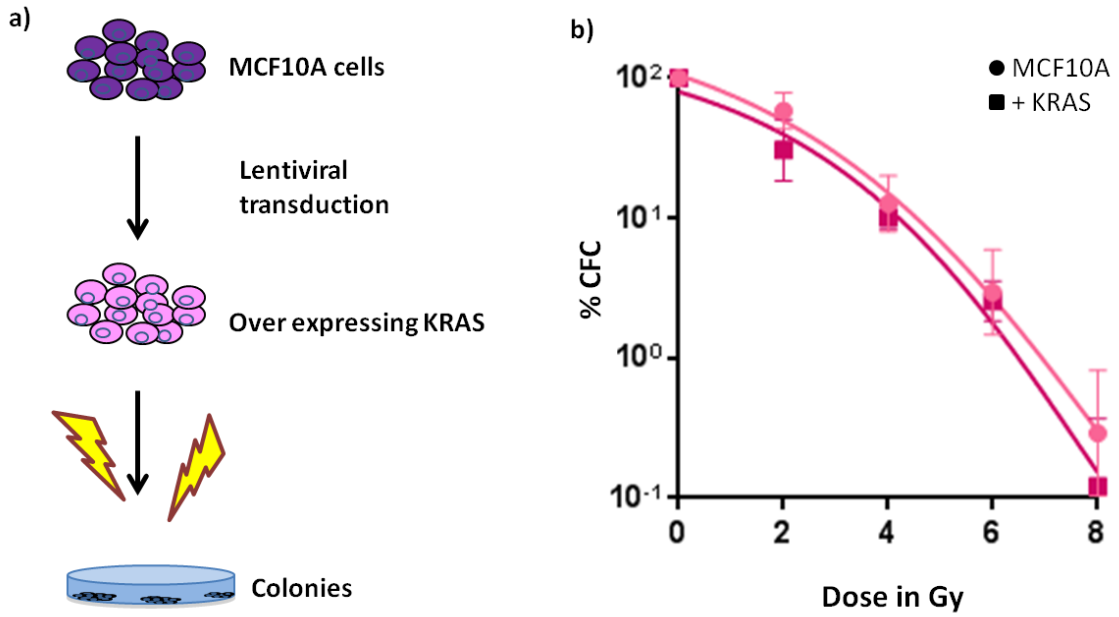

Figure 2.13: Assessment of the radiosensitivity of *KRAS*^{G12D}-transduced MCF-10A CFCs.

a) Experimental design. MCF-10A cells were transduced with the lentiviral *KRAS*^{G12D} vector, irradiated and assayed in 2D CFC assays. After 7-10 days, colony numbers were counted and the percentages of CFC survival were calculated. b) Results showing the % surviving CFCs with increasing doses of radiation. No change in radiosensitivity ($p>0.05$) was observed when computed by student's t-test, in transduced cells compared to those that were not transduced. Results are pooled from 3 experiments.

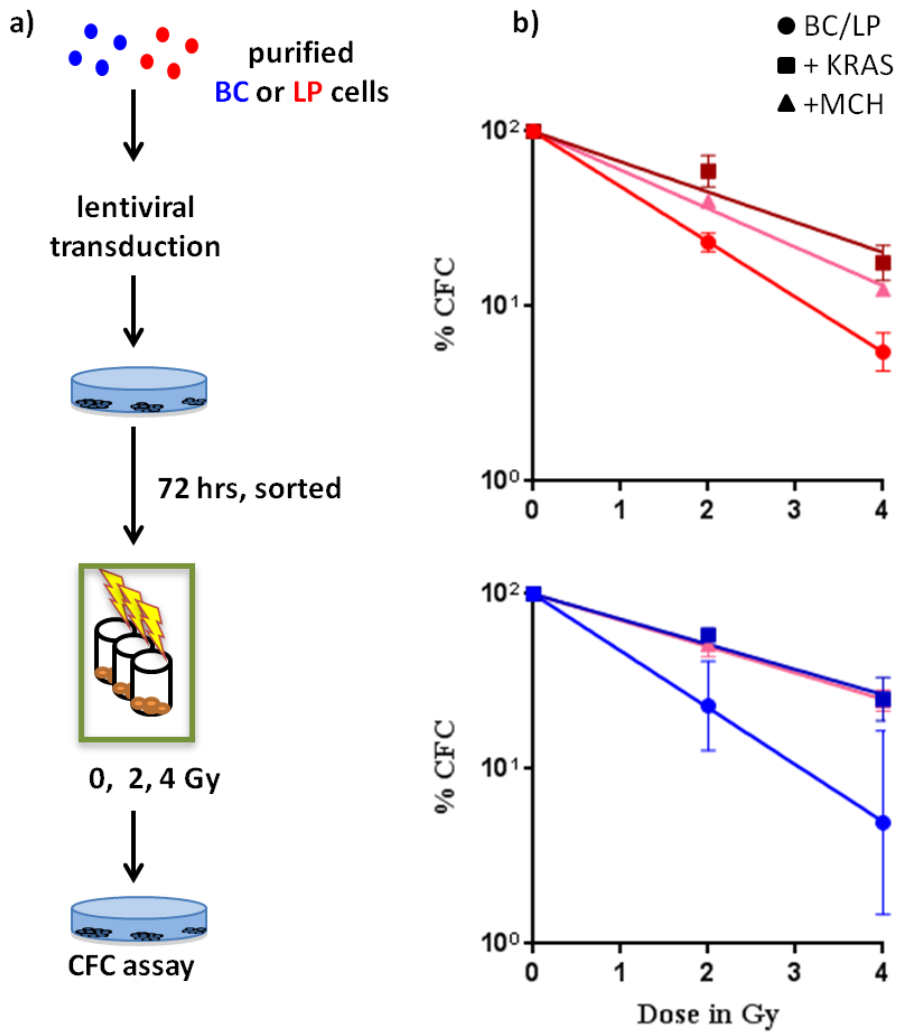

Figure 2.14: Assessment of the radiosensitivity of *KRAS*^{G12D}-transduced primary CFCs immediately post-transduction. .

a) Experimental design. Purified cells were transduced with lentiviral *KRAS*^{G12D} vector (squares) or control mCherry vector (triangles) and cultured for 72 hours. These cells were then irradiated in suspension and assayed in 2D CFC assays. b) Results. All LP CFCs show increased radioresistance (p=0.0172 for LP vs. LP+KRAS^{G12D}, p=0.0270 for LP vs. LP+mCh at 4 Gy, as computed by student's t-test), compared to unaltered primary cultured cells independent of *KRAS*^{G12D}. Results are pooled from 3 experiments with matched LP and BC isolates from different donors in each experiment.

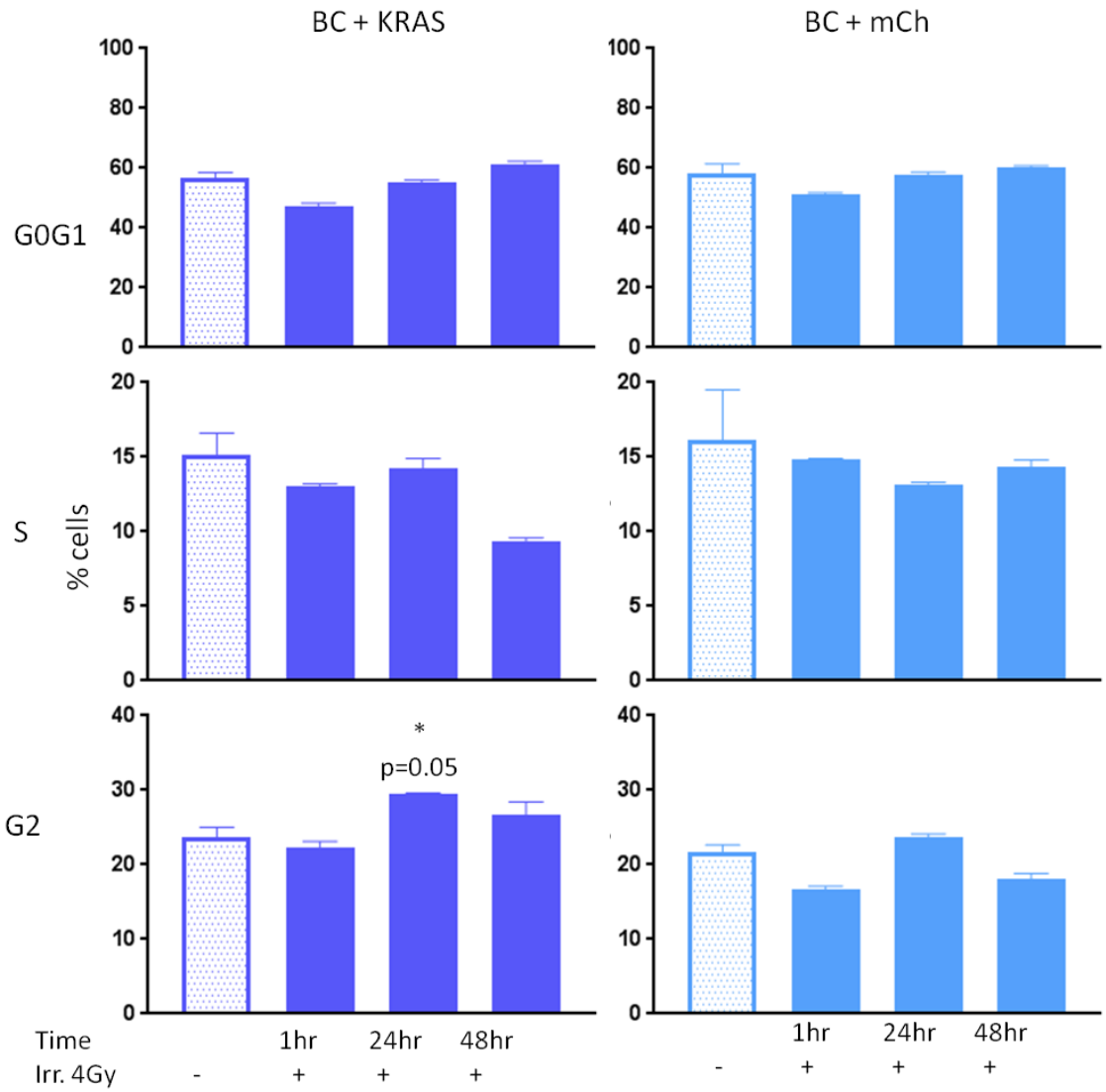

Figure 2.15a: Quantification of cell cycle distribution of BCs transduced with *KRAS^{G12D}* or mCherry vectors assessed at different times after exposure to 0 or 4 Gy 72 hours post-transduction.

BCs transduced with *KRAS^{G12D}* show a significant increase (p=0.05 as computed by student's t-test) in cells arrested in the G_2-phase after irradiation relative to non-irradiated cells. Results are pooled from 3 experiments with matched LP and BC isolates from 3 different donors.

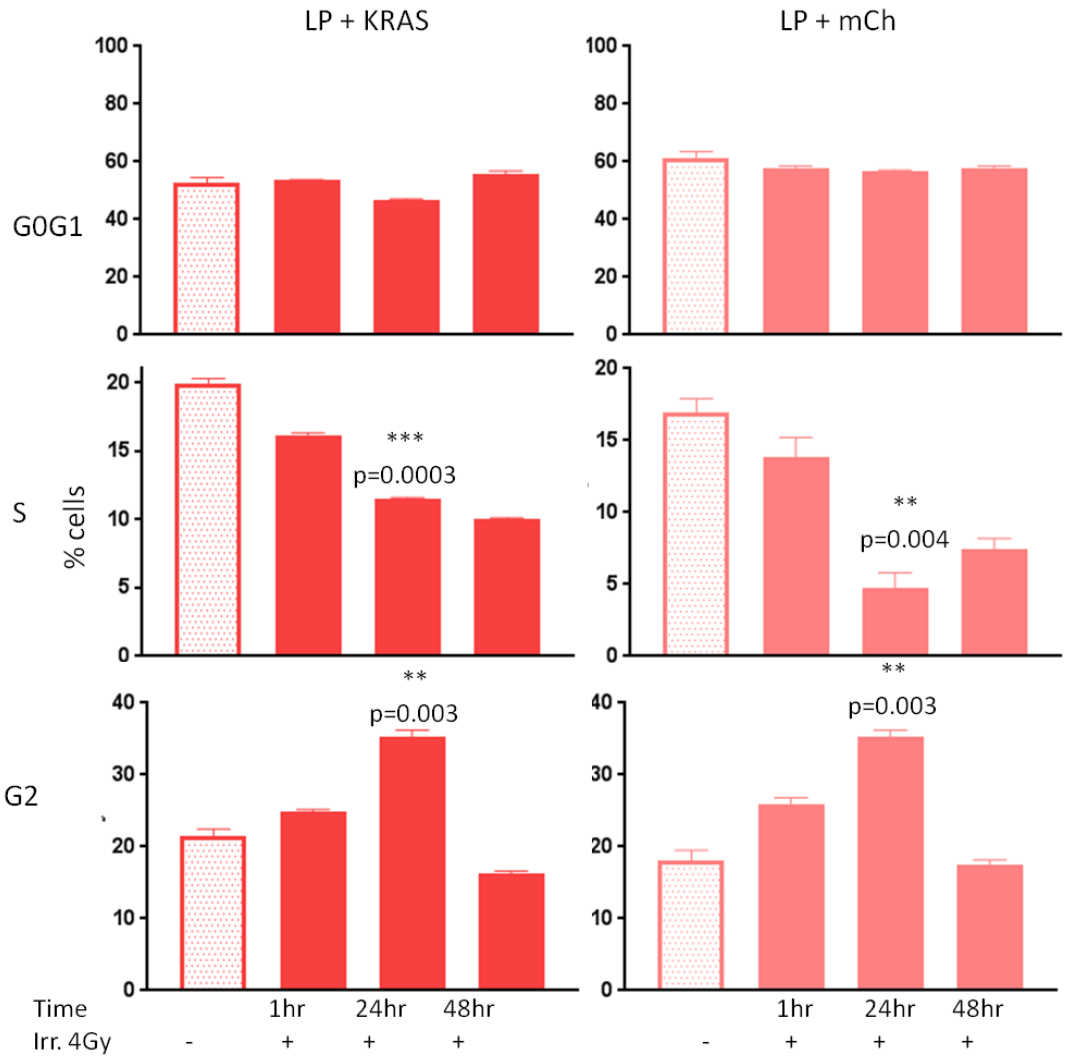

Figure 2.15b: Quantification of the cell cycle distribution of LPs transduced with *KRAS*^{G12D} or mCherry vectors assessed at different times after exposure to 0 or 4 Gy 72 hours post-transduction.

LPs show a significant decrease in the percentage of cells in S-phase (p=0.0003 for LP +KRAS, p=0.004 for LP+mCh) and increase in cells arrested in G_2-phase (p=0.003 for both LP +KRAS and LP+mCh), irrespective of the vector used after irradiation relative to non-irradiated cells. Results are pooled from 3 experiments with matched LP and BC isolates from 3 different donors and computed by student's t-test.

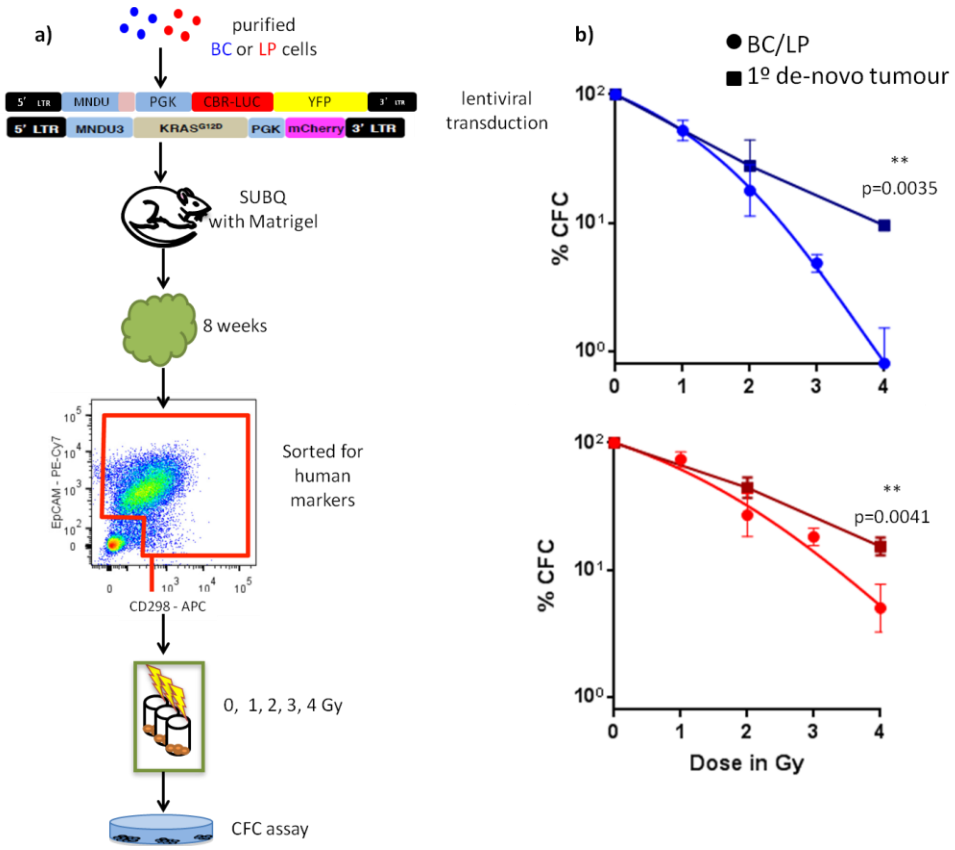

Figure 2.16: Assessment of the radiosensitivity of CFCs present in tumours generated *de novo* with BCs and LPs.

a) Experimental design. Purified cells were transduced with lentiviral *KRAS*^{G12D} and CBR-Luciferase vectors and injected into NRG mice subcutaneously with Matrigel to make a tumour. Tumours were harvested after 8 weeks, sorted for human cells by using human cell surface markers EpCAM & CD298, irradiated in suspension at different doses and then assayed in the 2D CFC assay. Colonies were counted after 7-10 days. b) Results. CFCs from tumours generated from both cell sources were more radioresistant (p=0.0035 for BC- and p=0.0041 for LP-*denovo* at 4Gy computed by student's t-test) than corresponding normal primary cell subtypes from which they were derived. Results are pooled from 3 experiments with matched LP- and BC-derived tumours generated from different donors in each experiment. Results for normal CFCs are redrawn from Fig. 2.2.

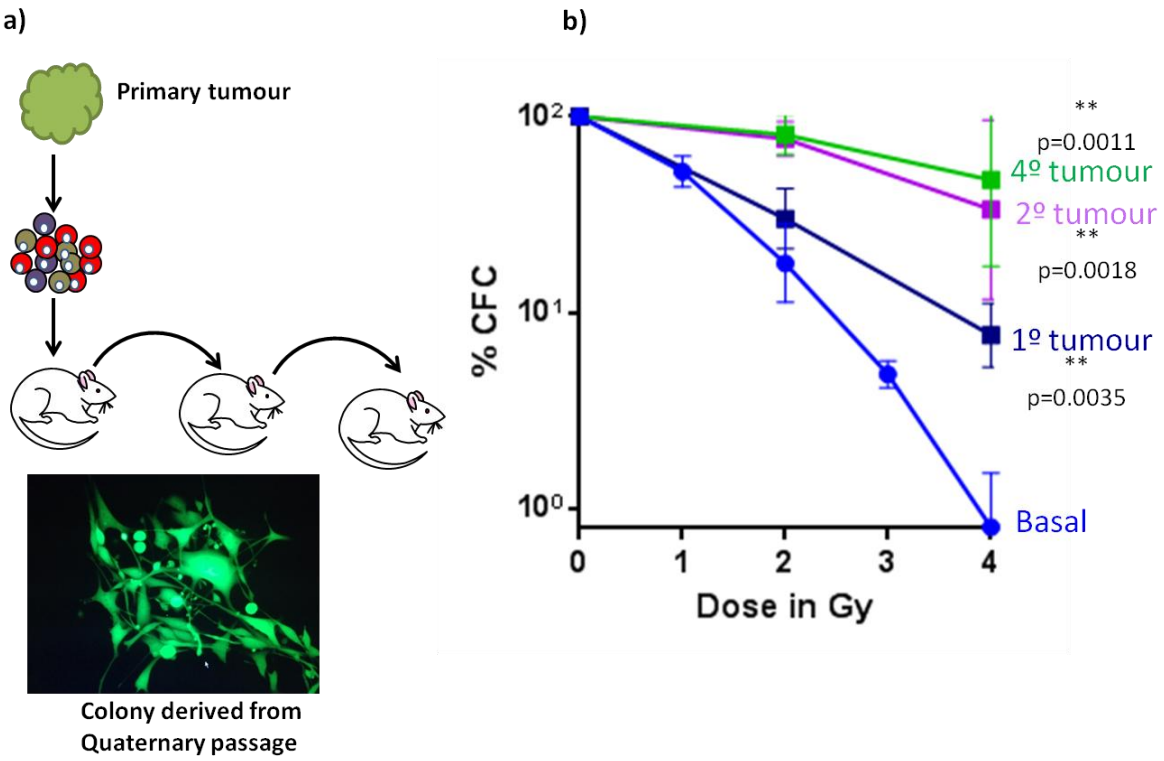

Figure 2.17: Assessment of the radiosensitivity of CFCs from serially passaged *de novo* tumours.

a) Experimental design. Cells from primary, and serially passaged secondary and quaternary derivative lines (originally derived from BCs) were irradiated in suspension *in vitro* with increasing doses of radiation and assayed in the 2D CFC assay. b) Results. CFCs from the serially passaged tumours were more radioresistant than those from BCs-CFCs (data from Fig. 2.2). Significance indicated by asterisks at where p=0.0035 for BC vs. BC-derived primary tumour, p=0.0018 for BC vs. secondary tumour and p=0.0011 for BC vs. quaternary tumour at 4 Gy, as computed by student's t-test.

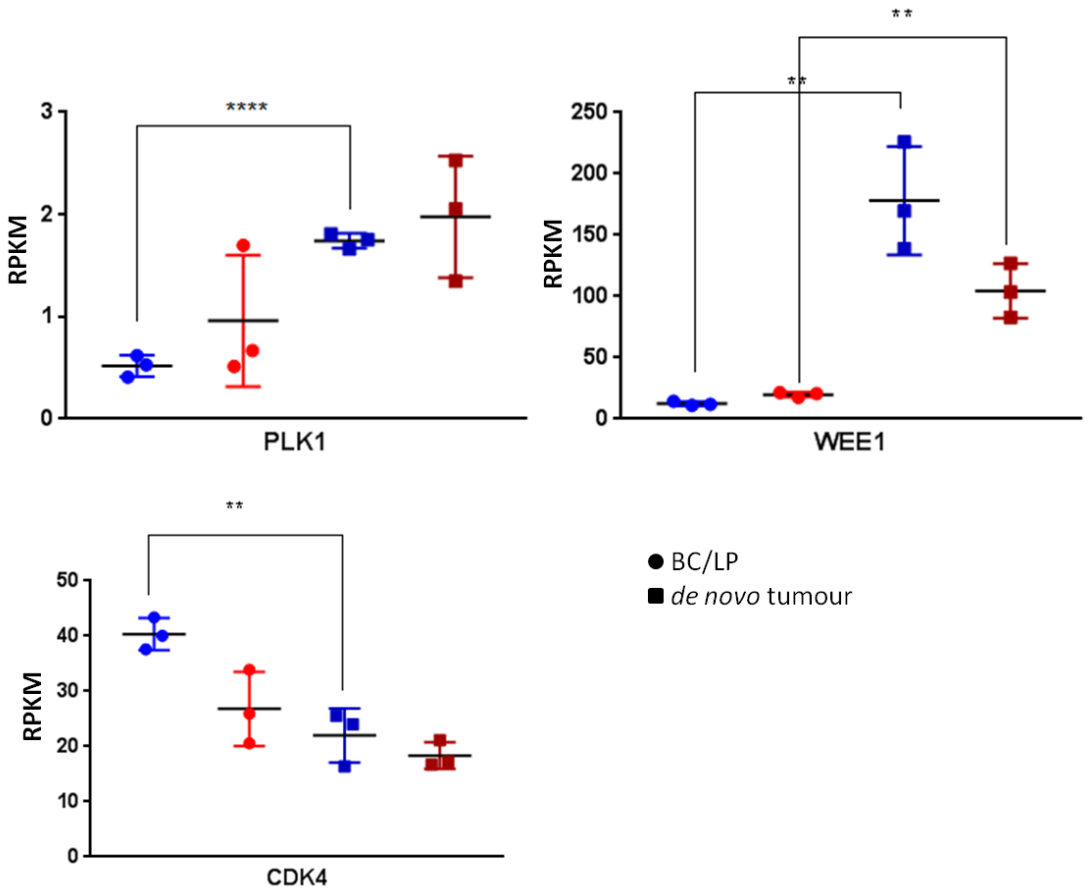

Figure 2.18: Comparison of the relative levels of PLK1, WEE1 and CDK4 in normal BCs, LPs and tumours generated *de novo* from BCs and LPs transduced with lentiviral *KRAS*^{G12D} vector derived from published RNA-seq data [130].

BC-derived *de novo* tumours show significantly higher expression of *PLK1* compared to normal BCs (p=<0.0001) and both BC and LP-derived *de novo* tumours show significantly higher expression of *WEE1* compared to their respective starting populations (p=0.0029 for BCs and p=0.0027 for LPs). BC-derived *de novo* tumours show significantly lower expression of *CDK4* compared to normal BCs (p=0.0051). No statistically significant differences were seen in the expression of *CHK1*, *CHK2*, *CDC25C*, *CDK1*, *ATM*, *ATR*, *CDKN1A* and *CDK 2* in *de novo* derived tumours relative to their corresponding starting cell populations. Significance computed by student's t-test.

Chapter 3: Development of a method to quantify the *in vivo* treatment response of transformed cells with clonogenic activity

3.1 Introduction

The need for models that can predict the *in vivo* responses of patient tumours to candidate treatments is widely appreciated but as yet poorly developed. A popular recent approach has been the use of patient-derived xenografts (PDXs) in immunodeficient mice [28, 69]. However, these have numerous limitations including their lack of applicability to a large fraction of breast cancers [178], non-representative content of available samples [75], and frequent failure to regenerate or sustain the clonal composition of the original sample [69]. *In vitro* clonal methods to assess the effects of *in vivo* treatments might be theoretically more attractive, but these have generally not been proven possible. The recent development of organoid technology may be adapted to circumvent this historic limitation [179]. Nevertheless, these approaches may not adequately recapture the responses obtained in an *in vivo* context.

DNA barcoding offers a powerful alternative approach to track clonal dynamics in experimental systems and has been used to analyze the clonal dynamics of transplants of normal cells, cell lines as well as normal cells that are transduced with an oncogenic lentivirus to make breast tumours in immunocompromised mice and in PDX models with and without treatments [27, 28, 79, 130]. This technology labels individual cells with a unique DNA barcode so that its' subsequently generated progeny can be clonally identified in large mixtures and hence, allows us to make inferences about the clonal

composition of normal tissue or tumour formation in xenografts. As a prelude to using such an approach to monitor the responses of clonogenic cells (and their progeny) to various treatments, we initiated a series of baseline experiments with two human breast cancer cell lines to first determine how clonal growth *in vivo* is related to the number of clonogenic cells present and then define appropriate assays to compare the effects of exposing a tumour initiated with DNA-barcoded cells on its tumorigenic cell content to its clonal response *in vivo*.

In this chapter, the results of these experiments are presented. A first study indicated that the *in vivo* tumorigenic activity of cells from one of the two breast cancer cell lines used in these studies was grossly inhibited by radiation doses that cause a 1-2.5-fold reduction in their *in vitro* CFC activity (Fig. 2.12). However, follow-up experiments revealed surprising evidence of an inverse relationship between the number of unirradiated tumorigenic cells present when a tumour is starting to grow and the number of these that actually grow to produce detectable clones. This prompted an effort to develop an *in vivo* clonal assay for *de novo* derived tumorigenic cells to enable future analyses of the determinants of their clonal growth activity *in vivo* and the effects of candidate anti-tumour treatments on this activity.

3.2 Materials and Methods

3.2.1 Cell lines

MDA-MB231 and SUM149 cells were maintained as cultures as described in Chapter 2.

3.2.2 Generation of tumours from cell lines

Cell lines were cultured for 2 days in respective media, plates trypsinized and cells harvested as described in Chapter 2. Cells were counted and centrifuged. Cells were then mixed with equal volumes of Matrigel before they were injected subcutaneously into adult virgin female NRG mice.

3.2.3 Isolation of human mammary epithelial cells

Cells were enzymatically dissociated into single cells as described in Chapter 2.

3.2.4 Flow cytometry to separate cell subsets

Cells were isolated into subsets on the basis of cell surface markers as described in Chapter 2.

3.2.5 Irradiation of cells

Cells were irradiated in suspension as described in Chapter 2.

3.2.6 Transduction protocol

Cells were transduced according to the protocol described in Chapter 2. Cells were exposed to the DNA-barcoded lentiviral library preparation [27] at a dilution of 1:300 ($3x10^5$ infectious units/100 ul) to avoid double integrations.

3.2.7 Generation of *de novo* tumours

De novo tumours were generated as described in Chapter 2.

3.2.8 Luciferase assessment

Mice were injected intraperitoneally with 150 mg/kg body weight VivoGlo Luciferin (Promega) prepared in PBS and imaged 10 minutes later on the Xenogen IVIS Lumina In Vivo Imaging System with Living Image version 3.0 software (Caliper Life Sciences). Luciferin is a firefly luciferase substrate capable of generating light when it reacts with CBR-Luciferase produced by cells transduced with a cDNA that encodes this protein.

3.2.9 Histology

Tumours retrieved from mice were fixed in 10% formalin (Thermo Fisher Scientific), washed in 70% ethanol, embedded in paraffin and 3 mm sections stained with hematoxylin and eosin.

3.2.10 Statistics

LDA calculations were calculated using the ELDA program [180]. The values obtained are shown with calculated 95% confidence intervals.

3.3. Results

3.3.1 Preliminary assessment of the effect of radiation on the *in vivo* tumorigenic activity of SUM149 cells

Preliminary experiments showed that palpable tumour formation could be consistently obtained within 6-8 weeks in female NRG mice injected subcutaneously with 500,000

SUM149 cells. Accordingly, to obtain a first assessment of the effect of radiation on their overall tumorigenic capacity, we first transduced SUM149 cells with a luciferase vector and then exposed them to doses of radiation *in vitro* that had suppressed their CFC activity *in vitro* by 1-2.5-fold (Fig. 2.12). The cells from each of the different treatment groups were then injected directly into female NRG mice at doses of 500,000 cells per mouse. The luciferase activity subsequently detectable in each mouse was then monitored over several weeks. Tumours were retrieved from mice euthanized after 11 weeks and then weighed before the number of cells per tumour was determined. The results of these measurements showed that the tumours generated were smaller with increasing doses of radiation (Figure 3.1, Table 3.1).

3.3.2 Clonal analysis of primary tumours generated from breast cancer cell lines cells

In order to first validate the use of clonal yield to serve as a measure of the number of cells in a tumour that had *in vivo* growth potential, we designed a series of experiments to examine this relationship using varying doses of untreated cells from both the SUM149 and MDA-MB231 cell lines. Serial dilutions of cells in Matrigel ranging from 1 to 500,000 cells per mouse were tested, with innocula of >30,000 cells being first labeled with a DNA barcode (Figures 3.2 - 3.4). In a first set of experiments mice were euthanized 6-8 weeks post-transplant and tumours were harvested. Tumour weights were recorded and then the tumours were enzymatically dissociated into single cells and the total number of cells present was determined (Table 3.2). A linear response between both

of these endpoints and cell input number was observed up to approximately 500 input MDA-MB231 cells and up to approximately 10,000 SUM149 cells (a ~20-fold difference), above which the tumour sizes plateaued (Figure 3.3). LDA calculations were computed using the ELDA program [180] to relate the presence or absence of a detectable tumour, which yielded 6- to 7-week TIC frequencies of 1 in 9 (95% CI=1/5.7-1/14) for MDA-MB231 cells and 1 in 65 (95% CI=1/36-1/116) for SUM149 cells (Table 3.3 and Figure 3.4). Additional experiments in which injected mice were monitored for up to 13 weeks, showed that the frequency of MDA-MB231 TICs increased to 1 in 3 (95%CI=1/1.9-1/5.4).

To further analyze the basis of the plateau in tumour size obtained from innocula of > 3,000 cells, we performed a second set of experiments in which the same cells were DNA-barcoded just prior to injection at 30,000 – 500,000 cells/mouse. The number of clones detectable in the tumours harvested 6-8 weeks later was then determined by sequencing the DNA barcode inserts found within tumour extracts. The results of this analysis revealed an innoculum dose-dependent *inhibition* of detectable clones which appeared more pronounced for SUM149 cells than MDA-MB231 cells (Figure 3.5).

3.3.3 Frequency of TICs within *KRAS*^{G12D}-transduced BCs and LPs assessed in a transplant assay

Previous experiments designed to estimate the frequency of TICs in *KRAS*^{G12D}-transduced LPs and BCs made use of DNA barcoding [130]. Although these experiments yielded TIC values of 1/200-1/4100 for BCs and 1/150-1/9100 for LPs, they relied on an

experimental design in which the input cell doses ranged from a lower limit of 30,000 cells to 10^6 cells. Given the inhibition of clone detection evident in the breast cancer cell lines that used similar sized innocula, we initiated experiments to examine TIC frequencies directly from transplant assays using lower input innocula. Accordingly, BCs and LPs were sorted and co-transduced with lentiviral vectors containing *KRAS*^{G12D} and CBR-luciferase and then injected subcutaneously into NRG mice with Matrigel at serially diluted doses ranging from 30 to 30,000 cells (Figure 3.6). Mice were monitored by luciferase assessment every few weeks for up to a maximum of 40 weeks (Figure 3.7, total age of the mice 50-54 weeks), by which time all mice were euthanized and tumours retrieved. LDA calculations gave TIC frequencies of 1/6,400 (95% CI=1/2969-1/13981) BCs and 1/1,500 (95% CI=1/571-1/4352) LPs, using 10^5 photons/second as a threshold for detecting a positive growth [180] (Table 3.4 and Figure 3.8).

3.3.4 Enhanced detection of TICs in *KRAS*^{G12D}-transduced BCs and LPs by co-transplantation of irradiated fibroblasts

Detection of clones by LDA depends on optimizing the assay to detect clone formation under limiting input cell conditions and normal human mammary CFCs *in vitro* [2] and MRU detection *in vivo* [17] is known to be compromised in the absence of added irradiated fibroblasts. Therefore, we wondered whether “tumour” formation by initially transduced *KRAS*^{G12D} BCs and/or LPs might also be enhanced by a similar inclusion of irradiated fibroblasts in the transplant innoculum. To further improve the sensitivity of

the assay, we also sorted the cells 2 days post-transduction to ensure that all of the cells injected were doubly transduced with *KRAS*^{G12D} and CBR-luciferase (Figure 3.9).

The results for a series of mice injected with serial dilutions of sorted doubly transduced BCs spanning a range from 30 to 30,000 cells together with 10T1/2 fibroblasts irradiated at 50Gy are shown in Figure 3.8. A comparison between the two methodologies showed that adding fibroblasts and a post-transduction sort gave a higher frequency of TIC detection using 10^5 photons as threshold for a positive tumour (Figure 3.10 – 3.12 and Table 3.5). LDA of these data gave TIC values of 1 in 211 (95% CI=1/139-1/320) BCs and 1 in 2,100 LPs (95% CI=1/1264-1/3518) [180]. An example of the type of "clonal" populations obtained as visualized by fluorescence microscopy is shown in Figure 3.13 and in a standard histological preparation in Figure 3.14.

3.3.5 Frequency of secondary tumour formation from *KRAS*^{G12D}-transduced BCs and LPs is related to the primary input innoculum

Serial transplantability is often considered a hallmark of "complete" transformation, and this property has been shown to be a feature of some of the progeny of *KRAS*^{G12D}-transduced BCs and LPs, although as separable entities from the initially detectable TICs [130]. It was therefore of interest to determine how well the acquisition of serial transplantability might relate to the frequency of primary TICs. To address this question, primary tumours generated from different input numbers of *KRAS*^{G12D}-transduced BCs or LPs were enzymatically digested to produce single cell suspensions and aliquots were then transplanted into secondary NRG mice with Matrigel. Table 3.6 summarizes to the

results obtained. Secondary tumours were consistently generated only from primary tumours generated with ≥30,000 input cells. Limited attempts were made with 3,000 input cells but no secondary tumours could be generated from these tumours (data not shown). Thus, the frequency of secondary TICs appeared to be lower than that of primary TICs.

3.4 Discussion

The rationale of this chapter was to develop an assay for studying transformed cells that are clonogenic *in vivo*. The cell line SUM149 was used to generate tumours in mice after exposure to radiation *in vitro* (pre-transplant). It was observed that with increasing radiation doses the tumours generated were smaller as predicted from *in vitro* studies. However, a counter-intuitive observation was that with input cell doses of >10,000 cells, the tumours formed contained fewer, albeit bigger clones. Tumours generated from lower doses of SUM149 and MDA-MB231 cells revealed TIC frequencies of 1 in 65 and 1 in 9, respectively (using a 6/7-week endpoint). In the *de novo* model system (which involved transducing primary BCs and LPs with an oncogenic $KRAS^{G12D}$ lentiviral vector and transplanting them immediately into immunocompromised mice – see Chapter 2), corresponding TIC frequencies of 1 in 200 for BCs and 1 in 2100 for LPs in the presence of fibroblasts were obtained.

The suppressed growth of cell line clones observed with high innocula is a novel finding and has important implications for any attempt to analyze the effects of a treatment on malignant cells with *in vivo* clonogenic activity. This consideration led to an

effort to first understand the relationship between input cells dose and clone initiation. The two cell lines studied have generally been assumed to be relatively homogenous populations. The cell dose-response experiments reported here support this concept but also indicate that interactions obtained with high cell numbers *in vivo* may create circumstances that suppress expression of their growth activity without necessarily suppressing their viability or growth potential as also evident from serial transplant experiments [28]. These experiments also light on shed the importance of permissivity of a model system for the study of TICs, for example the increase in TIC frequency with the addition of fibroblasts.

Intratumour heterogeneity, which fosters tumour evolution, is a key challenge in cancer medicine and often the cause of therapeutic failure and drug resistance. Targeting clonal events present in every cell, therefore, presents an attractive model for drug development, however resistance is frequent in the advanced disease setting and may be driven by the selection of resistant cells present at low frequencies prior to therapy [29] or may evolve through mutations acquired during therapy [181]. Predicting the innumerable interactions of cancer subclones with each other and the microenvironment is a formidable task; however, the establishment of a quantitative system to assess the TIC frequency of cells using a *de novo* model of tumorigenesis constitutes a first critical step to enable the study of the effect of relevant therapies on the *in vivo* growth capacity of these cells.

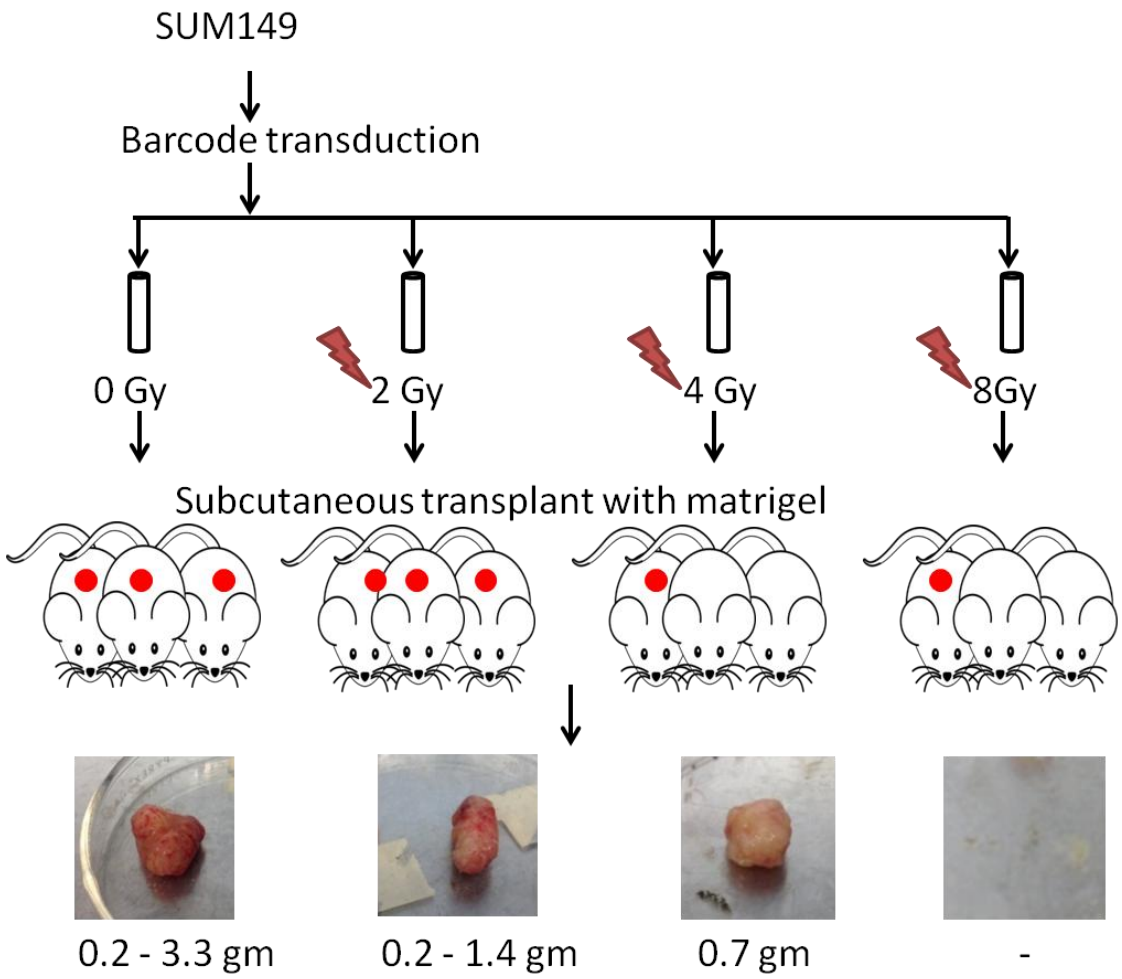

Figure 3.1: Experimental design for assessing the effect of radiation on the i*n vivo* tumorigenic activity of SUM149 cells

SUM149 cells were irradiated in suspension at increasing doses and then subcutaneously transplanted into NRG mice together with Matrigel (500,000 cells/mouse). After 11 weeks, mice were euthanized and tumours were collected. As illustrated, the tumour sizes decreased as a function of the dose of irradiation that the input cells had received.

Table 3.1: Table showing tumours retrieved from initially irradiated transplanted cells, at different time points

Radiation Gy	@ 11 wks	@ 14 wks	@ 24 wks	Tumour weight (g)*
0	100% (3/3)			3.3, 0.2, 0.8
2	100% (3/3)			0.4, 1.4, 0.2
4	33% (1/3)			0.7
		1/2		1.2
			1/1	0.3
8	0% (0/3)			-
		0/2		-
			2/2	1.0, 0.2

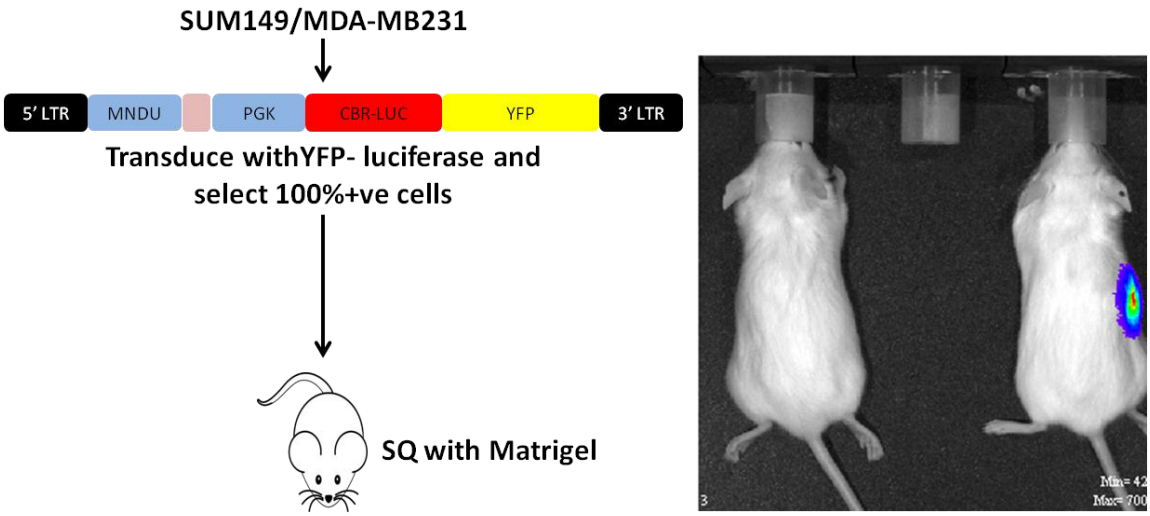

Figure 3.2: Experimental design used to analyze the *in vivo* tumorigenic activity of SUM149 and MDA-MB231 cells.

Cells from the SUM149 and MDA-MB231 cell lines were transduced with a lentiviral CBR-luciferase vector and YFP-positive cells were isolated by FACS after 48 hours in culture. Graded doses of each cell line were then injected into female NRG mice subcutaneously with Matrigel and resulting tumour formation was assessed by the detection of luciferase activity.

Table 3.2: Table showing weight of tumours and number of cells/tumour generated from SUM149 and MDA-MB231

SUM149					
Cell dose	Tumour #	Tumour weight (gm)	Cells/tumour	Average weight (gm)	Average cells/tum
250,000	1	1.08	2.70E+07		
	2	0.38	1.80E+07		
				0.73	2.25E+07
50,000	1	0.07	3.60E+06		
	2	0.38	1.05E+07		
	3	0.38	2.15E+07		
	4	0.235	1.11E+07		
	5	0.35	2.50E+07		
	6	0.775	3.75E+07		
				0.365	1.82E+07
10,000	1	0.63	2.00E+07		
	2	0.76	1.76E+07		
	3	0.55	1.65E+07		
	4	0.46	2.34E+07		
	5	0.325	1.97E+07		
	6	0.335	2.40E+07		
	7	0.35	2.90E+07		
				0.49	1.88E+07

Cell dose	Tumour #	weight (gm)	Cells/tumour	Avg wt (gm)	Avg cells/tum
2000	1	0.11	4.50E+06		
	2	0.15	4.60E+06		
	3	0.24	4.80E+06		
	4	0.27	6.30E+06		
	5	0.23	3.25E+06		
	6	0.295	9.00E+06		
	7	0.22	5.80E+06		
	8	0.3	1.12E+07		
				0.226875	6.18E+06
400	1	0.01	1.00E+05		
	2	0.076	3.30E+06		
	3	0.116	5.60E+03		
	4	0.03	1.30E+06		
				0.058	1.18E+06
200	1	0.02	1.05E+06		
	2	0.0185	1.15E+06		
	3	0.175	3.50E+06		
	4	0.085	5.00E+06		
				0.074625	2.68E+06
20	1	0.85	5.00E+06		
	2	0.04	3.00E+06		
	3	0.1	5.00E+06		
	4	0.03	5.00E+05		
				0.26	3.38E+06

MDA-MB231					
Cell dose	**Tumour #**	**weight (gm)**	**Cells/tumour**	**Avg wt (gm)**	**Avg cells/tum**
200,000	**1**	**0.21**	**9.00E+06**		
20,000	**1**	**0.18**	**9.50E+06**		
	2	**0.20**	**2.50E+07**		
	3	**0.32**	**4.76E+07**		
				0.23	**2.74E+07**
10,000	**1**	**0.195**	**1.76E+07**		
	2	**0.215**	**3.48E+07**		
				0.21	**2.62E+07**
2,000	**1**	**0.11**	**3.67E+06**		
	2	**0.27**	**3.08E+07**		
	3	**0.17**	**2.21E+07**		
				0.18	**1.88E+07**
200	**1**	**0.16**	**1.12E+07**		
	2	**0.165**	**5.36E+07**		
	3	**0.14**	**1.60E+07**		
				0.16	**2.69E+07**
20	**1**	**0.04**	**2.57E+06**		
	2	**0.02**	**1.60E+06**		
	3	**0.0225**	**2.40E+06**		
	4	**0.05**	**4.20E+06**		
				0.03	**2.69E+06**
2	**1**	**0.02**	**9.00E+05**		

Cell dose	Tumour #	weight (gm)	Cells/tumour	Avg wt (gm)	Avg cells/tum
1	**1**	**0.02**	**6.00E+05**		
	2	**0.017**	**9.00E+05**		
				0.0185	**7.50E+05**

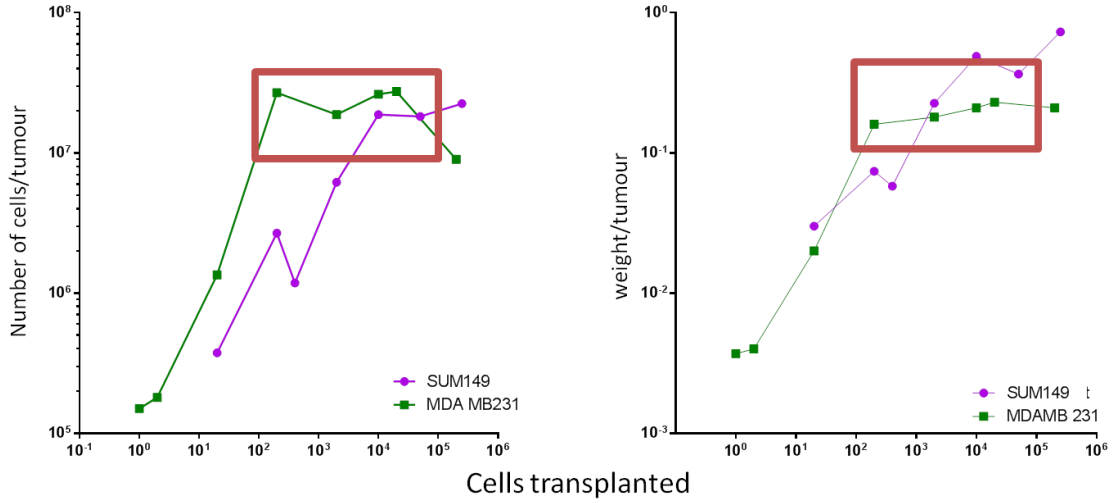

Figure 3.3: Dose-response relationships of tumour formation endpoints vs. input cell numbers.

Different numbers of MDA-MB231 and SUM149 cells were injected into NRG mice and two measurements of tumour size (weight and number of cells per tumour) were made after the mice were euthanized 6-8 weeks later. The results showed a linear correlation between the number of cells transplanted and tumour size up to approximately 500 input MDA-MB231 cells and 10,000 input SUM149 cells (i.e., a 20-fold difference). The red boxes show doses at which there is a loss of a linear relationship between the number of cells transplanted to generate a tumour and the number of cell retrieved- and weight- per tumour, respectively.

Table 3.3: LDA of TIC frequency in SUM149 and MDA-MB231 cells

Cells per mouse	+/total mice (SUM149)
1	2/20
20	5/20
200	11/12
400	4/4
2000	12/12

Cells per mouse	+/total mice (MDA-MB231)
1	9/20*
2	3/14
20	17/22
200	11/11
2000	11/11

* at 6-7 weeks, 12/30 at 13 weeks

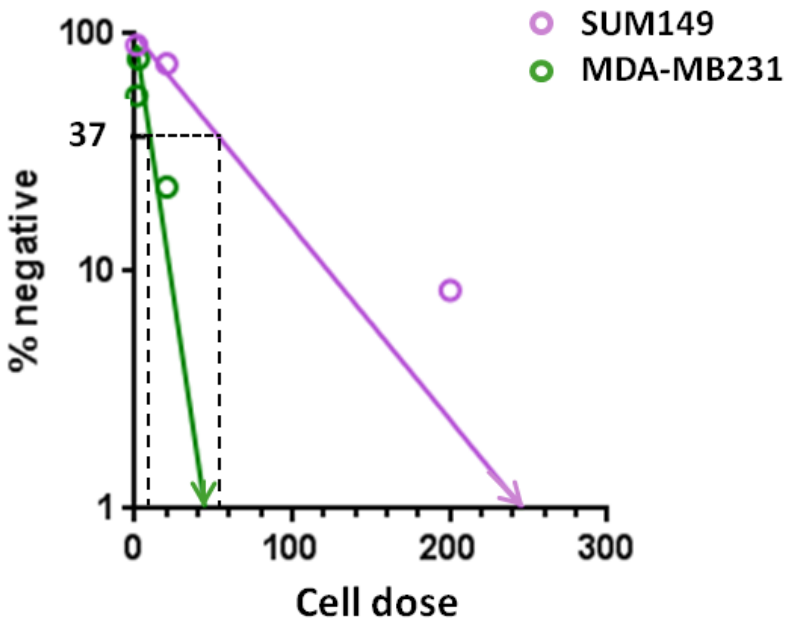

Figure 3.4: LDA of the frequency of TIC of SUM149 and MDA-MB231cells at 6 weeks.

Assuming a Poisson distribution, the frequency of the cell of interest is determined by the relationship $F_0 = e^{(-m)}$ where F_0 is the fraction of negative readout at a particular cell dose transplanted and m is the average number of cells per transplant. Thus, to calculate the cell dose where, on average, one TIC is transplanted, m=1 and F_0=0.368 (or 37% fraction negative readout). TIC frequencies from Table 3.3 are computed to be 1 in 65 SUM149 cells (95% CI= 1/36 – 1/116) and 1 in 9 MDA-MB231 cells (95% CI= 1/5.7 – 1/14).

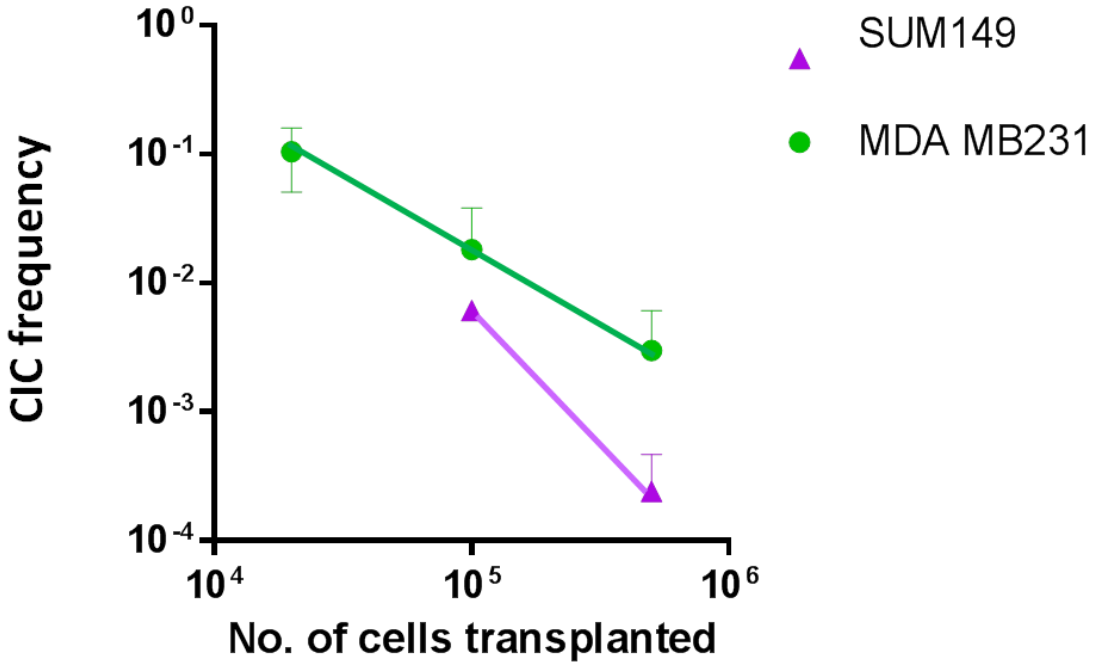

Figure 3.5: Inverse relationship between number of SUM149 or MDA-MB231 cells transplanted and the number of clones detected.

Results of DNA analysis of the number of clones formed in tumours derived from >30,000 viable input cells are shown. Adapted from [28]. CIC frequency refers to the frequency of cells capable of making detectable clonal progeny in a polyclonal tumour as assessed by lentivirally barcoding the cells initially transplanted.

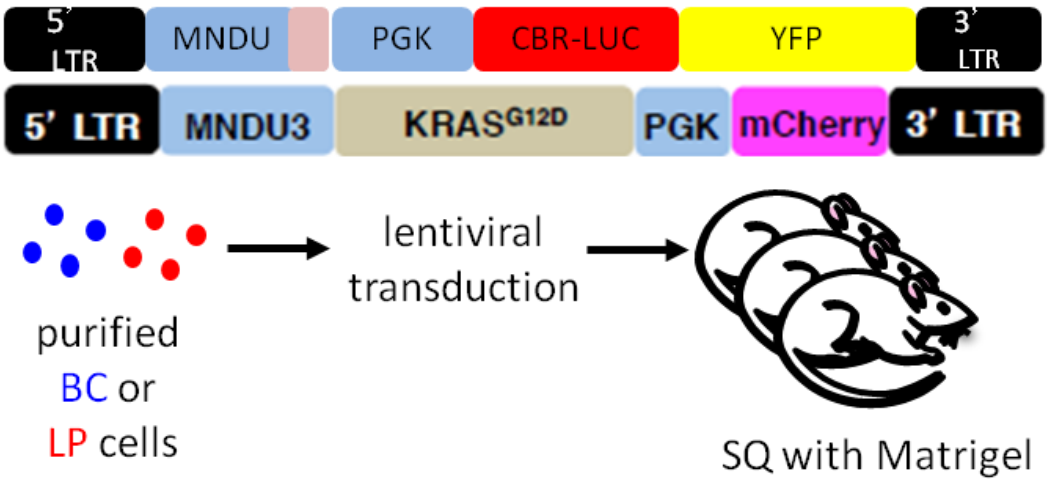

Figure 3.6: Experimental design to measure primary tumour growth from decreasing numbers of *KRAS*^{G12D}-transduced normal mammary cells.

Purified BCs and LPs were co-transduced with two lentiviral constructs, one containing CBR-Luciferase and the other containing the oncogenic *KRAS*^{G12D}. These transduced cells were then transplanted into NRG mice subcutaneously with Matrigel in serially diluted input cell doses.

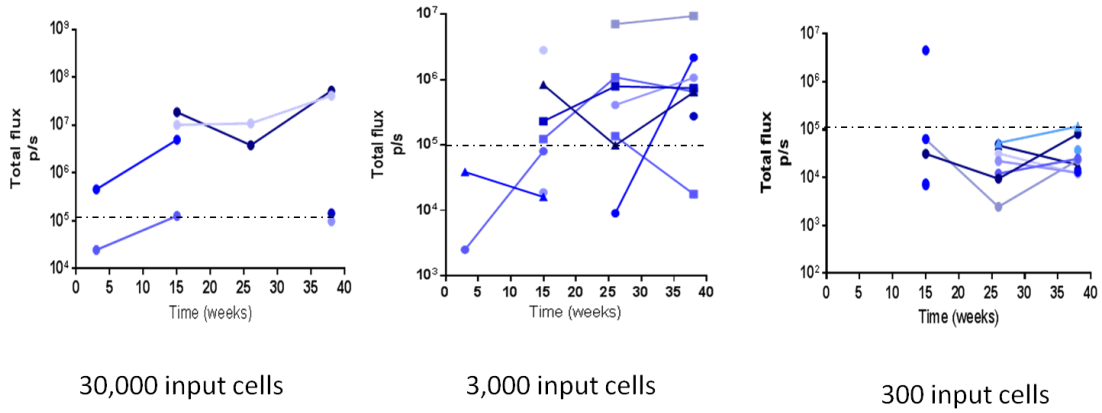

Figure 3.7: Kinetics of tumour growth with different input doses of *KRAS*^{G12D}-transduced BCs.

Shown here in photons/second (p/s) are luciferase signals obtained in a representative series of mice injected with input cell doses ranging from 300 to 30,000 transduced cells. 10^5 p/s was chosen as the threshold to indicate a positive signal. Data shown is from 3 different experiments, each assessed and terminated at different time points ranging from 3 to 40 weeks post-transplant. Lines between individual points show kinetics of tumour growth in individual mice.

Table 3.4: LDA to examine the relationship between transplanted *KRAS*^{G12D}-transduced BCs or LPs and the appearance of a positive luciferase signal (=measure of tumour formation)

Number of BCs or LPs transplanted	+/total mice (BCs)	+/total mice (LPs)
30	**0/8**	**0/8**
300	**2/16**	**2/6**
3000	**7/12**	**3/4**
30000	**5/6**	**2/2**

Calculated by luciferase assessment over 40 weeks.

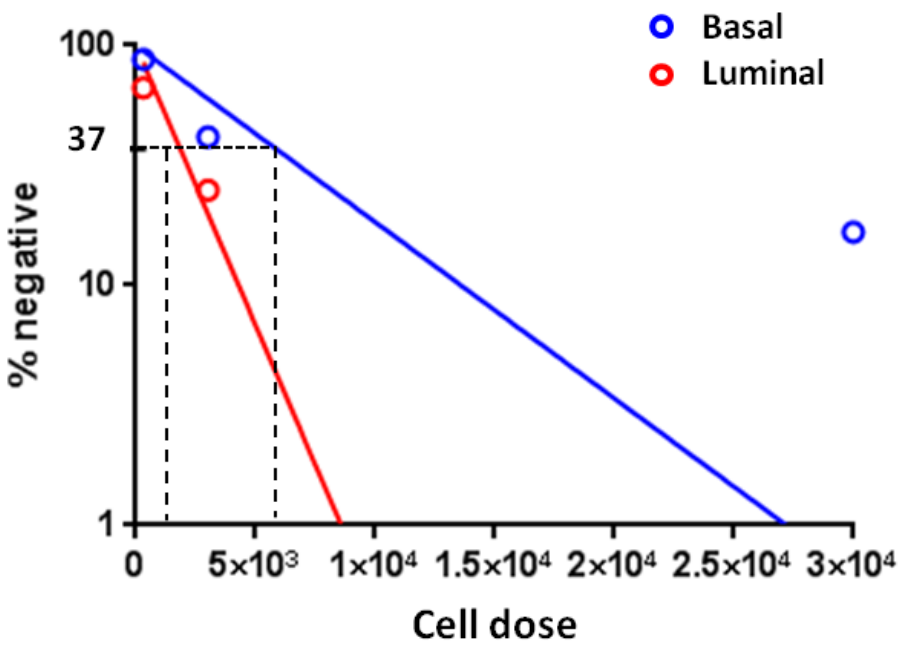

Figure 3.8: LDA of the frequency of TICs of transplanted BCs and LPs transduced with *KRAS*^{G12D}.

Assuming a Poisson distribution, the frequency of the cell of interest is determined by the relationship $F_0 = e^{(-m)}$ where F_0 is the fraction of negative readout at a particular cell dose transplanted and m is the average number of cells per transplant. Thus, to calculate the cell dose where on average one TIC is transplanted, m=1 and F_0=0.368 (or 37% fraction negative readout). TIC frequencies computed from Table 3.4 are 1 in 6,400 cells (95% CI= 1/2969 – 1/13981) for BCs and 1 in 1,500 cells (95% CI= 1/571 – 1/4352) for LPs [180].

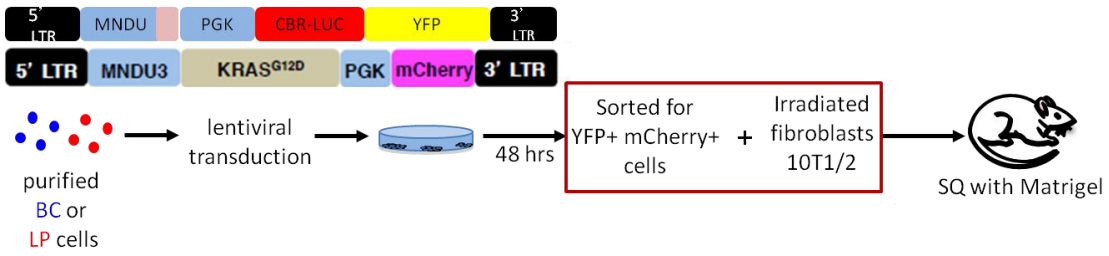

Figure 3.9: Protocol to obtain enhanced detection of TICs from low numbers of *KRAS^{G12D}*-transduced primary cells.

After the initial transduction of purified BCs and LPs with the lentiviral constructs, transduced cells were cultured *in vitro* for 48 hours and then YFP+mCherry+ cells were isolated by FACS. These cells were then co-transplanted subcutaneously with irradiated 10T1/2 fibroblasts suspended in Matrigel into NRG mice.

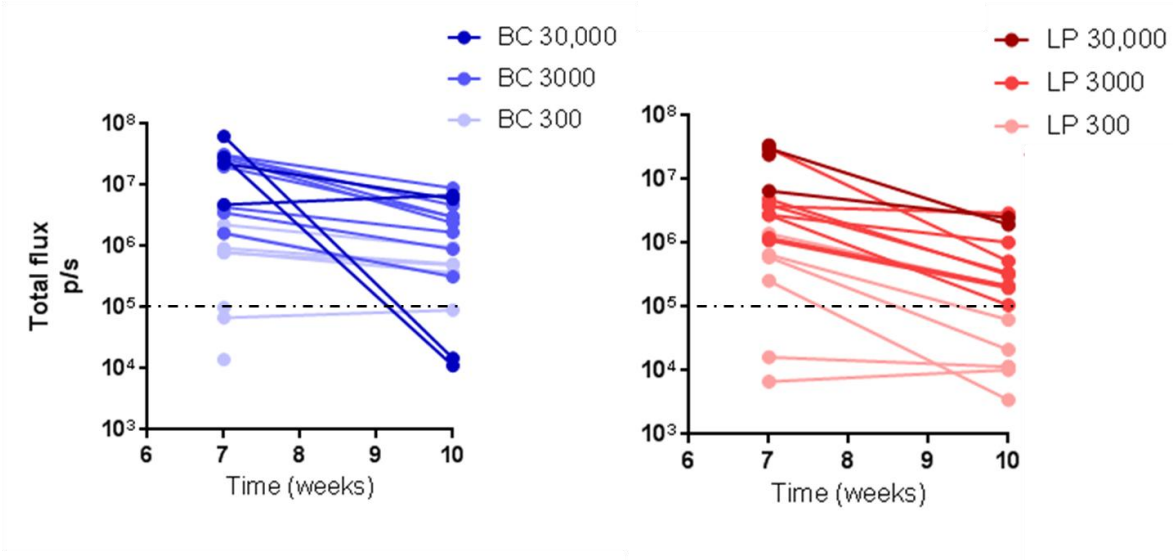

Figure 3.10: Luciferase detection of outputs of decreasing numbers of *KRAS^{G12D}*-transduced BCs or LPs when co-transplanted with irradiated fibroblasts.

Each pair of points indicates data for a single transplant 10^5 photons/second as a threshold to identify positive outputs.

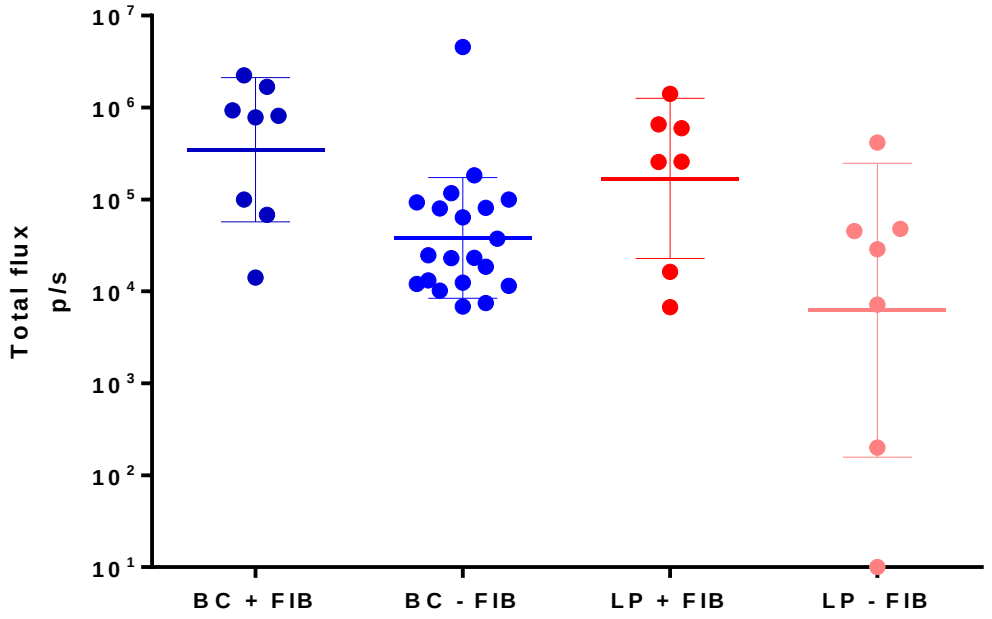

Figure 3.11: Comparison of luciferase signals generated by the outputs of 300 *KRAS*^{G12D}-transduced cells with and without co-injected irradiated fibroblasts.

Shown here are data comparing output signals when these were maximal (at 7-10 weeks post-transplant when fibroblasts were co-injected and at 15-38 weeks when no fibroblasts were injected). Data shown are taken from Fig 3.6 (and matching LP data not shown) and Fig 3.8.

Table 3.5: LDA of the frequency of TICs in *KRAS*^{G12D}-transduced cells assayed with co-transplanted irradiated fibroblasts

Number of BCs or LPs transplanted	+/total mice (BCs)	+/total mice (LPs)
30	5/16	0/12
200	8/8	6/8
300	14/24	6/20
2000	4/4	6/6
3000	10/10	10/12
30000	2/2	5/6

Calculated by luciferase assessment at 8 weeks.

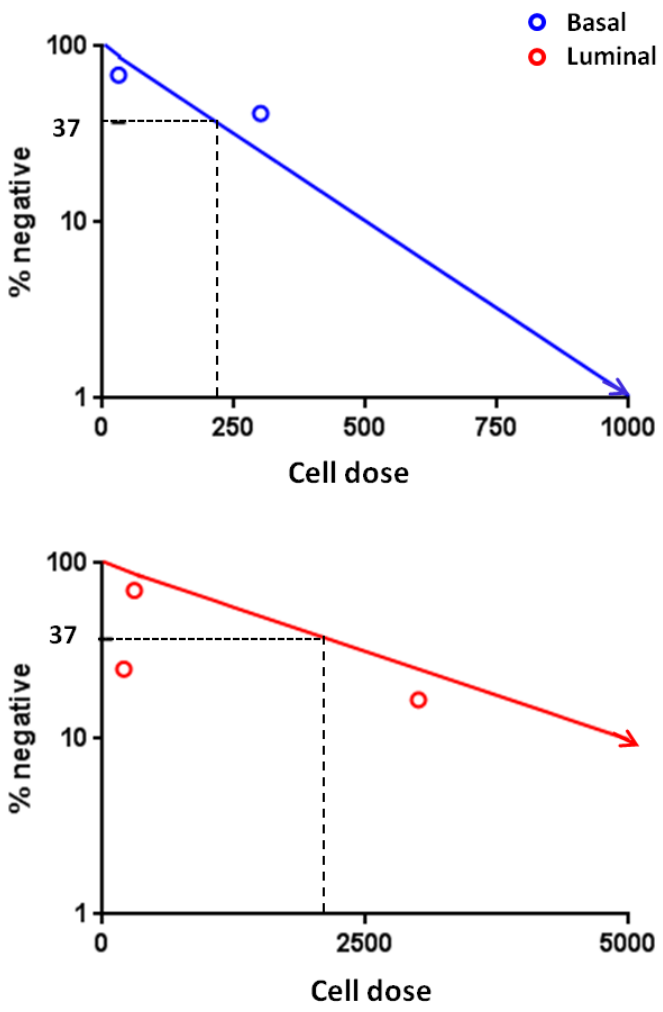

Figure 3.12: LDA of the frequency of TICs in *KRAS*^{G12D}-transduced cells assayed with co-transplanted irradiated fibroblasts.

Assuming a Poisson distribution, the frequency of cell of interest is determined by the relationship $F_0 = e^{(-m)}$ where F_0 is the fraction of negative readout at a particular cell dose transplanted and m is the average number of cells per transplant. Thus, to calculate the cell dose where on average one TIC is transplanted, m=1 and F_0=0.368 (or 37% fraction negative readout). TIC frequencies computed from Table 3.5 are 1 in 211 BCs (95% CI=1/139 - 1/320) and 1 in 2,100 LPs (95% CI=1/1264 – 1/3518) [180].

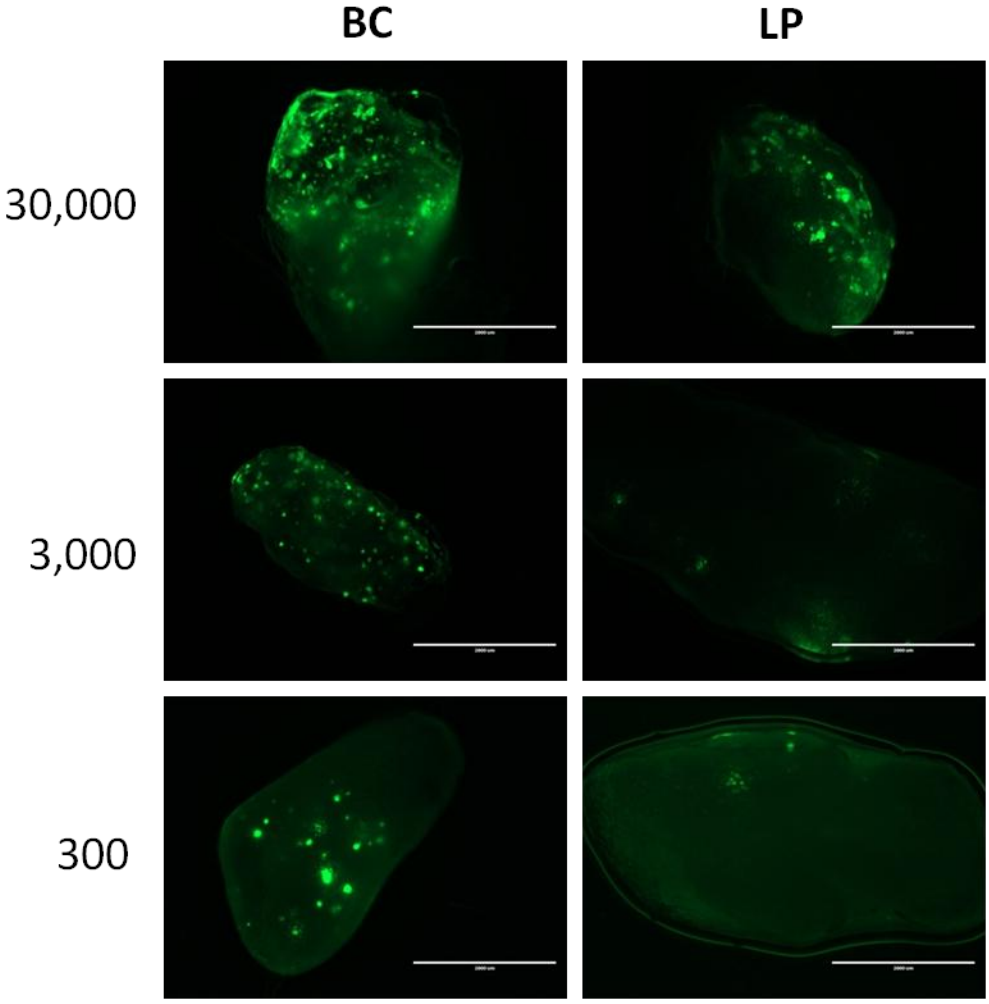

Figure 3.13: Representative fluorescence images of cell outputs from low transplant doses of *KRAS*^{G12D}-transduced primary cells.

Shown here are photomicrographs of gels retrieved from mice transplanted with different input BCs and LPs cell doses (numbers shown to the left of the photomicrographs) and harvested 8 weeks later. Bars show scale: 2000µm.

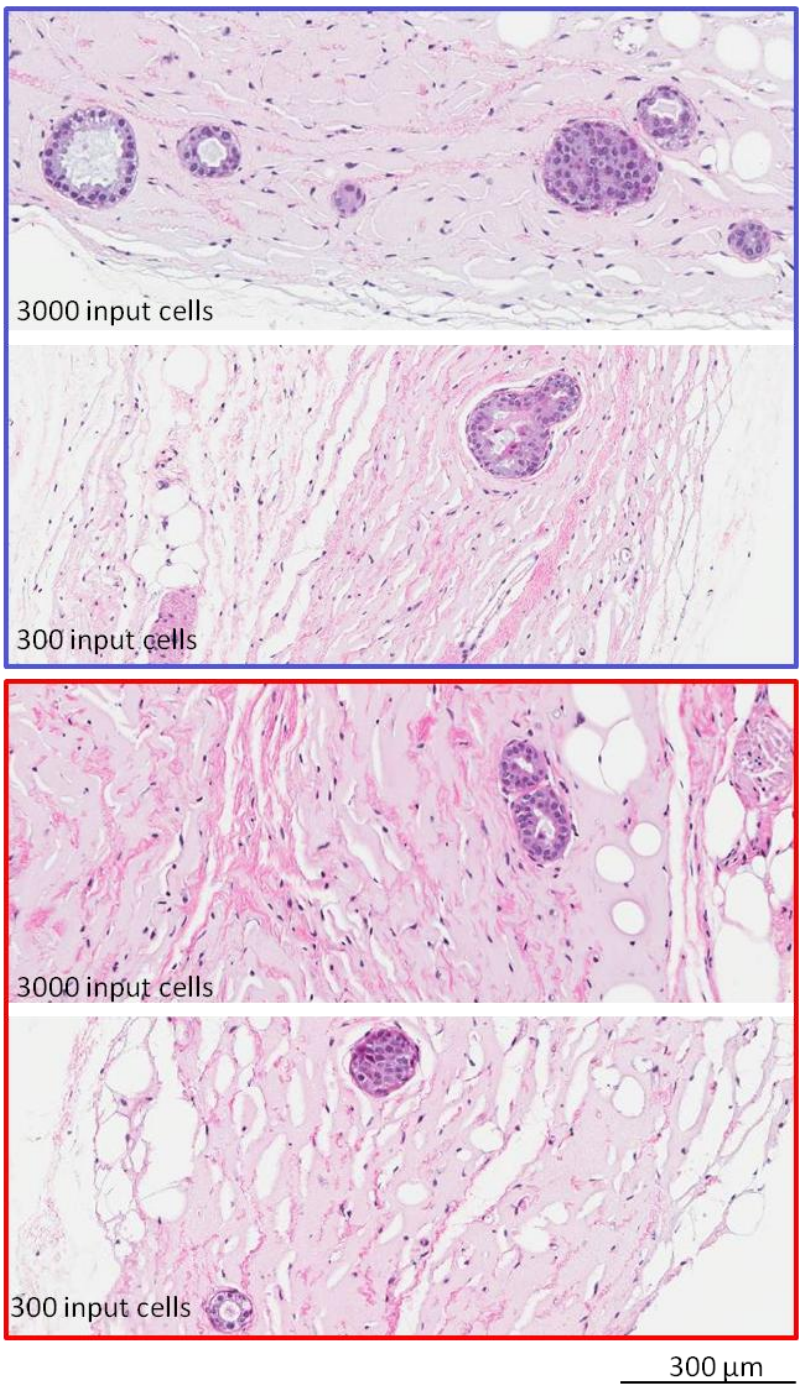

Figure 3.14: Representative H and E stained sections of abnormal structures generated from 300-3,000 *KRAS*^{G12D}-transduced BCs (in blue) or LPs (in red) in gels harvested 8 weeks post-transplant.

These tumours were positive by luciferase imaging.

Table 3.6: Table showing frequency of serial transplantable tumours obtained from primary tumours generated from different inputs of *KRAS*^{G12D}-transduced BCs or LPs

Donor	Initiating cells (source & number)	Primary Tumor	Secondary Tumor	Tertiary Tumor	Quaternary Tumor
42-14	BC (100K)	Yes (>460K)	Yes (>200K)	Yes	No
19-15	BC (30K)	Yes	No		
42-14	LP (220K)	Yes (>22K)	Yes (>60K)	Yes (3K)	No
28-14	LP (100K)	Yes	Yes	Yes	Yes
29-15	LP (100K)	Yes (>120K)	Yes (8K)	No	
30-15	LP (100K)	Yes (>460K)	Yes (6K)	No	
32-15	LP (100K)	Yes (>103K)	Yes (5K)	No	
4-15	LP (100K)	Yes	Yes	No	
34-15	LP (100K)	Yes (>63K)	No		
44-15	LP (100K)	Yes (>43K)	No		
23-14	LP (100K)	Yes	No		
29-15	LP (60K) cult	Yes (>280K)	Yes (6K)	Yes	
32-15	LP (30K) cult	Yes (>160K)	Yes (12K)	Yes	
19-15	LP (30K)	Yes	Yes		
41-15	LP (30K)	Yes	No		

Chapter 4: Conclusions and future perspectives

4.1 Summary of Findings

The objective of this thesis was to determine if and how primary sources of two major subsets of normal human mammary epithelial cells, BCs and LPs respond to radiation and how this might compare to their representative *de novo* transformed counterparts. Overall the major findings from can be summarized as follows:

LP-CFCs are more radioresistant than BC-CFCs: Survival curves for acute X-ray dose-responses of the proliferative activity of these cells revealed typical log-linear relationships similar to other mammalian cells [182-186] with a ~1.5-fold greater radioresistance of LP- versus BC-CFCs as reflected in the slopes of their respective survival curves. This finding is consistent with the rapidly reduced (within 48 hours) X-ray-induced levels of apoptosis exhibited by the entire LP versus BC populations, but was not predicted by immediate X-ray induced γH2AX foci which were higher in the LPs than in the BCs. However, the latter finding is in keeping with previous evidence of higher levels of ROS, ROS-regulating enzymes and resistance to H_2O_2-induced increases in ROS in untreated LPs and tolerated DNA damage [118]. This may also explain the unexpected finding of a lack of sub-lethal damage repair activity in LP-CFCs inferred from the fractionated dose experiments in comparison to BC-CFC where evidence of repair was revealed despite the reduced "shoulder" on the BC-CFC survival curve and their intrinsically greater radiosensitivity.

In search of other mechanisms to explain the different radiosensitivities of these two normal human mammary cell types, we also assessed those implicated in checkpoint adaptation. This mechanism has been extensively studied in yeast [160, 161] but previously only in human cell lines [163-166]. Here we report evidence from RNA-seq and western blot analysis of increased phospho-PLK1 levels in LPs, suggesting that LPs may escape cell cycle arrest after radiation by upregulating *PLK1* activity.

Cell of origin may play a role in responsiveness to therapy: Access to a *de novo* human breast cancer model system offered the possibility to look directly at the effect of the cell-of-origin of a tumour on the radiosensitivity of its clonogenic cells. Interestingly, when primary human mammary BCs and LPs were transduced with $KRAS^{G12D}$ or a control vector and assessed immediately there was no immediate effect on the radiosensitivity of their CFCs attributable specifically to the expression of the $KRAS^{G12D}$-transgene, although their radiation sensitivities were increased by being subjected to the transduction procedure itself. The results presented here also showed that the clonogenic cells obtained from tumours derived from $KRAS^{G12D}$-induced transformation of either BCs and LPs were more radioresistant than their respective starting populations, although, when compared to one another, a slightly greater radioresistance was displayed by CFCs from the LP-derived tumours. Together, these findings suggest that the cell of origin may play a role in determining the intrinsic radiosensitivity of a given tumour, but other properties potentially linked to the process of tumorigenesis itself may be more significant determinants of the radiation sensitivity of the cells present.

Differential effects of growth responses of malignant cells ascertained *in vivo* and *in vitro:* It was found by transplanting different input cells into mice that the TIC for two cell lines MDA-MB231 and SUM149 was 1 in 9 and 1 in 63, respectively at 6-7 weeks. This frequency further increases for MDA-MB231 to 1 in 3 when assessed at 13 weeks. The TIC of BCs and LPs transduced with $KRAS^{G12D}$ was found to be 1/6400 for BCs and 1/1500 for LPs. However, the addition of fibroblasts increased this frequency to 1/211 for BCs and 1/2100 for LPs indicating the contribution of fibroblasts in the proliferation of cells.

Strengths and limitations: While this was the first study to understand the radiosensitivity in primary mammary epithelial cells, all analysis were performed *in vitro*. The *in vivo* clonogenic cells may behave differently and cannot be assayed *in vitro*. Secondly, the cells are removed from the living system and studied under atmospheric oxygen. Oxygen has a definite effect on radiation and this is not taken into account. However the goal was to study the innate responses of cells independent of external factors and so although an interesting question, these studies are beyond the scope of this thesis. Similarly, the microenvironment and immune cells both in a normal as well as a malignant system are important players in the response of cells towards radiation. The use of *in vitro* systems and the use of immunocompromised mice as *in vivo* hosts to study tumorigenesis again prevent the investigation of these possibilities. It will be interesting to see how cells respond in the presence of these influencers.

Clonal tracking of TICs in large tumours also poses challenges. As was observed here in cell lines, the number of clones detected in tumours decreased with increasingly

large numbers of input cells used to generate the tumour. There are still questions left unanswered here. A possible mechanism at play for this observation can be cell-cell contact. Early competition for nutrients seems unlikely since these cells were injected subcutaneously in suspension as isolated cells. Another possibility could, however, be that cells may produce factors that inhibit their neighbouring cells through a process of lateral inhibition. Lateral inhibition regulated by *Notch* is known to play an integral role in mammary gland development and branching [187]. Finally, there is the possibility of inherent heterogeneity within the cells in their ability to initiate growth *in vivo* despite the high TIC content, given the prolonged interval of time taken for some tumours to arise from single cells transplanted *in vivo*.

Although even careful exploitation of the barcoding approach may be one of very few ways to analyze TIC responses *in vivo*, a technical difficulty inherent in its use is the threshold limit of detecting clones containing <100 cells. This limitation can be reduced using known barcodes and fluorochromes, but also restricts the total number of TICs that can be examined to ~200. This is not a barrier to studies of cell lines but may not yet be sufficient for primary cells.

Significance/Clinical Implications: These studies have provided new foundational data required to interpret *in vivo* treatment effects on clonogenic tumorigenic human mammary cells by first establishing a range of clonogenic cell frequencies for which there is a positive relationship between their number and their activity. In addition, they have addressed the utility and defined protocols for using DNA barcoding to examine the ability of different treatments to suppress the growth potential of tumorigenic human

mammary cells. In particular, the definition and comparison of sensitivities of tumorigenic cells originating from different human mammary epithelial cells isolated directly from normal tissue and transformed with the same mutant oncogenes have provided some definitive answers to the contribution of the cell of origin to the X-ray sensitivity of tumorigenic cells originating from different cell types. These results can serve as an interesting basis of comparison with cells from breast cancers that arise in patients and also subtypes that have been previously described and shown to have a high rate of relapse. It is also interesting to note that secondary tumours were generated only from primary tumours initiated with 10-100 times more $KRAS^{G12D}$-transduced LPs or BCs than the number shown to be able to produce primary tumours. This suggests that secondary TICs may have different properties and be more relevant assessing a clinical response to a given treatment.

4.2 Future Directions

4.2.1. Technological advances for future analysis of TIC genesis and characterizations

Technological advances are well known to be the drivers of new information. Nowhere is this more relevant than to current issues of interest in the general arena of biomedicine. In the field of human cell oncogenesis, three technologies are of particular relevance here: organoid cultures, reprogramming and CRISPR/Cas9. Organoid culture systems allow more faithful tissue generation from primitive normal cells and are showing promise for

supporting the expansion *in vitro* of cells derived directly from human tumours [179, 188, 189]. Reprogramming allows permanent clonal lines of induced pluripotent stem cells (iPSCs) to be generated from individual malignant cells. CRISPR/Cas9 enables the use of precise gene editing to create new models of human tumours and to test the role of specific genetic alterations in establishing or maintaining the transformed status of patient-derived malignant cells.

Organoids: This term refers to 3D structures generated in suspension cultures under conditions where 2D growth of attached cells is blocked or prevented (either by suspending the cells in a semi-solid medium like Matrigel or by the use of a culture container that prevents cell attachment). The generation of 3D organoids to engineer tissues that are histologically and functionally more similar to their *in vivo* counterparts will facilitate the modeling of human disorders, performing drug screens, and the creation *in vitro* of replacement tissues and/or organs. Methods combining directed differentiation of cells in culture systems that promote organoid formation are being developed for many complex tissues such as the liver, kidney, intestine, eye, and brain, to name a few [190]. The advantages of human organoid cultures include better control of the cellular milieu than is associated with tumorigenesis *in vivo*, better spatial organization of cell types than is achieved in 2D *in vitro* systems and improved mimicry of *in vivo* cell behaviour, potential for larger scale testing of variables and drug effects, and reduced ethical concerns and costs associated with animal xenograft experiments.

iPSCs: iPSC technology offers a novel method of capturing the genomic state of single cells from almost any source, including transformed cells. However, this comes at the cost of losing the malignant phenotype of the original cells from which each iPSC clone is derived. Nevertheless, from the limited experience where it has been applied to the study of cancer to date, it appears that at least some properties of the malignant cells of origin may be reactivated by stimulating the iPSCs to differentiate back into the lineage or tissue from which the malignant cells arose and may then also be used for drug screening [191, 192]. iPSCs have been derived from human chronic phase CML cells with documented retention and expression of the signature *BCR-ABL1* fusion gene[193-195]. Additional examples of human hematopoietic cells from which iPSCs (or iPSC-like cells) have been obtained include cells from patients with myelodysplastic syndromes (MDS) [196], polycythemia vera [197], juvenile myelomonocytic leukemia [198], as well as originally normal human hematopoietic cells forced to overexpress *MLL* [199]. iPSCs have also been generated from human pancreatic ductal adenocarcinomas [200], multiple endocrine neoplasia type 2A (MEN2A) [201], bladder cancer cell lines [202] and cells from an individual with Li Fraumeni syndrome, a congenital cancer predisposition genotype in which one allele of the p53 gene is mutated [203]. In this case, the iPSCs were used to study the epigenetic states of tumour formation [204] and the bidirectional reversibility of epigenetic processes associated with iPSC reprogramming [205].

The advantages of using iPSC are a reduced chance of immunorejection since the transplanted iPSCs can be generated from the patients, themselves. iPSCs also have the potential for unlimited expansion and are thus amenable to gene targeting, correction and disease modeling hence providing a personalized approach for evaluating drugs on a

patient-by-patient basis, lowering costs and risk of clinical trials and with lower ethical issues compared to embryonic stem cells [206]. On the flipside, iPSCs appear largely restricted to differentiate into embryonic/fetal tissues and suffer from line variability [207].

CRISPR/Cas9: The CRISPR/Cas9 technology originates from type II CRISPR-Cas systems that evolved to provide bacteria with a form of adaptive immunity to viruses and plasmids. The CRISPR-associated Cas9 protein is an endonuclease that introduces a site-specific double-strand break into DNA. The ability of CRISPR/Cas9 to introduce DSBs at defined positions using a guide RNA can also be used to generate human cell lines and primary cells bearing chromosomal translocations resembling those described in human cancers. Examples to date include lung cancer [208], AML [209], and Ewing's sarcoma [210]. An improved method to generate models of liver cancer or myeloid malignancy in mice using CRISPR/Cas9 was also recently reported [211, 212]. Combining CRISPR/Cas9 with barcoding has been used to track the clonal dynamics of lung cancer cells during their acquired resistance to EGFR inhibitors and subsequent response to combined drug therapies [213, 214]. Combining the generation of iPSCs with CRISPR/Cas9 holds the future possibility of both creating new models of human cancer and of testing the ultimate therapeutic potential of gene targeting approaches.

Implications for present findings: The findings presented in this thesis suggest many new avenues of investigation. Here shown are the advantages and importance of exploiting *de novo* models of primary human cell oncogenesis to interrogate independently different parameters that determine treatment sensitivities and responses at

the level of the clonogenic cells responsible for normal tissue and tumour maintenance. From the results presented here, it should now be possible to assess the *responses* to X-irradiation of LP and BC-derived *KRAS*^{G12D}-transformed TICs within tumours at a clonal level and compare the results with their independently measured *sensitivity*. For this, the use of tumours generated from barcoded cells may be useful to track clones that respond differently to radiation, as long as clonal competition or overcrowding in the initiation of tumour formation is avoided. Such studies, in turn, will help to focus on factors associated with the ability of the cells within the tumour to grow after exposure as compared to their assessment under *in vitro* or *in vivo* conditions optimized for clonal growth. Such studies might then also be extended to assessment of the response determinants of cells in patient-derived-xenografts.

Further studies to determine whether alterations in *PLK1* are responsible for checkpoint adaptation in irradiated mammary LPs and hence for the greater radioresistance of their CFC will also be of interest. For example, genetic strategies to reduce *PLK1* in LPs and BCs might reveal differential effects on their arrest in G_2 and subsequent death. *PLK1* can play a role in mitosis, damage and repair. Recent studies now support the notion of *PLK1* as a master regulator and coordinator of mitotic kinase signaling by having direct effects on kinases such as Aurora B and Haspin [215]. *PLK1* promotes mitotic entry, thus it is inactivated and degraded upon induction of a DNA damage response [216]. It also negatively regulates DNA damage signaling cascade by phosphorylating checkpoint scaffolding proteins causing inactivation of Chk2 [217]. Furthermore, *PLK1* may also play a role in *p53* and *FoxM1* regulation further influencing DNA damage response [218], as well as regulating *BRCA1*, a key mediator of efficient

DSB repair through homologous recombination [219]. Due to *PLK1*'s involvement in the cell-cycle progression and regulation that are relevant to cancer, it is considered a targetable gene. Hence inhibitors against *PLK1* are now available and in different phases of clinical trial [220]. It is also possible that checkpoint adaptation alone is not solely able to explain why more CFCs survive after radiation. Further exploration into the roles of various DNA repair pathways will thus clearly be of interest.

References

1. Novaro V, Roskelley CD, Bissell MJ: **Collagen-IV and laminin-1 regulate estrogen receptor alpha expression and function in mouse mammary epithelial cells**. *J Cell Sci* 2003, **116**(14):2975-2986.
2. Eirew P, Stingl J, Raouf A, Turashvili G, Aparicio S, Emerman JT, Eaves CJ: **A method for quantifying normal human mammary epithelial stem cells with in vivo regenerative ability**. *Nature medicine* 2008, **14**(12):1384-1389.
3. Lim E, Vaillant F, Wu D, Forrest NC, Pal B, Hart AH, Asselin-Labat ML, Gyorki DE, Ward T, Partanen A *et al*: **Aberrant luminal progenitors as the candidate target population for basal tumor development in BRCA1 mutation carriers**. *Nature medicine* 2009, **15**(8):907-913.
4. Shehata M, Teschendorff A, Sharp G, Novcic N, Russell IA, Avril S, Prater M, Eirew P, Caldas C, Watson CJ *et al*: **Phenotypic and functional characterisation of the luminal cell hierarchy of the mammary gland**. *Breast cancer research : BCR* 2012, **14**(5):R134.
5. Guo W, Keckesova Z, Donaher JL, Shibue T, Tischler V, Reinhardt F, Itzkovitz S, Noske A, Zurrer-Hardi U, Bell G *et al*: **Slug and Sox9 cooperatively determine the mammary stem cell state**. *Cell* 2012, **148**(5):1015-1028.
6. Lim E, Wu D, Pal B, Bouras T, Asselin-Labat ML, Vaillant F, Yagita H, Lindeman GJ, Smyth GK, Visvader JE: **Transcriptome analyses of mouse and human mammary cell subpopulations reveal multiple conserved genes and pathways**. *Breast cancer research : BCR* 2010, **12**(2):R21.
7. Makarem M, Kannan N, Nguyen LV, Knapp DJ, Balani S, Prater MD, Stingl J, Raouf A, Nemirovsky O, Eirew P *et al*: **Developmental changes in the in vitro activated regenerative activity of primitive mammary epithelial cells**. *PLoS biology* 2013, **11**(8):e1001630.
8. Kannan N, Huda N, Tu L, Droumeva R, Aubert G, Chavez E, Brinkman RR, Lansdorp P, Emerman J, Abe S *et al*: **The luminal progenitor compartment of the normal human mammary gland constitutes a unique site of telomere dysfunction**. *Stem cell reports* 2013, **1**(1):28-37.
9. Fu N, Lindeman GJ, Visvader JE: **The mammary stem cell hierarchy**. *Current topics in developmental biology* 2014, **107**:133-160.
10. Raouf A, Zhao Y, To K, Stingl J, Delaney A, Barbara M, Iscove N, Jones S, McKinney S, Emerman J *et al*: **Transcriptome analysis of the normal human mammary cell commitment and differentiation process**. *Cell stem cell* 2008, **3**(1):109-118.
11. Chakrabarti R, Hwang J, Andres Blanco M, Wei Y, Lukacisin M, Romano RA, Smalley K, Liu S, Yang Q, Ibrahim T *et al*: **Elf5 inhibits the epithelial-mesenchymal transition in mammary gland development and breast cancer metastasis by transcriptionally repressing Snail2**. *Nature cell biology* 2012, **14**(11):1212-1222.

12. Theodorou V, Stark R, Menon S, Carroll JS: **GATA3 acts upstream of FOXA1 in mediating ESR1 binding by shaping enhancer accessibility**. *Genome research* 2013, **23**(1):12-22.
13. Gascard P, Bilenky M, Sigaroudinia M, Zhao J, Li L, Carles A, Delaney A, Tam A, Kamoh B, Cho S *et al*: **Epigenetic and transcriptional determinants of the human breast**. *Nature communications* 2015, **6**:6351.
14. Pellacani D, Bilenky M, Kannan N, Heravi-Moussavi A, Knapp D, Gakkhar S, Moksa M, Carles A, Moore R, Mungall AJ *et al*: **Analysis of Normal Human Mammary Epigenomes Reveals Cell-Specific Active Enhancer States and Associated Transcription Factor Networks**. *Cell reports* 2016, **17**(8):2060-2074.
15. Knapp D, Kannan N, Pellacani D, Eaves CJ: **Mass Cytometric Analysis Reveals Viable Activated Caspase-3(+) Luminal Progenitors in the Normal Adult Human Mammary Gland**. *Cell reports* 2017, **21**(4):1116-1126.
16. Stingl J, Eirew P, Ricketson I, Shackleton M, Vaillant F, Choi D, Li HI, Eaves CJ: **Purification and unique properties of mammary epithelial stem cells**. *Nature* 2006, **439**(7079):993-997.
17. Eirew P, Stingl J, Eaves CJ: **Quantitation of human mammary epithelial stem cells with in vivo regenerative properties using a subrenal capsule xenotransplantation assay**. *Nature protocols* 2010, **5**(12):1945-1956.
18. Kuperwasser C, Chavarria T, Wu M, Magrane G, Gray JW, Carey L, Richardson A, Weinberg RA: **Reconstruction of functionally normal and malignant human breast tissues in mice**. *P Natl Acad Sci USA* 2004, **101**(14):4966-4971.
19. Shackleton M, Vaillant F, Simpson KJ, Stingl J, Smyth GK, Asselin-Labat ML, Wu L, Lindeman GJ, Visvader JE: **Generation of a functional mammary gland from a single stem cell**. *Nature* 2006, **439**(7072):84-88.
20. Imren S, Fabry ME, Westerman KA, Pawliuk R, Tang P, Rosten PM, Nagel RL, Leboulch P, Eaves CJ, Humphries RK: **High-level beta-globin expression and preferred intragenic integration after lentiviral transduction of human cord blood stem cells**. *The Journal of clinical investigation* 2004, **114**(7):953-962.
21. Bystrykh LV, Verovskaya E, Zwart E, Broekhuis M, de Haan G: **Counting stem cells: methodological constraints**. *Nature methods* 2012, **9**(6):567-574.
22. Harkey MA, Kaul R, Jacobs MA, Kurre P, Bovee D, Levy R, Blau CA: **Multiarm high-throughput integration site detection: limitations of LAM-PCR technology and optimization for clonal analysis**. *Stem cells and development* 2007, **16**(3):381-392.
23. Kustikova O, Fehse B, Modlich U, Yang M, Dullmann J, Kamino K, von Neuhoff N, Schlegelberger B, Li Z, Baum C: **Clonal dominance of hematopoietic stem cells triggered by retroviral gene marking**. *Science* 2005, **308**(5725):1171-1174.
24. Schmidt M, Hoffmann G, Wissler M, Lemke N, Mussig A, Glimm H, Williams DA, Ragg S, Hesemann CU, von Kalle C: **Detection and direct genomic**

sequencing of multiple rare unknown flanking DNA in highly complex samples. *Human gene therapy* 2001, **12**(7):743-749.
25. Gerrits A, Dykstra B, Kalmykowa OJ, Klauke K, Verovskaya E, Broekhuis MJ, de Haan G, Bystrykh LV: **Cellular barcoding tool for clonal analysis in the hematopoietic system**. *Blood* 2010, **115**(13):2610-2618.
26. Schepers K, Swart E, van Heijst JW, Gerlach C, Castrucci M, Sie D, Heimerikx M, Velds A, Kerkhoven RM, Arens R *et al*: **Dissecting T cell lineage relationships by cellular barcoding**. *The Journal of experimental medicine* 2008, **205**(10):2309-2318.
27. Nguyen LV, Makarem M, Carles A, Moksa M, Kannan N, Pandoh P, Eirew P, Osako T, Kardel M, Cheung AM *et al*: **Clonal analysis via barcoding reveals diverse growth and differentiation of transplanted mouse and human mammary stem cells**. *Cell stem cell* 2014, **14**(2):253-263.
28. Nguyen LV, Cox CL, Eirew P, Knapp DJ, Pellacani D, Kannan N, Carles A, Moksa M, Balani S, Shah S *et al*: **DNA barcoding reveals diverse growth kinetics of human breast tumour subclones in serially passaged xenografts**. *Nature communications* 2014, **5**:5871.
29. Bhang HE, Ruddy DA, Krishnamurthy Radhakrishna V, Caushi JX, Zhao R, Hims MM, Singh AP, Kao I, Rakiec D, Shaw P *et al*: **Studying clonal dynamics in response to cancer therapy using high-complexity barcoding**. *Nat Med* 2015, **21**(5):440-448.
30. Klauke K, Broekhuis MJ, Weersing E, Dethmers-Ausema A, Ritsema M, Gonzalez MV, Zwart E, Bystrykh LV, de Haan G: **Tracing dynamics and clonal heterogeneity of Cbx7-induced leukemic stem cells by cellular barcoding**. *Stem cell reports* 2015, **4**(1):74-89.
31. Wu C, Li B, Lu R, Koelle SJ, Yang Y, Jares A, Krouse AE, Metzger M, Liang F, Lore K *et al*: **Clonal tracking of rhesus macaque hematopoiesis highlights a distinct lineage origin for natural killer cells**. *Cell stem cell* 2014, **14**(4):486-499.
32. Cheung AM, Nguyen LV, Carles A, Beer P, Miller PH, Knapp DJ, Dhillon K, Hirst M, Eaves CJ: **Analysis of the clonal growth and differentiation dynamics of primitive barcoded human cord blood cells in NSG mice**. *Blood* 2013, **122**(18):3129-3137.
33. Verovskaya E, Broekhuis MJ, Zwart E, Ritsema M, van Os R, de Haan G, Bystrykh LV: **Heterogeneity of young and aged murine hematopoietic stem cells revealed by quantitative clonal analysis using cellular barcoding**. *Blood* 2013, **122**(4):523-532.
34. Naik SH, Perie L, Swart E, Gerlach C, van Rooij N, de Boer RJ, Schumacher TN: **Diverse and heritable lineage imprinting of early haematopoietic progenitors**. *Nature* 2013, **496**(7444):229-232.
35. Barabe F, Kennedy JA, Hope KJ, Dick JE: **Modeling the initiation and progression of human acute leukemia in mice**. *Science* 2007, **316**(5824):600-604.
36. Van Keymeulen A, Rocha AS, Ousset M, Beck B, Bouvencourt G, Rock J, Sharma N, Dekoninck S, Blanpain C: **Distinct stem cells contribute to**

mammary gland development and maintenance. *Nature* 2011, **479**(7372):189-193.

37. Tsai YC, Lu Y, Nichols PW, Zlotnikov G, Jones PA, Smith HS: **Contiguous patches of normal human mammary epithelium derived from a single stem cell: implications for breast carcinogenesis**. *Cancer research* 1996, **56**(2):402-404.
38. **Breast Cancer Signs and Symptoms** [https://www.cancer.org/cancer/breast-cancer/about/breast-cancer-signs-and-symptoms.html] February 6, 2018.
39. Ferlay J, Soerjomataram I, Dikshit R, Eser S, Mathers C, Rebelo M, Parkin DM, Forman D, Bray F: **Cancer incidence and mortality worldwide: sources, methods and major patterns in GLOBOCAN 2012**. *International journal of cancer* 2015, **136**(5):E359-386.
40. Ferlay J, Steliarova-Foucher E, Lortet-Tieulent J, Rosso S, Coebergh JW, Comber H, Forman D, Bray F: **Cancer incidence and mortality patterns in Europe: estimates for 40 countries in 2012**. *Eur J Cancer* 2013, **49**(6):1374-1403.
41. Torre LA, Siegel RL, Ward EM, Jemal A: **Global Cancer Incidence and Mortality Rates and Trends--An Update**. *Cancer epidemiology, biomarkers & prevention : a publication of the American Association for Cancer Research, cosponsored by the American Society of Preventive Oncology* 2016, **25**(1):16-27.
42. Ginsburg O, Bray F, Coleman MP, Vanderpuye V, Eniu A, Kotha SR, Sarker M, Huong TT, Allemani C, Dvaladze A *et al*: **The global burden of women's cancers: a grand challenge in global health**. *Lancet* 2017, **389**(10071):847-860.
43. **Canadian Cancer Statistics 2016** [www.cancer.ca/statistics] November 22, 2017.
44. Winters S, Martin C, Murphy D, Shokar NK: **Breast Cancer Epidemiology, Prevention, and Screening**. *Progress in molecular biology and translational science* 2017, **151**:1-32.
45. Nattinger AB, Mitchell JL: **Breast Cancer Screening and Prevention**. *Annals of internal medicine* 2016, **164**(11):ITC81-ITC96.
46. **Canadian Task Force on Preventive Health Care** [https://canadiantaskforce.ca/breast-cancer-clinician-mammography-recommendation/]
47. Andre F, Pusztai L: **Molecular classification of breast cancer: implications for selection of adjuvant chemotherapy**. *Nature clinical practice Oncology* 2006, **3**(11):621-632.
48. Perou CM, Sorlie T, Eisen MB, van de Rijn M, Jeffrey SS, Rees CA, Pollack JR, Ross DT, Johnsen H, Akslen LA *et al*: **Molecular portraits of human breast tumours**. *Nature* 2000, **406**(6797):747-752.
49. Sorlie T, Perou CM, Tibshirani R, Aas T, Geisler S, Johnsen H, Hastie T, Eisen MB, van de Rijn M, Jeffrey SS *et al*: **Gene expression patterns of breast carcinomas distinguish tumor subclasses with clinical implications**. *P Natl Acad Sci USA* 2001, **98**(19):10869-10874.

50. Prat A, Perou CM: **Deconstructing the molecular portraits of breast cancer**. *Molecular oncology* 2011, **5**(1):5-23.
51. Herschkowitz JI, Simin K, Weigman VJ, Mikaelian I, Usary J, Hu Z, Rasmussen KE, Jones LP, Assefnia S, Chandrasekharan S *et al*: **Identification of conserved gene expression features between murine mammary carcinoma models and human breast tumors**. *Genome biology* 2007, **8**(5):R76.
52. Prat A, Parker JS, Karginova O, Fan C, Livasy C, Herschkowitz JI, He X, Perou CM: **Phenotypic and molecular characterization of the claudin-low intrinsic subtype of breast cancer**. *Breast cancer research : BCR* 2010, **12**(5):R68.
53. Kim HS, Park I, Cho HJ, Gwak G, Yang K, Bae BN, Kim KW, Han S, Kim HJ, Kim YD: **Analysis of the potent prognostic factors in luminal-type breast cancer**. *Journal of breast cancer* 2012, **15**(4):401-406.
54. Gonzalez-Angulo AM, Iwamoto T, Liu S, Chen H, Do KA, Hortobagyi GN, Mills GB, Meric-Bernstam F, Symmans WF, Pusztai L: **Gene expression, molecular class changes, and pathway analysis after neoadjuvant systemic therapy for breast cancer**. *Clinical cancer research : an official journal of the American Association for Cancer Research* 2012, **18**(4):1109-1119.
55. Bastien RR, Rodriguez-Lescure A, Ebbert MT, Prat A, Munarriz B, Rowe L, Miller P, Ruiz-Borrego M, Anderson D, Lyons B *et al*: **PAM50 breast cancer subtyping by RT-qPCR and concordance with standard clinical molecular markers**. *BMC medical genomics* 2012, **5**:44.
56. Ellis MJ, Suman VJ, Hoog J, Lin L, Snider J, Prat A, Parker JS, Luo J, DeSchryver K, Allred DC *et al*: **Randomized phase II neoadjuvant comparison between letrozole, anastrozole, and exemestane for postmenopausal women with estrogen receptor-rich stage 2 to 3 breast cancer: clinical and biomarker outcomes and predictive value of the baseline PAM50-based intrinsic subtype--ACOSOG Z1031**. *Journal of clinical oncology : official journal of the American Society of Clinical Oncology* 2011, **29**(17):2342-2349.
57. Paik S, Shak S, Tang G, Kim C, Baker J, Cronin M, Baehner FL, Walker MG, Watson D, Park T *et al*: **A multigene assay to predict recurrence of tamoxifen-treated, node-negative breast cancer**. *The New England journal of medicine* 2004, **351**(27):2817-2826.
58. Sotiriou C, Wirapati P, Loi S, Harris A, Fox S, Smeds J, Nordgren H, Farmer P, Praz V, Haibe-Kains B *et al*: **Gene expression profiling in breast cancer: understanding the molecular basis of histologic grade to improve prognosis**. *Journal of the National Cancer Institute* 2006, **98**(4):262-272.
59. Tutt A, Wang A, Rowland C, Gillett C, Lau K, Chew K, Dai H, Kwok S, Ryder K, Shu H *et al*: **Risk estimation of distant metastasis in node-negative, estrogen receptor-positive breast cancer patients using an RT-PCR based prognostic expression signature**. *BMC cancer* 2008, **8**:339.
60. van de Vijver MJ, He YD, van't Veer LJ, Dai H, Hart AA, Voskuil DW, Schreiber GJ, Peterse JL, Roberts C, Marton MJ *et al*: **A gene-expression signature as a**

predictor of survival in breast cancer. *The New England journal of medicine* 2002, **347**(25):1999-2009.
61. Curtis C, Shah SP, Chin SF, Turashvili G, Rueda OM, Dunning MJ, Speed D, Lynch AG, Samarajiwa S, Yuan Y *et al*: **The genomic and transcriptomic architecture of 2,000 breast tumours reveals novel subgroups**. *Nature* 2012, **486**(7403):346-352.
62. Dawson SJ, Rueda OM, Aparicio S, Caldas C: **A new genome-driven integrated classification of breast cancer and its implications**. *The EMBO journal* 2013, **32**(5):617-628.
63. Ali HR, Rueda OM, Chin SF, Curtis C, Dunning MJ, Aparicio SA, Caldas C: **Genome-driven integrated classification of breast cancer validated in over 7,500 samples**. *Genome biology* 2014, **15**(8):431.
64. Shah SP, Morin RD, Khattra J, Prentice L, Pugh T, Burleigh A, Delaney A, Gelmon K, Guliany R, Senz J *et al*: **Mutational evolution in a lobular breast tumour profiled at single nucleotide resolution**. *Nature* 2009, **461**(7265):809-813.
65. Nik-Zainal S, Van Loo P, Wedge DC, Alexandrov LB, Greenman CD, Lau KW, Raine K, Jones D, Marshall J, Ramakrishna M *et al*: **The life history of 21 breast cancers**. *Cell* 2012, **149**(5):994-1007.
66. Shah SP, Roth A, Goya R, Oloumi A, Ha G, Zhao Y, Turashvili G, Ding J, Tse K, Haffari G *et al*: **The clonal and mutational evolution spectrum of primary triple-negative breast cancers**. *Nature* 2012, **486**(7403):395-399.
67. Greaves M, Maley CC: **Clonal evolution in cancer**. *Nature* 2012, **481**(7381):306-313.
68. Pereira B, Chin SF, Rueda OM, Vollan HK, Provenzano E, Bardwell HA, Pugh M, Jones L, Russell R, Sammut SJ *et al*: **The somatic mutation profiles of 2,433 breast cancers refines their genomic and transcriptomic landscapes**. *Nature communications* 2016, **7**:11479.
69. Eirew P, Steif A, Khattra J, Ha G, Yap D, Farahani H, Gelmon K, Chia S, Mar C, Wan A *et al*: **Dynamics of genomic clones in breast cancer patient xenografts at single-cell resolution**. *Nature* 2015, **518**(7539):422-426.
70. Gerlinger M, Rowan AJ, Horswell S, Math M, Larkin J, Endesfelder D, Gronroos E, Martinez P, Matthews N, Stewart A *et al*: **Intratumor heterogeneity and branched evolution revealed by multiregion sequencing**. *The New England journal of medicine* 2012, **366**(10):883-892.
71. Takahashi K, Kohno T, Matsumoto S, Nakanishi Y, Arai Y, Yamamoto S, Fujiwara T, Tanaka N, Yokota J: **Clonal and parallel evolution of primary lung cancers and their metastases revealed by molecular dissection of cancer cells**. *Clinical cancer research : an official journal of the American Association for Cancer Research* 2007, **13**(1):111-120.
72. Yachida S, Jones S, Bozic I, Antal T, Leary R, Fu B, Kamiyama M, Hruban RH, Eshleman JR, Nowak MA *et al*: **Distant metastasis occurs late during the genetic evolution of pancreatic cancer**. *Nature* 2010, **467**(7319):1114-1117.
73. Cariati M, Marlow R, Dontu G: **Xenotransplantation of breast cancers**. *Methods Mol Biol* 2011, **731**:471-482.

74. DeRose YS, Wang G, Lin YC, Bernard PS, Buys SS, Ebbert MT, Factor R, Matsen C, Milash BA, Nelson E *et al*: **Tumor grafts derived from women with breast cancer authentically reflect tumor pathology, growth, metastasis and disease outcomes**. *Nature medicine* 2011, **17**(11):1514-1520.
75. Ding L, Ellis MJ, Li S, Larson DE, Chen K, Wallis JW, Harris CC, McLellan MD, Fulton RS, Fulton LL *et al*: **Genome remodelling in a basal-like breast cancer metastasis and xenograft**. *Nature* 2010, **464**(7291):999-1005.
76. Zhang X, Claerhout S, Prat A, Dobrolecki LE, Petrovic I, Lai Q, Landis MD, Wiechmann L, Schiff R, Giuliano M *et al*: **A renewable tissue resource of phenotypically stable, biologically and ethnically diverse, patient-derived human breast cancer xenograft models**. *Cancer research* 2013, **73**(15):4885-4897.
77. Aparicio S, Caldas C: **The implications of clonal genome evolution for cancer medicine**. *The New England journal of medicine* 2013, **368**(9):842-851.
78. Nguyen LV, Vanner R, Dirks P, Eaves CJ: **Cancer stem cells: an evolving concept**. *Nature reviews Cancer* 2012, **12**(2):133-143.
79. Lan X, Jorg DJ, Cavalli FMG, Richards LM, Nguyen LV, Vanner RJ, Guilhamon P, Lee L, Kushida MM, Pellacani D *et al*: **Fate mapping of human glioblastoma reveals an invariant stem cell hierarchy**. *Nature* 2017, **549**(7671):227-232.
80. Wang Y, Waters J, Leung ML, Unruh A, Roh W, Shi X, Chen K, Scheet P, Vattathil S, Liang H *et al*: **Clonal evolution in breast cancer revealed by single nucleus genome sequencing**. *Nature* 2014, **512**(7513):155-160.
81. Bonadonna G, Veronesi U, Brambilla C, Ferrari L, Luini A, Greco M, Bartoli C, Coopmans de Yoldi G, Zucali R, Rilke F *et al*: **Primary chemotherapy to avoid mastectomy in tumors with diameters of three centimeters or more**. *Journal of the National Cancer Institute* 1990, **82**(19):1539-1545.
82. Middleman E, Luce J, Frei E, 3rd: **Clinical trials with adriamycin**. *Cancer* 1971, **28**(4):844-850.
83. Smalley RV, Carpenter J, Bartolucci A, Vogel C, Krauss S: **A comparison of cyclophosphamide, adriamycin, 5-fluorouracil (CAF) and cyclophosphamide, methotrexate, 5-fluorouracil, vincristine, prednisone (CMFVP) in patients with metastatic breast cancer: a Southeastern Cancer Study Group project**. *Cancer* 1977, **40**(2):625-632.
84. Fossati R, Confalonieri C, Torri V, Ghislandi E, Penna A, Pistotti V, Tinazzi A, Liberati A: **Cytotoxic and hormonal treatment for metastatic breast cancer: a systematic review of published randomized trials involving 31,510 women**. *Journal of clinical oncology : official journal of the American Society of Clinical Oncology* 1998, **16**(10):3439-3460.
85. Gregory RK, Smith IE: **Vinorelbine--a clinical review**. *British journal of cancer* 2000, **82**(12):1907-1913.
86. Takeda AL, Jones J, Loveman E, Tan SC, Clegg AJ: **The clinical effectiveness and cost-effectiveness of gemcitabine for metastatic breast cancer: a systematic review and economic evaluation**. *Health Technol Assess* 2007, **11**(19):iii, ix-xi, 1-62.

87. O'Shaughnessy JA, Kaufmann M, Siedentopf F, Dalivoust P, Debled M, Robert NJ, Harbeck N: **Capecitabine monotherapy: review of studies in first-line HER-2-negative metastatic breast cancer**. *The oncologist* 2012, **17**(4):476-484.
88. Yardley DA: **Activity of ixabepilone in patients with metastatic breast cancer with primary resistance to taxanes**. *Clinical breast cancer* 2008, **8**(6):487-492.
89. Pean E, Klaar S, Berglund EG, Salmonson T, Borregaard J, Hofland KF, Ersboll J, Abadie E, Giuliani R, Pignatti F: **The European medicines agency review of eribulin for the treatment of patients with locally advanced or metastatic breast cancer: summary of the scientific assessment of the committee for medicinal products for human use**. *Clinical cancer research : an official journal of the American Association for Cancer Research* 2012, **18**(17):4491-4497.
90. **Effects of chemotherapy and hormonal therapy for early breast cancer on recurrence and 15-year survival: an overview of the randomised trials**. *Lancet* 2005, **365**(9472):1687-1717.
91. Dowsett M, Cuzick J, Ingle J, Coates A, Forbes J, Bliss J, Buyse M, Baum M, Buzdar A, Colleoni M *et al*: **Meta-analysis of breast cancer outcomes in adjuvant trials of aromatase inhibitors versus tamoxifen**. *Journal of clinical oncology : official journal of the American Society of Clinical Oncology* 2010, **28**(3):509-518.
92. Slamon DJ, Clark GM, Wong SG, Levin WJ, Ullrich A, McGuire WL: **Human breast cancer: correlation of relapse and survival with amplification of the HER-2/neu oncogene**. *Science* 1987, **235**(4785):177-182.
93. Piccart-Gebhart MJ, Procter M, Leyland-Jones B, Goldhirsch A, Untch M, Smith I, Gianni L, Baselga J, Bell R, Jackisch C *et al*: **Trastuzumab after adjuvant chemotherapy in HER2-positive breast cancer**. *The New England journal of medicine* 2005, **353**(16):1659-1672.
94. Slamon DJ, Leyland-Jones B, Shak S, Fuchs H, Paton V, Bajamonde A, Fleming T, Eiermann W, Wolter J, Pegram M *et al*: **Use of chemotherapy plus a monoclonal antibody against HER2 for metastatic breast cancer that overexpresses HER2**. *The New England journal of medicine* 2001, **344**(11):783-792.
95. Geyer CE, Forster J, Lindquist D, Chan S, Romieu CG, Pienkowski T, Jagiello-Gruszfeld A, Crown J, Chan A, Kaufman B *et al*: **Lapatinib plus capecitabine for HER2-positive advanced breast cancer**. *The New England journal of medicine* 2006, **355**(26):2733-2743.
96. Harbeck N, Beckmann MW, Rody A, Schneeweiss A, Müller V, Fehm T, Marschner N, Gluz O, Schrader I, Heinrich G *et al*: **HER2 Dimerization Inhibitor Pertuzumab – Mode of Action and Clinical Data in Breast Cancer**. *Breast Care* 2013, **8**(1):49-55.
97. Baselga J, Campone M, Piccart M, Burris HA, 3rd, Rugo HS, Sahmoud T, Noguchi S, Gnant M, Pritchard KI, Lebrun F *et al*: **Everolimus in postmenopausal hormone-receptor-positive advanced breast cancer**. *The New England journal of medicine* 2012, **366**(6):520-529.

98. Mayer EL: **Targeting Breast Cancer with CDK Inhibitors**. *Current Oncology Reports* 2015, **17**(5):20.
99. Coleman RE, Rubens RD: **The clinical course of bone metastases from breast cancer**. *British journal of cancer* 1987, **55**(1):61-66.
100. Lin NU, Winer EP: **Brain metastases: the HER2 paradigm**. *Clinical cancer research : an official journal of the American Association for Cancer Research* 2007, **13**(6):1648-1655.
101. Baron R, Ferrari S, Russell RG: **Denosumab and bisphosphonates: different mechanisms of action and effects**. *Bone* 2011, **48**(4):677-692.
102. Sperduto PW, Chao ST, Sneed PK, Luo X, Suh J, Roberge D, Bhatt A, Jensen AW, Brown PD, Shih H *et al*: **Diagnosis-specific prognostic factors, indexes, and treatment outcomes for patients with newly diagnosed brain metastases: a multi-institutional analysis of 4,259 patients**. *International journal of radiation oncology, biology, physics* 2010, **77**(3):655-661.
103. Massacesi C, Di Tomaso E, Urban P, Germa C, Quadt C, Trandafir L, Aimone P, Fretault N, Dharan B, Tavorath R *et al*: **PI3K inhibitors as new cancer therapeutics: implications for clinical trial design**. *OncoTargets and therapy* 2016, **9**:203-210.
104. Nanda R, Chow LQM, Dees EC, Berger R, Gupta S, Geva R, Pusztai L, Pathiraja K, Aktan G, Cheng JD *et al*: **Pembrolizumab in Patients With Advanced Triple-Negative Breast Cancer: Phase Ib KEYNOTE-012 Study**. *Journal of Clinical Oncology* 2016, **34**(21):2460-2467.
105. Lipson EJ, Forde PM, Hammers H-J, Emens LA, Taube JM, Topalian SL: **Antagonists of PD-1 and PD-L1 in Cancer Treatment**. *Seminars in oncology* 2015, **42**(4):587-600.
106. Newton K, Strasser A: **Ionizing Radiation and Chemotherapeutic Drugs Induce Apoptosis in Lymphocytes in the Absence of FAS or Fadd/Mort1 Signaling: Implications for Cancer Therapy**. *The Journal of experimental medicine* 2000, **191**(1):195-200.
107. Phillips TM, McBride WH, Pajonk F: **The response of CD24(-/low)/CD44+ breast cancer-initiating cells to radiation**. *Journal of the National Cancer Institute* 2006, **98**(24):1777-1785.
108. Diehn M, Cho RW, Lobo NA, Kalisky T, Dorie MJ, Kulp AN, Qian D, Lam JS, Ailles LE, Wong M *et al*: **Association of reactive oxygen species levels and radioresistance in cancer stem cells**. *Nature* 2009, **458**(7239):780-783.
109. Bensimon J, Biard D, Paget V, Goislard M, Morel-Altmeyer S, Konge J, Chevillard S, Lebeau J: **Forced extinction of CD24 stem-like breast cancer marker alone promotes radiation resistance through the control of oxidative stress**. *Molecular carcinogenesis* 2016, **55**(3):245-254.
110. Chang CW, Chen YS, Chou SH, Han CL, Chen YJ, Yang CC, Huang CY, Lo JF: **Distinct subpopulations of head and neck cancer cells with different levels of intracellular reactive oxygen species exhibit diverse stemness, proliferation, and chemosensitivity**. *Cancer research* 2014, **74**(21):6291-6305.

111. Chen MS, Woodward WA, Behbod F, Peddibhotla S, Alfaro MP, Buchholz TA, Rosen JM: **Wnt/beta-catenin mediates radiation resistance of Sca1+ progenitors in an immortalized mammary gland cell line**. *J Cell Sci* 2007, **120**(Pt 3):468-477.
112. Hadjihannas MV, Bruckner M, Jerchow B, Birchmeier W, Dietmaier W, Behrens J: **Aberrant Wnt/beta-catenin signaling can induce chromosomal instability in colon cancer**. *P Natl Acad Sci USA* 2006, **103**(28):10747-10752.
113. Puc J, Keniry M, Li HS, Pandita TK, Choudhury AD, Memeo L, Mansukhani M, Murty VV, Gaciong Z, Meek SE *et al*: **Lack of PTEN sequesters CHK1 and initiates genetic instability**. *Cancer cell* 2005, **7**(2):193-204.
114. Jiang Z, Pore N, Cerniglia GJ, Mick R, Georgescu MM, Bernhard EJ, Hahn SM, Gupta AK, Maity A: **Phosphatase and tensin homologue deficiency in glioblastoma confers resistance to radiation and temozolomide that is reversed by the protease inhibitor nelfinavir**. *Cancer research* 2007, **67**(9):4467-4473.
115. Chakravarti A, Chakladar A, Delaney MA, Latham DE, Loeffler JS: **The epidermal growth factor receptor pathway mediates resistance to sequential administration of radiation and chemotherapy in primary human glioblastoma cells in a RAS-dependent manner**. *Cancer research* 2002, **62**(15):4307-4315.
116. Bianco C, Tortora G, Bianco R, Caputo R, Veneziani BM, Damiano V, Troiani T, Fontanini G, Raben D, Pepe S *et al*: **Enhancement of antitumor activity of ionizing radiation by combined treatment with the selective epidermal growth factor receptor-tyrosine kinase inhibitor ZD1839 (Iressa)**. *Clinical cancer research : an official journal of the American Association for Cancer Research* 2002, **8**(10):3250-3258.
117. Moeller BJ, Dreher MR, Rabbani ZN, Schroeder T, Cao Y, Li CY, Dewhirst MW: **Pleiotropic effects of HIF-1 blockade on tumor radiosensitivity**. *Cancer cell* 2005, **8**(2):99-110.
118. Kannan N, Nguyen LV, Makarem M, Dong Y, Shih K, Eirew P, Raouf A, Emerman JT, Eaves CJ: **Glutathione-dependent and -independent oxidative stress-control mechanisms distinguish normal human mammary epithelial cell subsets**. *P Natl Acad Sci USA* 2014, **111**(21):7789-7794.
119. Stingl J, Caldas C: **Molecular heterogeneity of breast carcinomas and the cancer stem cell hypothesis**. *Nature reviews Cancer* 2007, **7**(10):791-799.
120. Lim E, Vaillant F, Wu D, Forrest NC, Pal B, Hart AH, Asselin-Labat ML, Gyorki DE, Ward T, Partanen A *et al*: **Aberrant luminal progenitors as the candidate target population for basal tumor development in BRCA1 mutation carriers**. *Nature medicine* 2009, **15**(8):907-913.
121. Molyneux G, Geyer FC, Magnay FA, McCarthy A, Kendrick H, Natrajan R, Mackay A, Grigoriadis A, Tutt A, Ashworth A *et al*: **BRCA1 basal-like breast cancers originate from luminal epithelial progenitors and not from basal stem cells**. *Cell stem cell* 2010, **7**(3):403-417.

122. Scheel C, Eaton EN, Li SH, Chaffer CL, Reinhardt F, Kah KJ, Bell G, Guo W, Rubin J, Richardson AL *et al*: **Paracrine and autocrine signals induce and maintain mesenchymal and stem cell states in the breast**. *Cell* 2011, **145**(6):926-940.
123. Al-Hajj M, Wicha MS, Benito-Hernandez A, Morrison SJ, Clarke MF: **Prospective identification of tumorigenic breast cancer cells**. *P Natl Acad Sci USA* 2003, **100**(7):3983-3988.
124. Magee JA, Piskounova E, Morrison SJ: **Cancer stem cells: impact, heterogeneity, and uncertainty**. *Cancer cell* 2012, **21**(3):283-296.
125. Valent P, Bonnet D, De Maria R, Lapidot T, Copland M, Melo JV, Chomienne C, Ishikawa F, Schuringa JJ, Stassi G *et al*: **Cancer stem cell definitions and terminology: the devil is in the details**. *Nature reviews Cancer* 2012, **12**(11):767-775.
126. Goldstein AS, Huang J, Guo C, Garraway IP, Witte ON: **Identification of a cell of origin for human prostate cancer**. *Science* 2010, **329**(5991):568-571.
127. Matano M, Date S, Shimokawa M, Takano A, Fujii M, Ohta Y, Watanabe T, Kanai T, Sato T: **Modeling colorectal cancer using CRISPR-Cas9-mediated engineering of human intestinal organoids**. *Nature medicine* 2015, **21**(3):256-262.
128. Proia TA, Keller PJ, Gupta PB, Klebba I, Jones AD, Sedic M, Gilmore H, Tung N, Naber SP, Schnitt S *et al*: **Genetic predisposition directs breast cancer phenotype by dictating progenitor cell fate**. *Cell stem cell* 2011, **8**(2):149-163.
129. Keller PJ, Arendt LM, Skibinski A, Logvinenko T, Klebba I, Dong S, Smith AE, Prat A, Perou CM, Gilmore H *et al*: **Defining the cellular precursors to human breast cancer**. *P Natl Acad Sci USA* 2012, **109**(8):2772-2777.
130. Nguyen LV, Pellacani D, Lefort S, Kannan N, Osako T, Makarem M, Cox CL, Kennedy W, Beer P, Carles A *et al*: **Barcoding reveals complex clonal dynamics of de novo transformed human mammary cells**. *Nature* 2015, **528**(7581):267-271.
131. Wei J, Wunderlich M, Fox C, Alvarez S, Cigudosa JC, Wilhelm JS, Zheng Y, Cancelas JA, Gu Y, Jansen M *et al*: **Microenvironment determines lineage fate in a human model of MLL-AF9 leukemia**. *Cancer cell* 2008, **13**(6):483-495.
132. Lin S, Luo Roger T, Ptasinska A, Kerry J, Assi Salam A, Wunderlich M, Imamura T, Kaberlein Joseph J, Rayes A, Althoff Mark J *et al*: **Instructive Role of MLL-Fusion Proteins Revealed by a Model of t(4;11) Pro-B Acute Lymphoblastic Leukemia**. *Cancer cell* 2016, **30**(5):737-749.
133. Imren S, Heuser M, Gasparetto M, Beer PA, Norddahl GL, Xiang P, Chen L, Berg T, Rhyasen GW, Rosten P *et al*: **Modeling de novo leukemogenesis from human cord blood with MN1 and NUP98HOXD13**. *Blood* 2014, **124**(24):3608-3612.
134. Theocharides AP, Dobson SM, Laurenti E, Notta F, Voisin V, Cheng PY, Yuan JS, Guidos CJ, Minden MD, Mullighan CG *et al*: **Dominant-negative Ikaros cooperates with BCR-ABL1 to induce human acute myeloid leukemia in xenografts**. *Leukemia* 2015, **29**(1):177-187.

135. Leskov I, Pallasch CP, Drake A, Iliopoulou BP, Souza A, Shen CH, Schweighofer CD, Abruzzo L, Frenzel LP, Wendtner CM *et al*: **Rapid generation of human B-cell lymphomas via combined expression of Myc and Bcl2 and their use as a preclinical model for biological therapies**. *Oncogene* 2013, **32**(8):1066-1072.
136. Bruna A, Rueda OM, Greenwood W, Batra AS, Callari M, Batra RN, Pogrebniak K, Sandoval J, Cassidy JW, Tufegdzic-Vidakovic A *et al*: **A Biobank of Breast Cancer Explants with Preserved Intra-tumor Heterogeneity to Screen Anticancer Compounds**. *Cell* 2016, **167**(1):260-274 e222.
137. Navin N, Krasnitz A, Rodgers L, Cook K, Meth J, Kendall J, Riggs M, Eberling Y, Troge J, Grubor V *et al*: **Inferring tumor progression from genomic heterogeneity**. *Genome research* 2010, **20**(1):68-80.
138. Bashashati A, Ha G, Tone A, Ding J, Prentice LM, Roth A, Rosner J, Shumansky K, Kalloger S, Senz J *et al*: **Distinct evolutionary trajectories of primary high-grade serous ovarian cancers revealed through spatial mutational profiling**. *The Journal of pathology* 2013, **231**(1):21-34.
139. Gerlinger M, Rowan AJ, Horswell S, Larkin J, Endesfelder D, Gronroos E, Martinez P, Matthews N, Stewart A, Tarpey P *et al*: **Intratumor heterogeneity and branched evolution revealed by multiregion sequencing**. *The New England journal of medicine* 2012, **366**(10):883-892.
140. Shlush LI, Zandi S, Mitchell A, Chen WC, Brandwein JM, Gupta V, Kennedy JA, Schimmer AD, Schuh AC, Yee KW *et al*: **Identification of pre-leukaemic haematopoietic stem cells in acute leukaemia**. *Nature* 2014, **506**(7488):328-333.
141. Jiang X, Saw KM, Eaves A, Eaves C: **Instability of BCR-ABL gene in primary and cultured chronic myeloid leukemia stem cells**. *Journal of the National Cancer Institute* 2007, **99**(9):680-693.
142. Singh SK, Hawkins C, Clarke ID, Squire JA, Bayani J, Hide T, Henkelman RM, Cusimano MD, Dirks PB: **Identification of human brain tumour initiating cells**. *Nature* 2004, **432**(7015):396-401.
143. Bao S, Wu Q, McLendon RE, Hao Y, Shi Q, Hjelmeland AB, Dewhirst MW, Bigner DD, Rich JN: **Glioma stem cells promote radioresistance by preferential activation of the DNA damage response**. *Nature* 2006, **444**(7120):756-760.
144. O'Brien CA, Pollett A, Gallinger S, Dick JE: **A human colon cancer cell capable of initiating tumour growth in immunodeficient mice**. *Nature* 2007, **445**(7123):106-110.
145. Ricci-Vitiani L, Lombardi DG, Pilozzi E, Biffoni M, Todaro M, Peschle C, De Maria R: **Identification and expansion of human colon-cancer-initiating cells**. *Nature* 2007, **445**(7123):111-115.
146. Collins AT, Berry PA, Hyde C, Stower MJ, Maitland NJ: **Prospective identification of tumorigenic prostate cancer stem cells**. *Cancer research* 2005, **65**(23):10946-10951.
147. Suzuki S, Terauchi M, Umezu T, Kajiyama H, Shibata K, Nawa A, Kikkawa F: **Identification and characterization of cancer stem cells in ovarian yolk sac tumors**. *Cancer science* 2010, **101**(10):2179-2185.

148. Quintana E, Shackleton M, Sabel MS, Fullen DR, Johnson TM, Morrison SJ: **Efficient tumour formation by single human melanoma cells**. *Nature* 2008, **456**(7222):593-598.
149. Schatton T, Murphy GF, Frank NY, Yamaura K, Waaga-Gasser AM, Gasser M, Zhan Q, Jordan S, Duncan LM, Weishaupt C *et al*: **Identification of cells initiating human melanomas**. *Nature* 2008, **451**(7176):345-U311.
150. Bonnet D, Dick JE: **Human acute myeloid leukemia is organized as a hierarchy that originates from a primitive hematopoietic cell**. *Nature medicine* 1997, **3**(7):730-737.
151. Lapidot T, Sirard C, Vormoor J, Murdoch B, Hoang T, Caceres-cortes J, Minden M, Paterson B, Caligiuri MA, Dick JE: **A Cell Initiating Human Acute Myeloid-Leukemia after Transplantation into Scid Mice**. *Nature* 1994, **367**(6464):645-648.
152. Sarry JE, Murphy K, Perry R, Sanchez PV, Secreto A, Keefer C, Swider CR, Strzelecki AC, Cavelier C, Recher C *et al*: **Human acute myelogenous leukemia stem cells are rare and heterogeneous when assayed in NOD/SCID/IL2R gamma c-deficient mice**. *Journal of Clinical Investigation* 2011, **121**(1):384-395.
153. Notta F, Mullighan CG, Wang JCY, Poeppl A, Doulatov S, Phillips LA, Ma J, Minden MD, Downing JR, Dick JE: **Evolution of human BCR-ABL1 lymphoblastic leukaemia-initiating cells (vol 469, pg 362, 2011)**. *Nature* 2011, **471**(7337).
154. Ebinger S, Ozdemir EZ, Ziegenhain C, Tiedt S, Castro Alves C, Grunert M, Dworzak M, Lutz C, Turati VA, Enver T *et al*: **Characterization of Rare, Dormant, and Therapy-Resistant Cells in Acute Lymphoblastic Leukemia**. *Cancer cell* 2016.
155. Bystrykh LV, Belderbos ME: **Clonal Analysis of Cells with Cellular Barcoding: When Numbers and Sizes Matter**. *Methods Mol Biol* 2016, **1516**:57-89.
156. Elenbaas B, Spirio L, Koerner F, Fleming MD, Zimonjic DB, Donaher JL, Popescu NC, Hahn WC, Weinberg RA: **Human breast cancer cells generated by oncogenic transformation of primary mammary epithelial cells**. *Genes & Development* 2001, **15**(1):50-65.
157. Duss S, André S, Nicoulaz A-L, Fiche M, Bonnefoi H, Brisken C, Iggo RD: **An oestrogen-dependent model of breast cancer created by transformation of normal human mammary epithelial cells**. *Breast Cancer Research* 2007, **9**(3):R38.
158. Qin H, Malek S, Cowell JK, Ren M: **Transformation of human CD34+hematopoietic progenitor cells with DEK-NUP214 induces AML in an immunocompromised mouse model**. *Oncogene* 2016, **35**(43):5686-5691.
159. Ren M, Qin H, Wu Q, Savage NM, George TI, Cowell JK: **Development of ZMYM2-FGFR1 driven AML in human CD34+ cells in immunocompromised mice**. *International journal of cancer* 2016, **139**(4):836-840.

160. Sandell LL, Zakian VA: **Loss of a yeast telomere: arrest, recovery, and chromosome loss**. *Cell* 1993, **75**(4):729-739.
161. Toczyski DP, Galgoczy DJ, Hartwell LH: **CDC5 and CKII control adaptation to the yeast DNA damage checkpoint**. *Cell* 1997, **90**(6):1097-1106.
162. Yoo HY, Kumagai A, Shevchenko A, Dunphy WG: **Adaptation of a DNA replication checkpoint response depends upon inactivation of Claspin by the Polo-like kinase**. *Cell* 2004, **117**(5):575-588.
163. Syljuasen RG, Jensen S, Bartek J, Lukas J: **Adaptation to the ionizing radiation-induced G2 checkpoint occurs in human cells and depends on checkpoint kinase 1 and Polo-like kinase 1 kinases**. *Cancer research* 2006, **66**(21):10253-10257.
164. Rezacova M, Rudolfova G, Tichy A, Bacikova A, Mutna D, Havelek R, Vavrova J, Odrazka K, Lukasova E, Kozubek S: **Accumulation of DNA damage and cell death after fractionated irradiation**. *Radiation research* 2011, **175**(6):708-718.
165. Kubara PM, Kerneis-Golsteyn S, Studeny A, Lanser BB, Meijer L, Golsteyn RM: **Human cells enter mitosis with damaged DNA after treatment with pharmacological concentrations of genotoxic agents**. *The Biochemical journal* 2012, **446**(3):373-381.
166. Wang XQ, Zhu YQ, Lui KS, Cai Q, Lu P, Poon RT: **Aberrant Polo-like kinase 1-Cdc25A pathway in metastatic hepatocellular carcinoma**. *Clinical cancer research : an official journal of the American Association for Cancer Research* 2008, **14**(21):6813-6820.
167. Bartek J, Lukas J: **DNA damage checkpoints: from initiation to recovery or adaptation**. *Current opinion in cell biology* 2007, **19**(2):238-245.
168. Donzelli M, Draetta GF: **Regulating mammalian checkpoints through Cdc25 inactivation**. *EMBO reports* 2003, **4**(7):671-677.
169. Bartek J, Lukas J: **Chk1 and Chk2 kinases in checkpoint control and cancer**. *Cancer cell* 2003, **3**(5):421-429.
170. Taylor WR, Stark GR: **Regulation of the G2/M transition by p53**. *Oncogene* 2001, **20**(15):1803-1815.
171. Dotto GP: **p21(WAF1/Cip1): more than a break to the cell cycle?** *Biochimica et biophysica acta* 2000, **1471**(1):M43-56.
172. Brugarolas J, Moberg K, Boyd SD, Taya Y, Jacks T, Lees JA: **Inhibition of cyclin-dependent kinase 2 by p21 is necessary for retinoblastoma protein-mediated G1 arrest after gamma-irradiation**. *P Natl Acad Sci USA* 1999, **96**(3):1002-1007.
173. Ewen ME, Sluss HK, Sherr CJ, Matsushime H, Kato J, Livingston DM: **Functional interactions of the retinoblastoma protein with mammalian D-type cyclins**. *Cell* 1993, **73**(3):487-497.
174. Cheng L, Wu Q, Huang Z, Guryanova OA, Huang Q, Shou W, Rich JN, Bao S: **L1CAM regulates DNA damage checkpoint response of glioblastoma stem cells through NBS1**. *The EMBO journal* 2011, **30**(5):800-813.
175. Sancar A, Lindsey-Boltz LA, Unsal-Kacmaz K, Linn S: **Molecular mechanisms of mammalian DNA repair and the DNA damage checkpoints**. *Annual review of biochemistry* 2004, **73**:39-85.

176. Soule HD, Maloney TM, Wolman SR, Peterson WD, Brenz R, McGrath CM, Russo J, Pauley RJ, Jones RF, Brooks SC: **Isolation and Characterization of a Spontaneously Immortalized Human Breast Epithelial Cell Line, MCF-10**. *Cancer research* 1990, **50**(18):6075-6086.
177. Fiedler M, Weber F, Hautmann MG, Haubner F, Reichert TE, Klingelhöffer C, Schreml S, Meier JK, Hartmann A, Ettl T: **Biological predictors of radiosensitivity in head and neck squamous cell carcinoma**. *Clinical Oral Investigations* 2018, **22**(1):189-200.
178. DeRose YS, Gligorich KM, Wang G, Georgelas A, Bowman P, Courdy SJ, Welm AL, Welm BE: **Patient-derived models of human breast cancer: protocols for in vitro and in vivo applications in tumor biology and translational medicine**. *Current protocols in pharmacology* 2013, **Chapter 14**:Unit14 23.
179. Clevers H: **Modeling Development and Disease with Organoids**. *Cell* 2016, **165**(7):1586-1597.
180. Hu Y, Smyth GK: **ELDA: extreme limiting dilution analysis for comparing depleted and enriched populations in stem cell and other assays**. *Journal of immunological methods* 2009, **347**(1-2):70-78.
181. Hata AN, Niederst MJ, Archibald HL, Gomez-Caraballo M, Siddiqui FM, Mulvey HE, Maruvka YE, Ji F, Bhang HE, Krishnamurthy Radhakrishna V *et al*: **Tumor cells can follow distinct evolutionary paths to become resistant to epidermal growth factor receptor inhibition**. *Nature medicine* 2016, **22**(3):262-269.
182. Withers HR: **Recovery and repopulation in vivo by mouse skin epithelial cells during fractionated irradiation**. *Radiation research* 1967, **32**(2):227-239.
183. Thames HD, Jr., Withers R, Mason KA, Reid BO: **Dose-survival characteristics of mouse jejunal crypt cells**. *International journal of radiation oncology, biology, physics* 1981, **7**(11):1591-1597.
184. Withers HR, Hunter N, Barkley HT, Jr., Reid BO: **Radiation survival and regeneration characteristics of spermatogenic stem cells of mouse testis**. *Radiation research* 1974, **57**(1):88-103.
185. Withers HR, Mason KA, Thames HD, Jr.: **Late radiation response of kidney assayed by tubule-cell survival**. *The British journal of radiology* 1986, **59**(702):587-595.
186. McCulloch EA, Till JE: **The sensitivity of cells from normal mouse bone marrow to gamma radiation in vitro and in vivo**. *Radiation research* 1962, **16**:822-832.
187. Bouras T, Pal B, Vaillant F, Harburg G, Asselin-Labat M-L, Oakes SR, Lindeman GJ, Visvader JE: **Notch Signaling Regulates Mammary Stem Cell Function and Luminal Cell-Fate Commitment**. *Cell stem cell*, **3**(4):429-441.
188. Weeber F, van de Wetering M, Hoogstraat M, Dijkstra KK, Krijgsman O, Kuilman T, Gadellaa-van Hooijdonk CGM, van der Velden DL, Peeper DS, Cuppen EPJG *et al*: **Preserved genetic diversity in organoids cultured from biopsies of human colorectal cancer metastases**. *P Natl Acad Sci USA* 2015, **112**(43):13308-13311.

189. Baker LA, Tiriac H, Clevers H, Tuveson DA: **Modeling Pancreatic Cancer with Organoids**. *Trends in Cancer* 2016, **2**(4):176-190.
190. Lancaster MA, Knoblich JA: **Organogenesis in a dish: Modeling development and disease using organoid technologies**. *Science* 2014, **345**(6194).
191. Papapetrou EP: **Patient-derived induced pluripotent stem cells in cancer research and precision oncology**. *Nature medicine* 2016, **22**(12):1392-1401.
192. Lim KL, Teoh HK, Choong PF, Teh HX, Cheong SK, Kamarul T: **Reprogramming cancer cells: overview & current progress**. *Expert opinion on biological therapy* 2016, **16**(7):941-951.
193. Kumano K, Arai S, Hosoi M, Taoka K, Takayama N, Otsu M, Nagae G, Ueda K, Nakazaki K, Kamikubo Y *et al*: **Generation of induced pluripotent stem cells from primary chronic myelogenous leukemia patient samples**. *Blood* 2012, **119**(26):6234-6242.
194. Carette JE, Pruszak J, Varadarajan M, Blomen VA, Gokhale S, Camargo FD, Wernig M, Jaenisch R, Brummelkamp TR: **Generation of iPSCs from cultured human malignant cells**. *Blood* 2010, **115**(20):4039-4042.
195. Hu K, Slukvin I: **Generation of Transgene-Free iPSC Lines from Human Normal and Neoplastic Blood Cells Using Episomal Vectors**. In: *Pluripotent Stem Cells: Methods and Protocols.* edn. Edited by Lakshmipathy U, Vemuri MC. Totowa, NJ: Humana Press; 2013: 163-176.
196. Kotini A, Dolezal EK, Nimer S, Papapetrou EP: **An iPSC-Based Model Of MDS For Phenotype-Driven Gene and Drug Discovery**. *Blood* 2013, **122**(21):859-859.
197. Ye Z, Zhan H, Mali P, Dowey S, Williams DM, Jang YY, Dang CV, Spivak JL, Moliterno AR, Cheng L: **Human-induced pluripotent stem cells from blood cells of healthy donors and patients with acquired blood disorders**. *Blood* 2009, **114**(27):5473-5480.
198. Gandre-Babbe S, Paluru P, Aribeana C, Chou ST, Bresolin S, Lu L, Sullivan SK, Tasian SK, Weng J, Favre H *et al*: **Patient-derived induced pluripotent stem cells recapitulate hematopoietic abnormalities of juvenile myelomonocytic leukemia**. *Blood* 2013, **121**(24):4925-4929.
199. Muñoz-López A, Romero-Moya D, Prieto C, Ramos-Mejía V, Agraz-Doblas A, Varela I, Buschbeck M, Palau A, Carvajal-Vergara X, Giorgetti A *et al*: **Development Refractoriness of MLL-Rearranged Human B Cell Acute Leukemias to Reprogramming into Pluripotency**. *Stem cell reports*, **7**(4):602-618.
200. Kim J, Hoffman JP, Alpaugh RK, Rhim AD, Reichert M, Stanger BZ, Furth EE, Sepulveda AR, Yuan CX, Won KJ *et al*: **An iPSC line from human pancreatic ductal adenocarcinoma undergoes early to invasive stages of pancreatic cancer progression**. *Cell reports* 2013, **3**(6):2088-2099.
201. Hadoux J, Feraud O, Griscelli F, Opolon P, Divers D, Gobbo E, Schlumberger M, Bennaceur-Griscelli A, Turhan AG: **Generation of an induced pluripotent stem cell line from a patient with hereditary multiple endocrine**

neoplasia 2A (MEN2A) syndrome with RET mutation. *Stem cell research* 2016, **17**(1):154-157.
202. Iskender B, Izgi K, Canatan H: **Reprogramming bladder cancer cells for studying cancer initiation and progression**. *Tumour biology : the journal of the International Society for Oncodevelopmental Biology and Medicine* 2016, **37**(10):13237-13245.
203. Lee DF, Su J, Kim HS, Chang B, Papatsenko D, Zhao R, Yuan Y, Gingold J, Xia W, Darr H *et al*: **Modeling familial cancer with induced pluripotent stem cells**. *Cell* 2015, **161**(2):240-254.
204. Ron-Bigger S, Bar-Nur O, Isaac S, Bocker M, Lyko F, Eden A: **Aberrant epigenetic silencing of tumor suppressor genes is reversed by direct reprogramming**. *Stem Cells* 2010, **28**(8):1349-1354.
205. Ohnishi K, Semi K, Yamamoto T, Shimizu M, Tanaka A, Mitsunaga K, Okita K, Osafune K, Arioka Y, Maeda T *et al*: **Premature termination of reprogramming in vivo leads to cancer development through altered epigenetic regulation**. *Cell* 2014, **156**(4):663-677.
206. Singh VK, Kalsan M, Kumar N, Saini A, Chandra R: **Induced pluripotent stem cells: applications in regenerative medicine, disease modeling, and drug discovery**. *Frontiers in Cell and Developmental Biology* 2015, **3**:2.
207. Hockemeyer D, Jaenisch R: **Induced Pluripotent Stem Cells Meet Genome Editing**. *Cell stem cell*, **18**(5):573-586.
208. Choi PS, Meyerson M: **Targeted genomic rearrangements using CRISPR/Cas technology**. *Nature communications* 2014, **5**:3728.
209. Chen C, Liu Y, Rappaport AR, Kitzing T, Schultz N, Zhao Z, Shroff AS, Dickins RA, Vakoc CR, Bradner JE *et al*: **MLL3 is a haploinsufficient 7q tumor suppressor in acute myeloid leukemia**. *Cancer cell* 2014, **25**(5):652-665.
210. Torres R, Martin MC, Garcia A, Cigudosa JC, Ramirez JC, Rodriguez-Perales S: **Engineering human tumour-associated chromosomal translocations with the RNA-guided CRISPR-Cas9 system**. *Nature communications* 2014, **5**:3964.
211. Heckl D, Kowalczyk MS, Yudovich D, Belizaire R, Puram RV, McConkey ME, Thielke A, Aster JC, Regev A, Ebert BL: **Generation of mouse models of myeloid malignancy with combinatorial genetic lesions using CRISPR-Cas9 genome editing**. *Nat Biotech* 2014, **32**(9):941-946.
212. Xue W, Chen S, Yin H, Tammela T, Papagiannakopoulos T, Joshi NS, Cai W, Yang G, Bronson R, Crowley DG *et al*: **CRISPR-mediated direct mutation of cancer genes in the mouse liver**. *Nature* 2014, **514**(7522):380-384.
213. Guernet A, Mungamuri SK, Cartier D, Sachidanandam R, Jayaprakash A, Adriouch S, Vezain M, Charbonnier F, Rohkin G, Coutant S *et al*: **CRISPR-Barcoding for Intratumor Genetic Heterogeneity Modeling and Functional Analysis of Oncogenic Driver Mutations**. *Molecular cell* 2016, **63**(3):526-538.
214. Frieda KL, Linton JM, Hormoz S, Choi J, Chow K-HK, Singer ZS, Budde MW, Elowitz MB, Cai L: **Synthetic recording and in situ readout of lineage information in single cells**. *Nature* 2017, **541**(7635):107-111.

215. Combes G, Alharbi I, Braga LG, Elowe S: **Playing polo during mitosis: PLK1 takes the lead**. *Oncogene* 2017, **36**(34):4819-4827.
216. Smits VAJ, Klompmaker R, Arnaud L, Rijksen G, Nigg EA, Medema RH: **Polo-like kinase-1 is a target of the DNA damage checkpoint**. *Nature cell biology* 2000, **2**:672.
217. van Vugt MATM, Gardino AK, Linding R, Ostheimer GJ, Reinhardt HC, Ong S-E, Tan CS, Miao H, Keezer SM, Li J *et al*: **A Mitotic Phosphorylation Feedback Network Connects Cdk1, Plk1, 53BP1, and Chk2 to Inactivate the G2/M DNA Damage Checkpoint**. *PLoS biology* 2010, **8**(1):e1000287.
218. Bruinsma W, Raaijmakers JA, Medema RH: **Switching Polo-like kinase-1 on and off in time and space**. *Trends in biochemical sciences* 2012, **37**(12):534-542.
219. Chabalier-Taste C, Brichese L, Racca C, Canitrot Y, Calsou P, Larminat F: **Polo-like kinase 1 mediates BRCA1 phosphorylation and recruitment at DNA double-strand breaks**. *Oncotarget* 2016, **7**(3):2269-2283.
220. Gutteridge REA, Ndiaye MA, Liu X, Ahmad N: **Plk1 inhibitors in cancer therapy: From laboratory to clinics**. *Molecular cancer therapeutics* 2016, **15**(7):1427-1435.